NOL HYPERVELOCITY WIND TUNNEL
REPORT NO. 2: NOZZLE DESIGN

By
Walter J. Glowacki

30 APRIL 1971

NOL

NAVAL ORDNANCE LABORATORY, WHITE OAK, SILVER SPRING, MARYLAND

APPROVED FOR PUBLIC RELEASE;
DISTRIBUTION UNLIMITED

NOL Hypervelocity Wind Tunnel
Report No. 2: Nozzle Design

Prepared by

Walter J. Glowacki

ABSTRACT: The NOL Hypervelocity Wind Tunnel will provide a high
Reynolds number turbulent flow simulation in the Mach number range 10
to 20. This facility, much needed for large-scale testing of hyper-
sonic vehicles, is under construction and will be operational late in
1972. Supply pressures up to 40,000 psi will be maintained constant
for 1 to 4 seconds during which stable, condensation-free flow con-
ditions will prevail. Very high Reynolds numbers, ranging from 6.5 x
10^6 at Mach number 20 to 46 x 10^6 at Mach number 10 (based on the
nozzle exit diameter), are obtained by operating with nitrogen at
temperatures just sufficient to avoid test section condensation. This
report presents the detailed procedure used to design three nozzles
for this facility. The nozzles are forty feet long with five foot
exit diameters and are designed to operate at Mach numbers 10, 15, and
20 with supply pressure of 430, 2365, and 3110 atmospheres, respectively.
Pressure and temperature effects on the thermodynamic properties of
nitrogen are important at these elevated supply conditions and are
taken into account in both the inviscid core and the boundary layer
calculations. The supersonic portion of the inviscid core is cal-
culated by the method of characteristics and the subsonic portion is
approximated as a one-dimensional flow. The boundary layer calcula-
tion procedure is based on an integral moment-of-momentum equation
and is valid for thick as well as thin boundary layers. The design
conditions and the coordinates of both the nozzle wall and the inviscid
core contours are given.

U. S. Naval Ordnance Laboratory
White Oak, Silver Spring, Maryland

NOLTR 71-6   30 April 1971

NOL HYPERVELOCITY WIND TUNNEL REPORT NO. 2: NOZZLE DESIGN

This report is one of a series of technical reports describing the
design and performance of the NOL Hypervelocity Wind Tunnel. A
previous report describes the facility and its mode of operation in
very general terms and summarizes the more significant aspects of the
aerodynamic design of the facility. The present report describes more
completely the detailed procedure used to design the nozzles for this
facility. Future reports in the series will include more detailed
descriptions of individual design features or calculation methods used
in the development of the facility. Tunnel performance and test
results will be reported when available.

                              GEORGE G. BALL
                              Captain, USN
                              Commander

                              L. H. Schindel

                              L. H. SCHINDEL
                              By direction

CONTENTS

CONTENTS (Cont)

TABLES

Table   Title

1   Nitrogen Properties at Condensation Threshold

2   Nozzle Supply and Test Section Conditions

3   Intervals Used with Woolley's Program

4   Selected Inviscid Core and Nozzle Wall Coordinates

5   Card Input Data for ACP and RGTBLP Programs

6   Selected Nozzle Dimensions

7   Corrected Wall Radii in Subsonic Inlets

ILLUSTRATIONS

Figure   Title

1   Comparison of Pressure-Temperature Variations at High
         Densities with AEDC Data Tabulations

2   Variation of Reynolds Number in Test Section with Temperature
         for Constant Pressure or Condensation Threshold Operation
         at Mach 20

3   Variation of Pressure in Test Section with Temperature for
         Condensation Threshold Operation

ILLUSTRATIONS (Cont.)

ILLUSTRATIONS (Cont.)

List of Symbols

a	Sound speed
A	Nozzle cross-sectional area
B'	Constant in compressibility equation (1)
C'	Constant in compressibility equation (1)
C_f	Skin friction coefficient
h	Enthalpy
H_i	Shape factor
H_{i_f}	Shape factor for zero pressure gradient flow
M	Mach number
p	Pressure
Pr	Prandtl number
r	Radius
r_e	Radius of inviscid core at nozzle exit
R	Gas constant
Re	Reynolds number
s_w	Distance from throat along nozzle wall
S	Entropy
St	Stanton number
T	Temperature
T_R	Reduced temperature, equation (7)
T^*	Reduced temperature, equation (3)
u	Flow velocity
x	Distance from throat along nozzle axis
X	$\log_{10} \dfrac{\rho}{\rho_{st}}$
Z	Compressibility factor
α	Wall angle
γ	Ratio of specific heats
θ	Boundary layer momentum thickness
θ_r	Axisymmetric boundary layer momentum thickness
Θ	Characteristic temperature, equation (29)
μ	Viscosity
μ^*	Viscosity at atmospheric pressure
ρ	Density
ω	Flow angle
$\Omega^{(2,2)*}$	Collision integral, equation (5)

List of Symbols (Cont.)

Subscripts

aw	Adiabatic wall
e	Edge of boundary layer
ST	Standard conditions
T_c	Critical temperature
w	Wall
o	Supply or upstream end of inlet
1	At first characteristic point
*	Throat or sonic point

Superscripts

+	Length non-dimensionalized by r_e

INTRODUCTION

A new hypervelocity wind tunnel is currently being installed at the U.S. Naval Ordnance Laboratory (NOL). The facility, which operates for a minimum of one second in a blowdown mode, has separate legs for Mach number 10, 15, and 20 operation. Each leg is fitted with a storage heater and a forty-foot long, five-foot exit diameter contoured axisymmetric nozzle, but shares a common test section. Very high Reynolds numbers, ranging from 6.5×10^6 to 46×10^6 based on nozzle exit diameter, are obtained by operating with nitrogen at pressures up to 3110 atm and temperatures just sufficient to avoid test section condensation.

Various aspects of the mechanical and aerodynamic design of this facility were summarized in reference (1). The aerodynamic design was presented in somewhat more detail in reference (2). This report will present more completely the detailed procedure used to design the three nozzles for this facility.

PROPERTIES OF HIGH-DENSITY NITROGEN

THERMODYNAMIC PROPERTIES

The expansion of a gas in a nozzle is an isentropic process, provided the gas remains in local thermodynamic equilibrium during the expansion. If the expansion is not too fast, the small departures from local thermodynamic equilibrium can be neglected and the flow considered to be isentropic. The gas properties required for the nozzle design calculations are then the equilibrium thermodynamic properties of the gas and as such can be tabulated once the desired isentrope is identified. In practice, the isentrope can be determined by choosing either the nozzle supply conditions or the test section conditions desired. Once the required gas properties are tabulated,

1

only the tabulations need be introduced into the nozzle contour cal-
culations. This in effect uncouples the properties calculation from
the contour calculation and thereby simplifies the nozzle design
problem considerably. For the present nozzles, the flow conditions
and nozzle sizes discussed in later sections indicate that the nitrogen
will be very close to local thermodynamic equilibrium throughout the
expansion process. The small amount of energy frozen in the vibrational
mode will have little effect on the overall properties and can be
neglected. Thus, for the three nozzles discussed in this report, the
nitrogen test gas is assumed to remain in local thermodynamic equilibrium.

In a later section, it will be shown that in order to achieve the
desired range of free-stream Reynolds numbers in the tunnel test-
section at reasonable mass flow rates, it is necessary to use nozzle
supply pressures of several thousand atmospheres for operation at Mach
numbers of 15 and 20. The corresponding densities are sufficiently
high that compressibility corrections to the equation of state must
include at least the first two virial coefficients. Thermodynamic data
including such virial corrections are usually given in tabular form
(e.g. references (3) - (7)) or in the graphical form of a Mollier
diagram (e.g. reference (8)). These tabulations and diagrams were used
to provide the properties of nitrogen at high densities required for
calculations concerning tunnel components upstream of the nozzle.
Although such tabular and graphical forms are very useful for calcula-
tions done by hand, they are not very well suited to computer applications
such as the computation of nozzle contours.

The need for nitrogen properties at moderately high densities in
a form suitable for computer applications was filled by adapting a
versatile computer program developed by Dr. Harold W. Woolley (reference
(9))*. This program can compute the equilibrium thermodynamic properties
of arbitrary mixtures of various components** at moderately-high
densities by treating the mixture as a Cragoe-type gas with

---

*After this phase of the work was completed, Enkenhus and Culotta (ref-
erence (10)) presented analytical expressions for the thermodynamic
properties of nitrogen which agree with the tabulations of Brahinsky
(reference (3)) to better than one percent.
**Subroutines for the six components, nitrogen, oxygen, argon, neon,
carbon dioxide, water vapor, were included.

$$\frac{\ln Z}{\rho} = B' + C'\rho \tag{1}$$

where Z is the compressibility of the gas and ρ the density. The coefficients B' and C' have been determined as functions of temperature by fitting experimental data. Because of its form, this expression leads to nitrogen properties which agree quite well with published tabulations (see Figure 1) provided that the density is not too high. For the enthalpy and entropy required in the nozzle supply reservoir (i.e. the heater vessel), values of temperature, pressure, density, compressibility, and speed of sound obtained using Woolley's computer program deviated from values obtained from interpolation of Brahinsky's tabulations (reference (3)) by less than 0.4 percent, 1.2 percent, and 1.6 percent for the Mach number 10, 15, and 20 nozzles, respectively. Accordingly, the computer program was judged sufficiently accurate and was used to provide the nitrogen properties required for computing the nozzle contours. It must be kept in mind that the nozzle calculations are for moderately-high density conditions. For higher densities, such as in the gas supply vessels upstream of the heater, Woolley's program can be significantly in error and should not be used except with the utmost caution.

Given values for any two thermodynamic variables, Woolley's program will compute the corresponding values for most other thermodynamic variables of interest. Since temperature and density are the natural variables for the equations used in Woolley's program, a built-in iterative procedure beginning with initial guesses for temperature and density is used for other pairs of variables. The program is set up to perform multiple calculations either by reading successively pairs of values for the two chosen variables or by working through a specified range of the two variables with increments given by the user.

CONDENSATION LINE PROPERTIES

In order to attain the highest test-section Reynolds number for a given supply pressure and test-section Mach number, the test-section

3

temperature should be as low as possible. To see this, we anticipate
the results somewhat and assume that the temperature and pressure in
the test section are such that the perfect gas law applies, the
specific heats are constant, and the viscosity is a function of tem-
perature only. Then, for a given pressure and test-section Mach
number, the Reynolds number is proportional to about the -1.25 power
of the test-section temperature and, therefore, increases as the
temperature decreases. This behavior is evident in Figure 2 for three
supply pressures and a Mach number of 20.

In practice, a lower limit exists for the test-section temperature
for any given supply pressure because the gaseous nitrogen will
condense into the liquid phase if cooled sufficiently. This lower
limit is the temperature at which the nitrogen is on the verge of
condensing, i.e. the condensation temperature. Operation at this
limit then becomes "condensation threshold operation." Using the
equilibrium saturation temperature-pressure relation for the onset of
condensation given by Din (reference (4), p. 86)

$$\log_{10} p \text{ (mmHg)} = 6.49594 - \frac{255.821}{T \text{ (}^\circ K\text{)} - 6.6} \tag{2}$$

the Reynolds number per foot for condensation-threshold operation at
Mach number 20 is shown as a function of test-section temperature in
Figure 2, together with the curves for constant pressure operation.
The figure shows, as expected, that the minimum supply pressure
necessary to produce a given Reynolds number per foot in the test
section is the pressure corresponding to condensation threshold opera-
tion.

The expression given by Din for the onset of condensation applies
only if the nitrogen does not become supersaturated. Daum (reference
(11)) shows that a substantial amount of supersaturation can occur
when a test gas is expanded rapidly to high velocity and low pressure.
If the distance from the upstream end of the uniform flow region to
the test section is sufficiently short, the test gas will still be in
a supersaturated state when it reaches the test section. Applying
the procedure outlined by Daum, it was estimated that there could be

4

no supersaturation in the Mach number 10 and 15 nozzles and only a minimal amount in the Mach number 20 nozzle. Later calculations based on the final nozzle designs agreed with the early estimates.

For the Mach number 20 case, the analysis indicated that the test-section static temperature could be lowered about 2°K before the onset of condensation. This 2°K reduction leads to a five percent decrease in the required supply pressure and temperature for the same Reynolds number. However, it was decided that this five percent decrease in supply conditions was not sufficient to justify risking the possibility of condensation in the test section. Moreover, as will be seen in a later section, the Mach 20 nozzle will probably require film or transpiration cooling to protect the nozzle throat during the test run. Such cooling may reduce the stream temperature and precipitate condensation. This possibility is reduced somewhat by operating at the slightly higher temperature.

Since little or no supersaturation is indicated, Din's expression was chosen to represent the temperature-pressure relation at condensation threshold. If a temperature is given, the corresponding pressure for condensation threshold operation is obtained from Din's expression. The remaining thermodynamic properties can then be found from a Mollier diagram, perfect gas relations, or a computer program such as the one obtained from Woolley. Woolley's program was used so that the condensation line properties would be consistent with the properties obtained by using Woolley's program to compute isentropic expansions from the selected nozzle supply conditions. The pressure, density, entropy, enthalpy, and sound speed for condensation threshold operation are shown in Figures 3-7 and listed in Table 1. The mass flow per unit area and Reynolds number per foot are shown in Figures 8 and 9.

VISCOSITY

Low Temperature. The viscosity of nitrogen at low temperature required for Reynolds number calculations was obtained from the dilute-gas relation given by Hirschfelder, Curtiss, and Bird (reference (12))

$$\mu = \frac{266.93 \times 10^{-7} \sqrt{MT}}{\sigma^2 \, \Omega^{(2,2)*}(T^*)} \quad (\frac{g}{cm \; sec}) \tag{3}$$

where $T^* = kT/\varepsilon$.

For nitrogen $\quad\quad M = 28.016$

$$\sigma = 3.681 \text{\AA}$$

$$\varepsilon/k = 91.46°K$$

Substituting these values and changing units

$$\mu = 7.0066 \times 10^{-7} \frac{\sqrt{T}}{\Omega^{(2,2)^*}(T^*)} \quad (\frac{lbm}{ftsec}) \quad\quad\quad (4)$$

The collision integral $\Omega^{(2,2)^*}$ was obtained from the expression

$$\Omega^{(2,2)^*}(T^*) = \frac{1}{3}[6.771 - 6.38(T^*-.5) + 6.6(T^*-.5)^2 - 4(T^*-.5)^3] \quad\quad (5)$$

which represents the data tabulated in reference (12) for the Lennard-Jones (6-12) potential to better than 0.1 percent accuracy in the range 30-80°K. The viscosity calculated from these expressions (shown in Figure 10 and listed in Table 1) was used in the Reynolds number calculations mentioned previously.

Higher Temperature. The viscosity of nitrogen at higher temperatures and densities was obtained from the results of Brebach and Thodos (reference (13)) who give a reduced state correlation for the viscosity of diatomic gases at atmospheric pressure and a density-dependent correction to account for higher pressures. Experimental data for the viscosity at atmospheric pressure (μ^*) are correlated by the expressions

$$\frac{\mu^*}{\mu^*_{T_c}} = T_R^{0.979} \quad (T_R \leq 1.0) \quad\quad\quad (6)$$

$$\frac{\mu^*}{\mu^*_{T_c}} = 1.196 \, T_R^{0.659} \quad\quad (T_R \geq 3.5) \quad\quad\quad (7)$$

where $T_R = T/T_c$ and T_c is the critical temperature. For nitrogen, T_c is given as 126.2 degrees Kelvin and $\mu^*_{T_c}$ as .00865 centipoise. Since

Brebach and Thodos do not give an expression for μ^* in the range $1.0 < T_R < 3.5$, a Sutherland-type formula was fitted to the above expressions at the points $T_R = 1.0$ and $T_R = 3.5$ with the result

$$\frac{\mu^*}{\mu^*_{T_c}} = \frac{1.7884 \quad T_R^{1.5}}{0.7884 + T_R} \qquad (1.0 \leq T_R \leq 3.5) \qquad (8)$$

The viscosity obtained from this relation seems to fit the data shown by Brebach and Thodos to better than 0.1 percent in the range $1.0 \leq T_R \leq 3.5$. The viscosity obtained using the appropriate expressions given above for the three temperature ranges is shown in Figure 11.

High Density. Pressures higher than atmospheric are accounted for by a density-dependent correction to the viscosity at atmospheric pressure (μ^*) as given by the above expressions. This correction, obtained by fitting the nitrogen data shown by Brebach and Thodos to an accuracy of a few percent, is given by

$$\mu - \mu^* = .01198 \, \rho + .06410 \rho^2 \qquad (.01 \leq \rho \leq .35 g/cm^3) \qquad (9)$$

where μ and μ^* are expressed in centipoises and ρ in g/cm^3. The upper limit on the density range is dictated by the accuracy of the fit but is sufficient for present purposes*. The lower limit coincides with that of the data given but is sufficient also. For example, in the nozzle design calculations, the density of $.01 g/cm^3$ occurs at temperatures greater than 370°K. At this temperature and density, the viscosity correction is 0.6 percent and can be neglected.

The density-dependent correction to the viscosity discussed in the previous paragraph is non-negative. Thus, it does not account for the decrease in viscosity for pressures much less than atmospheric as shown in Figures 7 or 9 of reference (13). However, in the present

---

*The upper limit on equation (9) exceeds the highest supply density (Mach 20 case) by 30 percent. For cold wall nozzles, the local density at the wall can exceed the supply density. For the present nozzles, this probably does not occur, but at worst may occur only in the very beginning of the inlet section where its effects can be neglected.

calculations, the temperature-pressure combinations occurring are such that no correction of this type is needed.

Application of Formulas. The viscosities required for the turbulent boundary layer calculations were obtained using equations (6), (7), and (8) for the viscosity at atmospheric pressure (μ^*). For densities less than .01g/cm^3 (.0194 slug/ft^3), the required viscosity is equal to μ^*. For densities greater than .01g/cm^3, the density-dependent correction given by equation (9) is also used. For the sake of continuity, the viscosity at the lower temperatures is obtained from the Brebach-Thodos expression (equation (6)) rather than from the Lennard-Jones (6-12) expression (equation (3) or (4)) which yields viscosities about 2 percent lower than the Brebach-Thodos expression over the range 30-80°K. Thus, the Reynolds numbers near the nozzle exit obtained from the boundary layer calculation will be about 2 percent lower than those expected on the basis of Figure 9.

NOZZLE OPERATING CONDITIONS

SUPPLY CONDITIONS FOR CONDENSATION THRESHOLD OPERATION

Given the conditions along Din's condensation line, the corresponding nozzle supply (heater vessel) conditions can be calculated using Woolley's computer program. Since the expansion process in the nozzle is assumed to be isentropic, the supply entropy is given by Figure 5 or Table 1. Then, for a particular condensation-line temperature, the supply enthalpy h_0 can be calculated from

$$\frac{h_0}{R} = \frac{h}{R} + \frac{M^2 a^2}{2R} \tag{10}$$

using the desired Mach number and the condensation-line enthalpy and sound speed obtained either from Figures 6 and 7 or from Table 1. For each supply enthalpy-entropy pair, the remaining supply conditions can now be calculated using Woolley's computer program. The resulting supply pressure variations with condensation-line temperature are shown

in Figure 12 for selected Mach numbers between 10 and 20. The corresponding supply temperatures and densities are shown in Figures 13 and 14, respectively. For convenience, in Figure 15 the supply pressure is shown in terms of the Reynolds number per foot at the nozzle exit.

CHOICE OF NOZZLE SUPPLY AND TEST-SECTION CONDITIONS

The particular choice of supply and test conditions represents a compromise between a number of desirable but conflicting features. Consideration was given to such factors as test duration, Reynolds number capability, heater size and strength, nozzle size, pumping and vacuum requirements, and others, in order to find the optimum operating conditions which could be attained within the limitations of the allocated funds. Figures 16, 17, and 18, relating the supply pressure, Reynolds number, mass flow rate, volume flow rate in the supply vessel, and the nozzle core diameter, were made to simplify the search for the optimum operating conditions at Mach number 10, 15, and 20, respectively.* The nozzle supply and test section conditions resulting from this compromise are listed in Table 2.

ACCURACY OF NITROGEN PROPERTIES AT SUPPLY CONDITIONS

The thermodynamic properties of nitrogen obtained from Woolley's computer program become increasingly inaccurate at very high densities because only two coefficients are used in the compressibility equation (equation (1)). Figure 1 showed that, given the supply pressure and temperature, the calculated density is quite accurate. However, for the nozzle design computations, the properties must be calculated at constant entropy. To determine the accuracy of the properties for such computations, a more complete comparison was made with the tabulated results of Brahinsky and Neel (reference (3)). To avoid the need for interpolations in both the entropy and temperature, the comparison was made at the design entropy and at the temperature in Brahinsky's tabulations nearest to the design supply temperature. The results of this

---

*Similar figures for these and other Mach numbers can be prepared from the data given in Figures 8, 9, 12, and 14.

9

comparison, given in the table below , show that the nitrogen properties obtained from Woolley's program are sufficiently accurate for the nozzle design computations. Positive percent differences indicate that Woolley's values are greater than those obtained from Brahinsky and Neel.

Mach Number	10	15	20
Entropy (S/R)	21.44	22.15	23.74
Temperature (supply) °K	1030	1843	2800
Temperature (comparison) °K	1000	1800	2800
Pressure difference %	-0.39	-0.11	-0.59
Density difference %	-0.28	-1.16	-1.52
Enthalpy difference %	-0.16	-0.28	0.05
Sound Speed difference %	-0.07	0.59	1.10
Compressibility difference %	-0.17	0.10	0.92

INVISCID CORE CALCULATION

ISENTROPIC EXPANSION FROM SUPPLY CONDITIONS

At the chosen nozzle supply conditions, the properties of the nitrogen test gas will differ substantially from the properties of an ideal gas because of pressure and temperature effects. Thus, the "real gas" properties of nitrogen must be taken into account in the calculation of the nozzle contours. Since the nitrogen is assumed to remain in local thermodynamic equilibrium, the expansion process is isentropic. The nitrogen properties can then be calculated and tabulated before beginning the nozzle contour calculations, greatly simplifying both calculations.

The nitrogen properties for the isentropic expansion from the chosen supply conditions to the test section conditions were calculated using Woolley's equilibrium thermodynamic properties computer program mentioned earlier. Choosing entropy and temperature as the independent variables for Woolley's program, the necessary nitrogen properties were calculated using the supply entropy together with temperatures ranging from the supply temperature to just below the test section

temperature. Since a constant temperature difference becomes a larger percentage difference at the lower temperatures, the temperature interval was decreased as the test section temperature was approached. The temperature intervals used in various temperature ranges are tabulated in Table 3 for the three nozzles.

Woolley's computer program was modified slightly so that the desired nitrogen properties were punched into cards. These cards were then read into a small computer program which transforms Woolley's properties and writes the results onto magnetic tape in the form required by the method of characteristics program used for the inviscid core calculations in the supersonic flow region.

SELECTION OF FLOW REGIONS FOR CALCULATION PURPOSES

The inviscid flow in the throat region of a supersonic nozzle can be divided into the four regions indicated in the following sketch. Region I represents the subsonic flow region upstream of the curved sonic line AA'. Region IV represents the supersonic flow region downstream of a characteristic line CC'
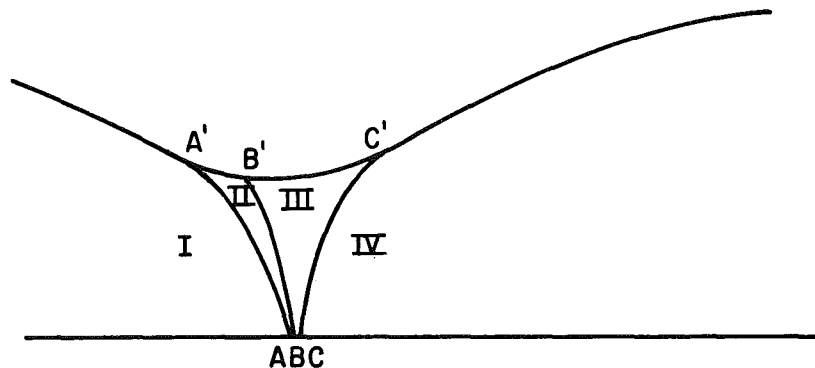
which starts an arbitrary, small distance downstream of the sonic point on the nozzle centerline and proceeds further downstream as the distance from the centerline increases. The supersonic flow region upstream of the characteristic CC' is divided into Regions II and III by some characteristic BB' of the family opposite to that of CC'. The characteristic BB' represents a limit upstream of which the method

of characteristics cannot be used effectively. Thus, the flow in Region III can be calculated by the method of characteristics.

The flow in Region II must be calculated by some other method, such as a series expansion method. Since such methods have not yet been developed for high-temperature, high-pressure gases, the flow in Region II is not calculated but treated in an approximate way as discussed in the subsonic flow section following. Although the flow in Region III can be calculated by the method of characteristics, the region is so small that it is treated in the same approximate way as Region II. For example, for the Mach number 10 and 15 nozzles, the point C' is less than one-quarter inch downstream of the sonic point A. For the Mach number 20 nozzle, the distance is less than one-tenth of an inch. For the present nozzles, there is little likelihood that the contours could be machined accurately enough to make the more exact calculation worthwhile.

For practical purposes, the inviscid flow through the nozzle can now be treated in two parts: The supersonic flow region downstream of some characteristic CC' and the combined subsonic flow and throat regions upstream of CC'.

SUPERSONIC FLOW REGION

A method of characteristics procedure for calculating the inviscid core contour in the supersonic flow region downstream of some characteristic such as CC' (see sketch, page 11) for uniform flow nozzles was presented in reference (14). The equations given are applicable to the isentropic flow of real and ideal gases through two-dimensional or axisymmetric nozzles. A FORTRAN IV computer program applying this procedure to the flow of air through axisymmetric nozzles was presented in reference (15) under the name Axisymmetric Core Program (ACP). The ACP program is written in such a way that the gas properties enter the program in the form of tabulated data read from an input tape. Thus, the program can be used unchanged for any gas for which an isentropic expansion has been calculated and stored on tape in the proper form. The utility program mentioned in a previous section was used to transform the isentropic flow data obtained from Woolley's program and store the results on tape in the form required for the ACP program.

The procedure incorporated into the ACP program requires the specification of the Mach number distribution along the nozzle centerline from the sonic point to the beginning of the uniform flow region near the nozzle exit. Initial calculations showed that the two centerline Mach number distribution formulas included in the program as given in reference (15) were unsuitable for use in the Mach number 15 and 20 nozzles. For forty-foot long nozzles at these Mach numbers, the included Mach number formulas lead to a large radius of curvature at the nozzle throat if the maximum expansion angle is kept under 12 degrees. Since the heat transfer rates near the throat are very high, such long narrow throat regions present a considerable design problem.

To decrease the throat radius of curvature and consequently the throat heating problem, a third centerline Mach number distribution formula was added to the ACP program. This formula is actually a composite using the Mach number distribution corresponding to radial flow with two patching distributions, one from the sonic point to the start of the radial flow region, and one from the radial flow region to the beginning of the uniform flow region*. Use of this Mach number distribution allowed the radius of curvature to be decreased significantly to 5.4 inches (6 throat diameters) and 2.6 inches (8 throat diameters) for the Mach number 15 and 20 nozzles, respectively. Although this increased the peak heat transfer at the nozzle throat, it reduced the total heat transfer to the throat region and decreased the length of the region that had to be cooled. Moreover, the nozzle throat region now became easier to machine to the desired accuracy.

SUBSONIC FLOW AND THROAT REGION

The calculation of the flow in the subsonic portion of the nozzle for a high-temperature, high-pressure gas is very difficult at best. The same is true for much of the small region of supersonic flow in the throat region (Regions II and III of sketch, page 11) not included in the method of characteristics calculation mentioned in the last

---

*Details of this third centerline Mach number distribution, its derivation, instructions for its use, and the changes made to ACP program are presented in Appendix A.

section. Consequently, the flow in the subsonic flow and throat regions has been approximated by using a one-dimensional flow analysis. A fourth-degree polynomial in x (axial distance from sonic point) is used to define the inviscid core contour in these regions. Previously a polynomial was used to define the nozzle wall contour in these regions. The present approach eliminates the sensitivity of the boundary layer calculation in the supersonic flow region to the choice of initial parameters. Moreover, although the present approach does not necessarily lead to a more accurate wall contour, the inviscid core contour, the boundary layer, and, thus, the nozzle wall contour are each on a firmer theoretical basis than previously.

The five constants in the fourth-degree polynomial are determined by specifying the length of the subsonic inlet and the radius and slope at the upstream end of the inlet, then matching at the throat (x = 0) the radius, slope (= 0), and curvature obtained from the characteristics calculation. The inlet is shown schematically in the following sketch.
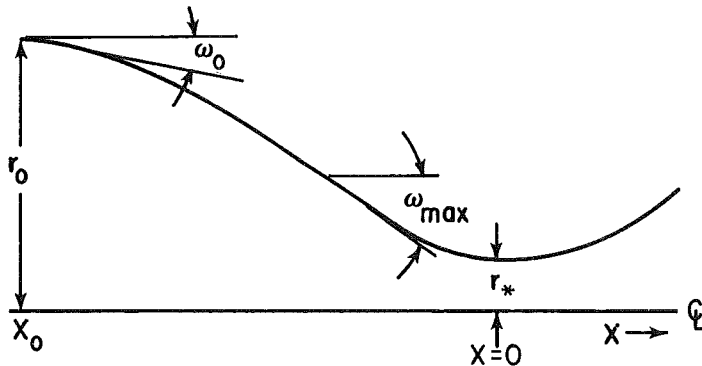
The inviscid core radius at the throat r_* is obtained from one-dimensional mass flow considerations and is supplied by the ACP characteristics calculation. The curvature (actually the second derivative r_*") at the throat is obtained from a second-degree polynomial (quadratic) fitted with zero slope at the throat to the throat radius r_* and the radius r_1 of the characteristics contour at some point x_1. The inlet length x_o ($x_o < 0$) and its upstream radius r_o and slope r_o' (= tan ω_o) are chosen to suit the particular application. For the present

nozzles, the radius r_o and slope r_o' were chosen, then the inlet length x_o was varied until the maximum slope of the inlet was about $-30°$. The inviscid core contour in the subsonic inlet is found from the polynomial

$$r = Ax^4 + Bx^3 + Cx^2 + Dx + E \qquad (11)$$

where

$$A = \frac{x_o(Cx_o + r_o') - 3(r_o - r_*)}{x_o^4} \qquad (12)$$

$$B = \frac{4(r_o - r_*) - x_o(2Cx_o + r_o')}{x_o^3} \qquad (13)$$

$$C = \frac{r_1 - r_*}{x_1^2} \qquad (14)$$

$$D = 0 \qquad (15)$$

$$E = r_* \qquad (16)$$

The inlet area ratio is given by

$$\frac{A}{A_*} = \left(\frac{r}{r_*}\right)^2 \qquad (17)$$

Since the flow in the subsonic inlet and the throat region is assumed to be one-dimensional, flow variables at various locations can be obtained from the isentropic expansion calculated earlier, once the area ratio is known. However, it is then necessary to interpolate six different flow variables (pressure, density, enthalpy, compressibility, sound speed and Mach number) at each location in the inlet. Unless this is done very carefully, the consistency between the flow variables

will be lost at the higher area ratios where the variables approach
their supply values asymptotically. To avoid this problem, it was
decided to invert the polynomial and find the location corresponding
to each area ratio tabulated in the isentropic expansion. The inversion
of the polynomial was carried out using the Newton-Raphson iteration
technique and proceeding from the throat upstream to the beginning of
the inlet.

The inviscid core contour in the supersonic portion of the nozzle
is obtained in dimensionless form by the method of characteristics
program and can be scaled to any exit diameter desired. This scaling
is usually done in the boundary layer program. The calculation of the
core contour for the subsonic flow and throat region is best done in
dimensional form and consequently has been incorporated into the
boundary layer program. This eliminates the need for a separate
program and simplifies the data input into the boundary layer program.
Since the subsonic portion of the isentropic expansion table input into
the characteristics program does not end up on the output tape, the
subsonic data is read into the boundary layer program on cards. A
program which punches the subsonic portion of the isentropic expansion
tape onto cards in the proper form is given in Appendix B. Selected
coordinates of the inviscid core contour for the three nozzles are
included in Table 4.

TURBULENT BOUNDARY LAYER CALCULATION

GENERAL THEORETICAL APPROACH

After the contour of the inviscid core has been determined, it
must be corrected in order to account for the growth of the boundary
layer on the nozzle wall. This correction was made by adding to the
inviscid core contour the displacement thickness determined using the
real gas turbulent boundary layer calculation method presented by
Tetervin in reference (16). In addition to an empirical skin friction
law and an integral momentum equation valid for thick as well as thin
boundary layers, Tetervin's method utilizes an integral moment-of-
momentum equation to calculate the momentum thickness, skin friction,

and a parameter which determines the shape of the velocity profile. From these quantities the required displacement and boundary layer thicknesses are obtained. Vector addition of the displacement thickness to the inviscid core contour then gives the contour of the nozzle wall.

A FORTRAN IV computer program was developed to apply Tetervin's turbulent boundary layer method to the present nozzle design calculations. The program as developed can be used for air or nitrogen and is compatible with the method of characteristics program of reference (15) which was used to compute the supersonic portion of the inviscid core contour. For convenience, the calculation of the subsonic portion of the inviscid core contour described in the preceding section was incorporated into the boundary layer program. The user has the option to omit the inlet core calculation and begin the boundary layer calculations at or downstream of the nozzle throat. The program and directions for its use are given in Appendix C. In the present calculations, the subsonic inviscid core option was utilized. Then the turbulent boundary layer growth was computed from the beginning of the subsonic inlet to the exit of the nozzle using the empirical Spalding-Chi skin friction law (reference (17)) and the Brebach-Thodos viscosity correlation for nitrogen discussed previously.

BASIC EQUATIONS AND MODIFICATIONS

The basic equations used are Tetervin's equations (38) to (41), (45), (51) to (54), (59), and (61). With the exception of the equations for A_0, B_0, and dH_i/dx, the equations are programmed as Tetervin gives them. Using Tetervin's notation and defining

$$\Sigma_1 = \int_0^1 \left(\frac{\rho_e}{\rho} - 1 \right) \frac{d\bar{Y}}{\Delta} = \int_0^1 \frac{\rho_e}{\rho} \frac{d\bar{Y}}{\Delta} - 1 \qquad (18)$$

$$\Sigma_2 = \int_0^1 \left(\frac{\rho_e}{\rho} - 1 \right) \frac{\bar{Y}}{\Delta} \frac{d\bar{Y}}{\Delta} = \int_0^1 \frac{\rho_e}{\rho} \frac{\bar{Y}}{\Delta} \frac{d\bar{Y}}{\Delta} - \frac{1}{2} \qquad (19)$$

17

A_o and B_o can be written as

$$A_o = \frac{u_e^2}{2h_o} \frac{1}{H_i+1} - 1 + \frac{h_e}{h_o}\left(\Sigma_2 + \frac{1}{2}\right) \tag{20}$$

$$B_o = \frac{u_e^2}{2h_o} \frac{1}{H_i} - 1 + \frac{h_e}{h_o}\left(\Sigma_1 + 1\right) \tag{21}$$

Tetervin concluded that the most reasonable variation of H_i with x resulted when the shear stress ratio τ/τ_w was taken equal to unity across the entire boundary layer. Moreover, the most plausible results were obtained when the first (H_i^2-1) in the equation for dH_i/dx was replaced by $(H_i^2 - H_{i_f}^2)$ with H_{i_f} assumed equal to its untransformed counterpart H_{u_f}. Combining these results and defining

$$F(x) \equiv -\left(\frac{1}{u_e}\frac{du_e}{dx} + \frac{1}{2\frac{h_o}{h_e}}\frac{d\frac{h_o}{h_e}}{dx}\right)\frac{h_e}{h_o} = \left(\frac{1}{2h_e}\frac{dh_e}{dx} - \frac{1}{u_e}\frac{du_e}{dx}\right)\frac{h_e}{h_o} \tag{22}$$

the equation for dH_i/dx for the nonporous wall ($v_w = 0$) case is obtained in the form

$$\frac{dH_i}{dx} = F(x)H_i(H_i+1)^2\left[\frac{H_i-1}{2} + H_i\Sigma_1 - (H_i+1)\Sigma_2\right] - \frac{C_f}{2}\frac{H_i^2-H_{i_f}^2}{\theta} \tag{23}$$

In the derivation of his equations, Tetervin uses the coordinates x and y to designate distances along and normal to the wall upon which the boundary layer is growing. For the nozzle calculations, it is more convenient and desirable to use distances measured along the nozzle centerline rather than along the nozzle wall. The derivative with respect to distance s_w (Tetervin's x) along the nozzle wall is related to the derivative with respect to distance x along the nozzle

centerline by the cosine of the wall angle α, i.e.

$$\frac{d}{dx} = \frac{ds_w}{dx} \frac{d}{ds_w} = \frac{1}{\cos \alpha} \frac{d}{ds_w} \tag{24}$$

Thus, Tetervin's differential equations for the momentum thickness θ_r and the transformed shape factor H_i (in the modified form given in the preceding paragraph) are obtained in terms of the desired center-line derivatives by multiplying through by $\frac{ds_w}{dx}$.

AUXILIARY RELATIONS

Wall Temperature. The turbulent boundary layer on the nozzle wall can be significantly affected by heat transfer to or from the nozzle wall. To uncouple the boundary layer development from the in-depth temperature response of the nozzle wall, eliminating the need for detailed knowledge of the wall construction and material properties, the wall surface temperature distribution is prescribed. Upstream of the nozzle throat, the wall temperature is taken to be constant, equal to the throat wall temperature. Downstream of the throat ($x = 0$), the temperature distribution is given by

$$T_w(x) = Ae^{-(Bx)^C} + D \tag{25}$$

The constants in this relation are determined by specifying the temperature of the nozzle wall at the nozzle throat, at the nozzle exit, and at two intermediate points. For the present nozzles, the throat wall temperature was taken to be approximately three-fourths of the supply temperature. The exit wall temperature was taken to be 300°K, approximately room temperature. The intermediate points and temperatures chosen are indicated in Figure 19 which shows the resulting wall temperature distributions for the three nozzles. Although this procedure is rather arbitrary, it should be kept in mind that, especially in the throat region and upstream, the nozzle wall which was initially near room temperature will be heated to nearly adiabatic wall conditions (zero heat transfer). Thus, for short test durations, the

processes are essentially time-dependent, so any steady-state wall temperature calculation is also rather arbitrary. The form of equation (25) for T_w is based on the assumption that, because of convective heating, the wall temperature is greatest at the nozzle throat and decreases continuously toward the nozzle exit. Other options available in the computer program as given in Appendix C are for a constant wall temperature throughout the nozzle and for adiabatic wall conditions.

Skin Friction. No single skin friction law seems to give good results for the wide range of flow conditions that can occur in hypersonic nozzles. The Ludwieg-Tillmann law (reference (18)) includes the effect of profile shape, but for compressible flows must be used with the reference enthalpy method (reference (19)). However, as Tetervin points out in his discussion, the reference enthalpy method can give skin friction coefficients that are much too large for very cool walls, i.e., for walls for which the gas enthalpy at the wall (h_w) is much less than the adiabatic wall enthalpy (h_{aw}). On the other hand, the Spalding-Chi skin friction law does not account for the effect of profile shape, but does seem to give fairly accurate results when h_w/h_{aw} is small. For the present calculations, the dependence on h_w/h_{aw} was considered the more important, so the Spalding-Chi law has been used. However, as these two skin friction laws tend to complement each other, both have been incorporated into the computer program.

Prandtl Number. The variation of the Prandtl number is difficult to calculate for most gases and conditions of interest in nozzle design. Consequently, a constant value of Prandtl number Pr equal to .72 has been used in the present calculations and incorporated into the computer program. The use of a constant Prandtl number results in constant values for such Prandtl number related quantities as the recovery factor and the Reynolds analogy factor. Thus,

$$\text{recovery factor} \equiv \frac{h_{aw} - h_e}{h_o - h_e} = Pr^{1/3} = .89628 \tag{26}$$

where h is the gas enthalpy and the subscripts aw, e, and o refer to

20

adiabatic wall, edge of the boundary layer, and supply conditions, respectively. Also, following Colburn,

$$\text{Reynolds analogy factor} \equiv \frac{St}{C_f/2} = Pr^{-2/3} = 1.2448 \qquad (27)$$

where St is the Stanton number and C_f the skin friction coefficient.

GAS PROPERTIES

The gas properties necessary for the boundary layer calculation are made available to the computer program in three ways. The supply and throat conditions and most of the necessary conditions along the edge of the boundary layer for the portion of the nozzle downstream of the throat are input from the tape produced by the Axisymmetric Core Program (ACP) discussed previously. The corresponding conditions for the nozzle portion upstream of the throat are input from cards as described in Appendix C. In addition to these constant entropy properties, the density distribution through the boundary layer, the viscosity at the edge of the boundary layer, and the enthalpy (or temperature for the adiabatic wall case) and viscosity at the wall are needed to complete the calculations. Thus, expressions for calculating these quantities must be incorporated into the computer program.

Since the available expressions often are not in terms of the desired variables, some procedure, usually iterative, must be used with the expressions to obtain the desired results. For example, the pressure through the boundary layer is assumed to be constant, equal to the known value p_e at the edge of the boundary layer. The enthalpy distribution through the boundary layer is calculated from the Crocco relation using the velocity distribution. Thus, the most natural variables for calculating the required density distribution are the pressure p ($=p_e$) and the enthalpy h. In functional form this may be written as $\rho(p, h)$. If an expression of the form $h(p, \rho)$ is used (as in the case of air), then an iterative procedure must be used which, from an initial guess for the density ρ, calculates h, and corrects ρ based on the difference between the desired and calculated values of h, repeating this procedure until the desired degree of convergence is

attained. If, on the other hand, an expression of the form h(T, ρ) is available (as in the case of nitrogen), then a different iterative procedure, this one involving the equation of state p (T, ρ), is needed. Since the available expressions for air and nitrogen differ and require different supporting procedures to achieve the desired results, the two cases will be discussed separately.

Nitrogen. It was pointed out in the preceding paragraphs that expressions must be incorporated into the computer program for calculating needed gas properties not input from cards or tape. For nitrogen, the expressions used are

$$p = \rho Z R T \tag{28}$$

$$\frac{h}{R} = (Z + \frac{5}{2}) \, T + \frac{\Theta}{\exp \, (\frac{\Theta}{T}) \, -1} \tag{29}$$

$$Z = \begin{cases} 1 & (X = \log_{10} (\frac{\rho}{\rho_{ST}}) \leq 0) \\ \\ 1 + .00482 X^2 e^X & (0 \leq X \leq 2.3) \end{cases} \tag{30}$$

where $\Theta = 3390°K$ and $\rho_{ST} = 2.423516 \times 10^{-3}$ slugs/ft^3. The expression for the compressibility Z was developed by Harris (reference (20)) using the thermodynamic data of Lewis and Neel (references (21) and (22)) and is valid for pressures up to 1000 atmospheres and temperatures up to 3000°K. For most applications this range is adequate. The pressure in the inlet and throat regions of the Mach 20 nozzle and in part of the Mach 15 inlet exceeds 1000 atmospheres, but in these regions the boundary layer is thin and the contour somewhat arbitrary. For these reasons, no attempt was made to extend the range to higher pressures.

Given the pressure p (=p_e) and the enthalpy h, these equations can be solved using the Newton-Raphson technique to obtain the density,

temperature, and compressibility.   This procedure is used to calculate
the density distribution through the boundary layer, the viscosities
at the edge of the boundary layer and at the wall (using equations (6)
to (9)), and the wall temperature for the case of an adiabatic wall.
The same equations can be solved, given the pressure and wall tem-
perature, by another, slightly different, Newton-Raphson procedure to
find the enthalpy at the wall.

Air. Air properties required for the boundary layer calculation,
but not input into the program from cards or tape, must be calculated
from appropriate expressions incorporated into the program.   To
calculate the density distribution in the boundary layer from the
pressure p ($=p_e$) and enthalpy h, i.e., to calculate $\rho(p,h)$, a form of
Newton's rule of false position is used with an expression for enthalpy
of the functional form $h(p,\rho)$.   Beginning with an initial guess for ρ,
the procedure is repeated until the desired degree of convergence is
attained.   The expression for $h(p,\rho)$ plus another for the compressibility
Z in the form $Z(p,\rho)$ were given originally by Grabau (reference (23))
and were corrected, evaluated, and presented as the subroutines ENTHLP
and COMP in reference (24).   The use of these enthalpy and compres-
sibility expressions together with the equation of state allows the
wall temperature for the case of an adiabatic wall to be calculated
from the pressure and enthalpy.

The wall enthalpy could be calculated from the pressure and tem-
perature using these expressions, but the procedure is rather involved.
Since the supply pressures for air nozzles are moderate and the wall
temperatures are not too high, the enthalpy is assumed to be a function
of temperature only and calculated from

$$\frac{h}{RT} = 3.48 + \frac{3.3175 \times 10^{-4} \ (T-499.17)}{1-\exp[-.012287 \ (T-499.17)]} \tag{31}$$

This expression is a fit to the ideal gas properties (pressure effects
neglected) of air and is good for temperatures in degrees Kelvin up to
approximately 2000°K.   The remaining quantities needed, the viscosities

at the wall and at the edge of the boundary layer, are calculated from fits of the form $\mu(p,h)$ to the viscosity data of Hansen (reference (25)).

RESULTS AND DISCUSSION

The more important results of the calculations of the nitrogen properties, the isentropic expansion, and the inviscid core contour have been presented in earlier sections of this report. In reference (16), Tetervin presented and discussed in detail most of the results of the boundary layer calculations for the three nozzles. Therefore, in.this section, only the remaining aspects of the boundary layer calculation and the final nozzle contours are considered.

INITIAL INPUT CHOICES

Before the boundary layer calculations can be carried out, several choices must be made from the options available. For the computer program as given in Appendix C, the user must decide whether to use the Spalding-Chi or the Ludwieg-Tillmann skin friction law, whether to use adiabatic wall conditions or a prescribed wall temperature distribution, whether to include the calculation of the subsonic inlet, and which numerical method to use to integrate the differential equations. The user must then specify certain input data appropriate to the choice of options being used, e.g., the wall temperature at four locations if the variable wall temperature distribution is being used, or the length and initial radius and slope of the subsonic inlet, if it is being included. For the present nozzle calculations, the Spalding-Chi skin friction law was used, the variable wall temperature distributions shown in Figure 19 were prescribed, and the subsonic inlet calculations were included.

The numerical integration of the differential equations for the momentum thickness θ_r and the shape factor H_i was performed using the utility subroutine FNOL2 (reference (26)) in the predictor-corrector mode. To begin the integration, values of θ_r and H_i had to be

24

specified at the initial station. These values can be specified arbitrarily. Alternatively, H_i can be obtained by setting it equal to the flat plate value H_{i_f} calculated from Tetervin's equation (61) using the specified value of θ_r. This procedure eliminates the need for specifying the initial value of H_i and was used in the present calculations.

If the boundary layer calculation is started at the nozzle throat position, the choice of the initial values for θ_r and H_i affect the calculated boundary layer thicknesses downstream of the throat, possibly all the way to the nozzle exit. However, by beginning the calculation upstream of the throat, this effect can be reduced. In particular, this effect can be minimized by beginning the calculation at the start of the subsonic inlet. This result is the major justification for including the approximate treatment of the subsonic inlet described earlier. For each of the present nozzles, the subsonic inlet calculation was included to minimize the effect of the initial value of θ_r. Figure 20 shows the variation of θ_r in the inlet for initial values differing by two orders of magnitude for the Mach number 15 nozzle. The curves converge to a single minimum value just upstream of the nozzle throat. The same behavior is observed for H_i. Thus, the boundary layer calculation downstream of the nozzle throat is independent of the choice of initial value for θ_r within a rather wide range. Moreover, in the upstream end of the inlet, the boundary layer is very thin compared to the inlet radius, so that the changes in the nozzle wall contour in this region are negligibly small. Thus, the calculated wall contour for the entire nozzle is unaffected by the initial value chosen for θ_r.

Values of the various parameters and initial values used in the final calculations are given in Table 5.

PRINCIPAL DIMENSIONS OF NOZZLES

In order to be able to use the same test cell and model support system for all three nozzles, the three nozzles were designed to have the same exit diameters and the same lengths. Preliminary calculations indicated that a throat-to-exit length of about 45 feet and an exit

diameter of about 5 feet would be necessary for the Mach number 20
nozzle if the maximum expansion half-angle was to be kept near 12 degrees.
It was decided to design the nozzles such that at a distance of 40 feet
from the nozzle throat the nozzle diameter would be five feet. The
remaining portion of the nozzle would not be fabricated, since, if
this cut-off portion was not too long, the nozzle performance would
not be appreciably affected. The optimum cut-off point is that axial
location at which the boundary layer enters the uniform flow region
inside the Mach cone (see Figure 21). Downstream of this point, the
usable test core decreases, even though the cross-sectional area of
the nozzle continues to increase. Iterations, involving the boundary
layer program only, were sufficient to produce contours for the Mach
number 10 and 15 nozzles in which the optimum cut-off point occurred
within a few inches of the 40-foot station. These small differences
made further iterations unnecessary and the nozzles were cut off at
the 40-foot station. The length of the cut-off portion was 1.72 and
1.50 feet for the Mach number 10 and 15 nozzles, respectively. For
the Mach number 20 nozzle, the optimum cut-off point occurred at the
44.7-foot station or 1.88 feet from the end of the uncut nozzle. To
move the optimum cut-off point nearer to the 40-foot station would
require a maximum expansion angle appreciably greater than any considered
acceptable. For this reason, no further iterations were made for the
Mach number 20 nozzle. The diameter of the usable test core was 18.2
inches at the 40-foot cut-off point rather than the 21 inches which
would have been attained if the nozzle had been cut off at the optimum
location. The seven square foot test core thus obtained was considered
adequate. Principal dimensions of the three nozzles are given in
Table 6.

HEAT TRANSFER TO NOZZLE WALL

The boundary layer calculations mentioned above assume that the
nozzle wall temperature can be kept to a reasonable level without
transpiration or film cooling. This can be done for the Mach number
10 nozzle and probably for the Mach number 15 nozzle. However, heat
transfer calculations for the Mach number 20 nozzle show that massive

transpiration or film cooling may be necessary in the throat region
to keep the nozzle throat from eroding early in the test run.

The nozzle wall temperature distributions for the three nozzles
were assumed to vary from about three-fourths of the supply temperature
at the throat to 300°K at the nozzle exit as shown in Figure 19. The
convective heat transfer from the boundary layer to the nozzle wall
was calculated from the skin friction coefficient using Colburn's
form of Reynolds analogy as given by equation (27). The throat region
is of particular interest since the heat transfer rate is much higher
there than elsewhere in the nozzle. For example, for the assumed
temperature distributions, the peak heat transfer rate occurs near the
nozzle throat and is 770, 19600, and 46000 BTU/ft^{2}sec for the Mach
number 10, 15, and 20 nozzles, respectively, while at the nozzle exit,
the rate is about 1 BTU/ft^{2}sec for each nozzle. The heat transfer
rates in the throat regions of the three nozzles are shown in Figure
22.

For the Mach number 20 nozzle, the heat transfer rate is extremely
high in the throat region. Coupling this with the rather high value
of 1600°K assumed for the wall temperature and the high static pressure
of 1560 atmospheres at the throat, it is clear that the design of the
throat region for the Mach 20 nozzle presents a formidable problem.
A number of possible solutions to this problem are now being studied.

The heat transfer rate in the throat region of the Mach number
15 nozzle is down to one-half the rate for the Mach 20 nozzle. More-
over, the wall temperature and pressure levels are more moderate. Thus,
there is a reasonable chance that the throat section of the Mach 15
nozzle can be made to have an acceptable lifetime without using trans-
piration or film cooling.

Conditions of temperature, pressure, and heat transfer rate in the
throat region of the Mach 10 nozzle are sufficiently moderate that no
transpiration or film cooling is needed.

NOZZLE WALL CONTOURS

The boundary layer program discussed in this report does not
include provisions for using transpiration or film cooling to protect

the nozzle during operation. In the previous section, it was shown
that the Mach number 10 and 15 nozzles can probably operate acceptably
without such cooling, but most likely the Mach number 20 nozzle can
not. Since calculations which take such cooling into account have not
yet been completed, the Mach 20 nozzle has been calculated with the
present program as though no such cooling is required. Thus, the
Mach 20 nozzle contour is considered preliminary at the present time.

During the boundary layer calculation, the inviscid core contour
(subsonic and supersonic flow regions) is automatically corrected to
account for the effect of the boundary layer and the resulting nozzle
contour is tabulated. However, inspection of the calculated contours
showed that each of the three nozzle contours required some smoothing
in a small portion of the subsonic inlet. The reason for this has not
yet been determined. The corrected nozzle wall radii, obtained by
hand-smoothing the calculated results, are given in Table 7 for each of
the nozzles. Selected coordinates of the nozzle contour, together
with the coordinates of the inviscid core, are presented in Table 4.

After the Mach number 10 and 15 nozzle contours had been submitted
for fabrication, an error was found in the boundary layer computer
program. The density-dependent correction to the viscosity was being
calculated incorrectly. The program was corrected and the contours
recalculated. The nozzle wall was found to be displaced outward
slightly with the increase in radius ranging from zero at the throat
to about one-thousandth of an inch at the nozzle exit. Since these
changes were quite small compared to the uncertainties inherent in the
boundary layer calculation, the changes were neglected. Thus, the
nozzle wall coordinates given in Table 4 are the uncorrected values
used in making the nozzles. The computer program given in Appendix C
is the corrected version.

ACCURACY OF CONTOURS

The nozzle design method presented in this report is subject to
error from a number of sources.

1.   The assumption of local thermodynamic equilibrium and
isentropic flow in the inviscid core is only an approximation.

For the present nozzle design calculations, this approximation should be very good. However, for more severe flow conditions and extreme nozzle shapes, this approximation can lead to errors which are no longer negligibly small.

2.   Inaccuracies in the gas properties for the flow conditions occurring in the nozzle can affect the calculated results substantially. Again, for the present nozzles, errors from this source are considered small.

3.   The assumptions of one-dimensional flow in the subsonic inlet and throat regions can cause errors which are very difficult to evaluate. For perfect gas flows, better (but more complicated) methods can be used. However, these methods are not yet applicable to flows in which high temperature or high pressure effects on the gas properties are important.

4.   Errors introduced by the method of characteristics procedure used for the supersonic inviscid core and by the numerical procedures used in the boundary layer program can be reduced to a negligible level by using sufficiently small step sizes. There is no difficulty here.

5.   The main sources of error in the boundary layer calculation seem to be in the accuracy of the available skin friction laws for highly cooled walls and in the assumed wall temperature distribution. For the design of nozzles (such as the present ones) having thick boundary layers, the errors in the boundary layer calculation probably outweigh all others. Fortunately, as Tetervin points out, errors in the boundary layer calculation are at least partially self-correcting. If, for example, the boundary layer is actually thicker than calculated, the flow Mach number will be less than the design value. However, for the same nozzle geometry and supply conditions, a decrease in the Mach number leads to a decrease in the boundary layer thickness which in turn acts to increase the Mach number. Thus, any tendency of the boundary layer to thicken or thin, brings about a change in the Mach number distribution which opposes that tendency. This equilibrium-like behavior tends to reduce the effect of inaccuracies in the boundary layer calculation.

6.   The final source of error in the nozzle contour is in the
actual fabrication of the nozzle. Prohibitive costs and the
capabilities of available equipment combine to limit the accuracy
with which the nozzle can be made.

In summary, the final nozzle is subject to errors from a number
of sources. Some of these errors can be made negligibly small, but
others cannot, at least at the present time. Because of the number
and nature of the possible errors, it is not possible to obtain a
numerical estimate of the overall accuracy of the calculated nozzle
contours. However, the three nozzle contours presented and discussed
in this report are considered to be as accurate as is now possible to
make them.

CONCLUDING REMARKS

The procedure used in designing axisymmetric nozzles for the NOL
Hypervelocity Wind Tunnel and the resulting nozzles for operation at
Mach numbers 10, 15, and 20 with high-density nitrogen and thick
turbulent boundary layers have been presented in detail.

The NOL Hypervelocity Wind Tunnel is a unique aerodynamic facility
for hypersonic research and developmental testing. The capability of
achieving a high Mach number - high Reynolds number flow with
relatively long run times and large model sizes will permit the
accumulation of large amounts of aerodynamic test data, greatly
facilitating the design and development of advanced, high-performance
re-entry vehicles.

This report summarizing the nozzle design for the facility is
one of a series. Other technical reports documenting various aspects
of the aerodynamic and mechanical design, tunnel performance, and
test results obtained will be published as the material becomes
available.

REFERENCES

1. Glowacki, W.J., Harris, E.L., Lobb, R.K., and Schlesinger, M.I., "The NOL Hypervelocity Wind Tunnel," AIAA Preprint 71-253, Albuquerque, N.M., Mar 1971

2. Harris, E.L., and Glowacki, W.J., "NOL Hypervelocity Wind Tunnel Report No. 1: Aerodynamic Design," NOLTR 71-5, Feb 1971

3. Brahinsky, H.S., and Neel, C.A., "Tables of Equilibrium Thermodynamic Properties of Nitrogen," AEDC-TR-69-126, Aug 1969

4. Din, F., Thermodynamic Functions of Gases, Vol. 3, Methane, Nitrogen, Ethane, Butterworths, London, 1961

5. Hilsenrath, J., and Klein, M., "Tables of Thermodynamic Properties of Nitrogen in Chemical Equilibrium Including Second Virial Corrections from 2000°K to 15,000°K," AEDC-TDR-63-162, Mar 1964

6. Smith, C.E., Jr., "Thermodynamic Properties of Nitrogen," LMSC L-90-62-111, Dec 1962

7. Grabau, M., and Brahinsky, H.S., "Thermodynamic Properties of Nitrogen from 300 to 5000°K and from 1 to 1000 Amagats," AEDC-TR-66-69, Aug 1966

8. Humphrey, R.L., and Piper, C.H., "Mollier Diagram for Nitrogen," NOLTR 67-32, 14 Mar 1967

9. Woolley, H.S., National Bureau of Standards, Gaithersburg, Maryland, private communication

10. Enkenhus, K.R., and Culotta, S., "Formulas for the Thermodynamic Properties of Dense Nitrogen," AIAA Journal, Vol. 7, No. 6, p 1188, Jun 1969

11. Daum, F.L., and Gyarmathy, G., "Condensation of Air and Nitrogen in Hypersonic Wind Tunnels," AIAA Journal, Vol. 6, No. 3, p. 458, Mar 1968

12. Hirschfelder, J.O., Curtiss, C.F., and Bird, R.B., Molecular Theory of Gases and Liquids, John Wiley and Sons, New York, 1954

13. Brebach, W.J. and Thodos, G., "Viscosity - Reduced State Correlation for Diatomic Gases," Ind. Eng. Chem, Vol. 50, No. 7, p 1095, July 1958

14. Conlan, J. and Trytten, G., "A High Speed Computer Technique to Determine Nozzle Contours for Supersonic Wind Tunnels," NOLTR 64-81, May 1964

15. Glowacki, W.J., "FORTRAN IV (IBM 7090) Program for the Design of Contoured Axisymmetric Nozzles for High Temperature Air," NOLTR 64-219, Feb 1965

16. Tetervin, N., "NOL Hypervelocity Wind Tunnel, Report No. 3: Theoretical Analysis of the Boundary Layer in the Nozzles," NOLTR 71-7, Feb 1971

17. Spalding, D.B. and Chi, S.W., "The Drag of a Compressible Turbulent Boundary Layer on a Smooth Flat Plate With and Without Heat Transfer," J. Fluid Mech., Vol. 18, pp 117-143, 1964

18. Ludwieg, H. and Tillmann, W., "Investigations of the Wall-Shearing Stress in Turbulent Boundary Layers," NACA TM 1285, May 1950

19. Eckert, E. R. G., "Survey on Heat Transfer at High Speeds," Aero Research Laboratory, WADC Technical Report 54-70, 1954

20. Harris, E.L., U.S. Naval Ordnance Laboratory, White Oak, Maryland, unpublished work

21. Lewis, C.H., and Neel, C.A., "Specific Heat and Speed of Sound Data for Imperfect Nitrogen - II. T = 100 to 2200°K," AEDC-TDR-64-114, Jun 1964

22. Lewis, C.H., and Neel, C.A., "Specific Heat and Speed of Sound Data for Imperfect Nitrogen - I. T = 2000 to 15,000°K," AEDC-TDR-64-113, Jun 1964

23. Grabau, M., "A Method of Forming Continuous Empirical Equations for the Thermodynamic Properties of Air From Ambient Temperatures to 15,000°K, With Applications," AEDC-TN-59-102, Aug 1959

24. Glowacki, W.J. and Maher, E.F., "IBM 7090 Subroutines for Real Gas Properties of High Temperature Air," NOLTR 63-223, Dec 1963

25. Hansen, C.F., "Approximation for the Thermodynamic and Transport Properties of High Temperature Air," NACA TN 4150, Mar 1958

26. Linnekin, J.S. and Belliveau, L.J., "FNOL2, A FORTRAN (IBM 7090) Subroutine for the Solution of Ordinary Differential Equations with Automatic Adjustment of the Interval of Integration," NOLTR 63-171, Jul 1963

27. Ames Research Staff, "Equations, Tables, and Charts for Compressible Flow," NACA Report 1135, 1953

TABLE 1

NITROGEN PROPERTIES AT CONDENSATION THRESHOLD

TEMPERATURE °K	PRESSURE ATM	DENSITY AMAGAT	ENTROPY*	ENTHALPY BTU/LBM	SOUND SPEED FT/SEC	VISCOSITY LBM/FT SEC
40.0	9.0327E-05	6.1656E-04	25.312	17.755	422.96	1.8470E-06
40.1	9.5210E-05	6.4826E-04	25.269	17.800	423.46	1.8514E-06
40.2	1.0033E-04	6.8140E-04	25.225	17.845	424.01	1.8557E-06
40.3	1.0568E-04	7.1600E-04	25.182	17.889	424.54	1.8601E-06
40.4	1.1129E-04	7.5214E-04	25.139	17.934	425.07	1.8644E-06
40.5	1.1716E-04	7.8986E-04	25.096	17.979	425.59	1.8688E-06
40.6	1.2331E-04	8.2923E-04	25.053	18.023	426.12	1.8731E-06
40.7	1.2973E-04	8.7030E-04	25.011	18.068	426.64	1.8775E-06
40.8	1.3645E-04	9.1315E-04	24.969	18.113	427.16	1.8818E-06
40.9	1.4348E-04	9.5783E-04	24.928	18.158	427.69	1.8862E-06
41.0	1.5082E-04	1.0044E-03	24.886	18.202	428.21	1.8906E-06
41.1	1.5850E-04	1.0529E-03	24.845	18.247	428.73	1.8949E-06
41.2	1.6652E-04	1.1035E-03	24.804	18.292	429.25	1.8993E-06
41.3	1.7489E-04	1.1562E-03	24.764	18.336	429.77	1.9037E-06
41.4	1.8363E-04	1.2111E-03	24.723	18.381	430.29	1.9080E-06
41.5	1.9276E-04	1.2682E-03	24.683	18.426	430.81	1.9124E-06
41.6	2.0228E-04	1.3277E-03	24.643	18.470	431.33	1.9168E-06
41.7	2.1222E-04	1.3895E-03	24.604	18.515	431.85	1.9212E-06
41.8	2.2258E-04	1.4539E-03	24.565	18.560	432.36	1.9256E-06
41.9	2.3339E-04	1.5209E-03	24.526	18.604	432.88	1.9299E-06
42.0	2.4465E-04	1.5905E-03	24.487	18.649	433.39	1.9343E-06
42.1	2.5639E-04	1.6628E-03	24.448	18.694	433.91	1.9387E-06
42.2	2.6862E-04	1.7380E-03	24.410	18.738	434.42	1.9431E-06
42.3	2.8137E-04	1.8162E-03	24.372	18.783	434.94	1.9475E-06
42.4	2.9464E-04	1.8974E-03	24.334	18.828	435.45	1.9519E-06
42.5	3.0846E-04	1.9817E-03	24.296	18.872	435.96	1.9563E-06
42.6	3.2284E-04	2.0693E-03	24.259	18.917	436.48	1.9607E-06
42.7	3.3781E-04	2.1601E-03	24.222	18.961	436.99	1.9651E-06
42.8	3.5339E-04	2.2545E-03	24.185	19.006	437.50	1.9695E-06
42.9	3.6959E-04	2.3523E-03	24.148	19.051	438.01	1.9739E-06
43.0	3.8644E-04	2.4539E-03	24.112	19.095	438.52	1.9783E-06
43.1	4.0396E-04	2.5592E-03	24.076	19.140	439.03	1.9827E-06
43.2	4.2217E-04	2.6683E-03	24.040	19.185	439.53	1.9871E-06
43.3	4.4109E-04	2.7815E-03	24.004	19.229	440.04	1.9915E-06
43.4	4.6076E-04	2.8988E-03	23.968	19.274	440.55	1.9959E-06
43.5	4.8118E-04	3.0204E-03	23.933	19.319	441.06	2.0004E-06
43.6	5.0240E-04	3.1463E-03	23.898	19.363	441.56	2.0048E-06
43.7	5.2443E-04	3.2768E-03	23.863	19.408	442.07	2.0092E-06
43.8	5.4729E-04	3.4119E-03	23.828	19.453	442.57	2.0136E-06
43.9	5.7103E-04	3.5517E-03	23.794	19.497	443.07	2.0180E-06
44.0	5.9566E-04	3.6965E-03	23.760	19.542	443.56	2.0225E-06
44.1	6.2121E-04	3.8464E-03	23.726	19.586	444.08	2.0269E-06
44.2	6.4771E-04	4.0014E-03	23.692	19.631	444.58	2.0313E-06
44.3	6.7519E-04	4.1618E-03	23.658	19.676	445.08	2.0357E-06
44.4	7.0368E-04	4.3277E-03	23.625	19.720	445.59	2.0402E-06
44.5	7.3322E-04	4.4992E-03	23.591	19.765	446.09	2.0446E-06
44.6	7.6383E-04	4.6765E-03	23.558	19.810	446.59	2.0490E-06
44.7	7.9555E-04	4.8599E-03	23.526	19.854	447.09	2.0535E-06
44.8	8.2841E-04	5.0493E-03	23.493	19.899	447.58	2.0579E-06
44.9	8.6244E-04	5.2451E-03	23.460	19.943	448.08	2.0624E-06

* ENTROPY S EXPRESSED IN DIMENSIONLESS FORM S/R

TABLE 1 (CONT.)

TEMPERATURE °K	PRESSURE ATM	DENSITY AMAGAT	ENTROPY*	ENTHALPY BTU/LBM	SOUND SPEED FT/SEC	VISCOSITY LBM/FT SEC
45.0	8.9769E-04	5.4473E-03	23.428	19.988	448.58	2.0668E-06
45.1	9.3418E-04	5.6562E-03	23.396	20.033	449.08	2.0713E-06
45.2	9.7195E-04	5.8719E-03	23.364	20.077	449.57	2.0757E-06
45.3	1.0110E-03	6.0946E-03	23.332	20.122	450.07	2.0802E-06
45.4	1.0515E-03	6.3245E-03	23.301	20.166	450.56	2.0846E-06
45.5	1.0933E-03	6.5618E-03	23.270	20.211	451.06	2.0891E-06
45.6	1.1366E-03	6.8067E-03	23.238	20.256	451.55	2.0935E-06
45.7	1.1814E-03	7.0593E-03	23.207	20.300	452.04	2.0980E-06
45.8	1.2277E-03	7.3199E-03	23.177	20.345	452.54	2.1024E-06
45.9	1.2755E-03	7.5887E-03	23.146	20.389	453.03	2.1069E-06
46.0	1.3250E-03	7.8659E-03	23.116	20.434	453.52	2.1114E-06
46.1	1.3761E-03	8.1517E-03	23.085	20.479	454.01	2.1158E-06
46.2	1.4289E-03	8.4462E-03	23.055	20.523	454.50	2.1203E-06
46.3	1.4835E-03	8.7498E-03	23.025	20.568	454.99	2.1247E-06
46.4	1.5398E-03	9.0626E-03	22.996	20.612	455.48	2.1292E-06
46.5	1.5980E-03	9.3850E-03	22.966	20.657	455.97	2.1337E-06
46.6	1.6581E-03	9.7170E-03	22.937	20.701	456.46	2.1382E-06
46.7	1.7201E-03	1.0059E-02	22.907	20.746	456.94	2.1426E-06
46.8	1.7841E-03	1.0411E-02	22.878	20.791	457.43	2.1471E-06
46.9	1.8502E-03	1.0774E-02	22.849	20.835	457.92	2.1516E-06
47.0	1.9183E-03	1.1147E-02	22.821	20.880	458.40	2.1561E-06
47.1	1.9887E-03	1.1531E-02	22.792	20.924	458.89	2.1605E-06
47.2	2.0612E-03	1.1926E-02	22.764	20.969	459.37	2.1650E-06
47.3	2.1360E-03	1.2333E-02	22.735	21.013	459.86	2.1695E-06
47.4	2.2131E-03	1.2752E-02	22.707	21.058	460.34	2.1740E-06
47.5	2.2926E-03	1.3182E-02	22.679	21.102	460.82	2.1785E-06
47.6	2.3746E-03	1.3625E-02	22.652	21.147	461.30	2.1830E-06
47.7	2.4591E-03	1.4080E-02	22.624	21.191	461.79	2.1875E-06
47.8	2.5461E-03	1.4548E-02	22.596	21.236	462.27	2.1920E-06
47.9	2.6358E-03	1.5029E-02	22.569	21.280	462.75	2.1965E-06
48.0	2.7282E-03	1.5524E-02	22.542	21.325	463.23	2.2010E-06
48.1	2.8234E-03	1.6032E-02	22.515	21.369	463.71	2.2054E-06
48.2	2.9214E-03	1.6555E-02	22.488	21.414	464.19	2.2099E-06
48.3	3.0223E-03	1.7091E-02	22.461	21.458	464.66	2.2144E-06
48.4	3.1262E-03	1.7642E-02	22.435	21.503	465.14	2.2190E-06
48.5	3.2331E-03	1.8208E-02	22.408	21.547	465.62	2.2235E-06
48.6	3.3431E-03	1.8789E-02	22.382	21.592	466.09	2.2280E-06
48.7	3.4564E-03	1.9386E-02	22.356	21.636	466.57	2.2325E-06
48.8	3.5729E-03	1.9999E-02	22.330	21.681	467.05	2.2370E-06
48.9	3.6928E-03	2.0628E-02	22.304	21.725	467.52	2.2415E-06
49.0	3.8161E-03	2.1274E-02	22.278	21.770	467.99	2.2460E-06
49.1	3.9429E-03	2.1936E-02	22.253	21.814	468.47	2.2505E-06
49.2	4.0733E-03	2.2616E-02	22.227	21.858	468.94	2.2550E-06
49.3	4.2073E-03	2.3313E-02	22.202	21.903	469.41	2.2595E-06
49.4	4.3451E-03	2.4028E-02	22.177	21.947	469.88	2.2641E-06
49.5	4.4868E-03	2.4762E-02	22.152	21.992	470.36	2.2686E-06
49.6	4.6324E-03	2.5514E-02	22.127	22.036	470.83	2.2731E-06
49.7	4.7820E-03	2.6285E-02	22.102	22.080	471.30	2.2776E-06
49.8	4.9357E-03	2.7076E-02	22.078	22.125	471.77	2.2821E-06
49.9	5.0936E-03	2.7887E-02	22.053	22.169	472.23	2.2867E-06

* ENTROPY S EXPRESSED IN DIMENSIONLESS FORM S/R

TABLE 1 (CONT.)

TEMPERATURE °K	PRESSURE ATM	DENSITY AMAGAT	ENTROPY*	ENTHALPY BTU/LBM	SOUND SPEED FT/SEC	VISCOSITY LBM/FT SEC
50.0	5.2558E-03	2.8718E-02	22.029	22.214	472.70	2.2912E-06
50.1	5.4223E-03	2.9569E-02	22.004	22.258	473.17	2.2957E-06
50.2	5.5934E-03	3.0442E-02	21.980	22.302	473.64	2.3003E-06
50.3	5.7690E-03	3.1336E-02	21.956	22.347	474.11	2.3048E-06
50.4	5.9493E-03	3.2252E-02	21.933	22.391	474.57	2.3093E-06
50.5	6.1344E-03	3.3190E-02	21.909	22.435	475.04	2.3138E-06
50.6	6.3244E-03	3.4150E-02	21.885	22.480	475.50	2.3184E-06
50.7	6.5193E-03	3.5134E-02	21.862	22.524	475.97	2.3229E-06
50.8	6.7193E-03	3.6142E-02	21.838	22.568	476.43	2.3275E-06
50.9	6.9245E-03	3.7173E-02	21.815	22.613	476.89	2.3320E-06
51.0	7.1350E-03	3.8229E-02	21.792	22.657	477.36	2.3365E-06
51.1	7.3509E-03	3.9309E-02	21.769	22.701	477.82	2.3411E-06
51.2	7.5724E-03	4.0415E-02	21.746	22.746	478.28	2.3456E-06
51.3	7.7995E-03	4.1547E-02	21.723	22.790	478.74	2.3502E-06
51.4	8.0323E-03	4.2705E-02	21.701	22.834	479.20	2.3547E-06
51.5	8.2710E-03	4.3889E-02	21.678	22.878	479.66	2.3593E-06
51.6	8.5157E-03	4.5101E-02	21.656	22.923	480.12	2.3638E-06
51.7	8.7665E-03	4.6341E-02	21.634	22.967	480.58	2.3684E-06
51.8	9.0235E-03	4.7608E-02	21.611	23.011	481.03	2.3729E-06
51.9	9.2868E-03	4.8905E-02	21.589	23.055	481.49	2.3775E-06
52.0	9.5567E-03	5.0230E-02	21.567	23.100	481.95	2.3820E-06
52.1	9.8331E-03	5.1585E-02	21.546	23.144	482.41	2.3866E-06
52.2	1.0116E-02	5.2970E-02	21.524	23.188	482.86	2.3911E-06
52.3	1.0406E-02	5.4386E-02	21.502	23.232	483.32	2.3957E-06
52.4	1.0703E-02	5.5833E-02	21.481	23.276	483.77	2.4002E-06
52.5	1.1007E-02	5.7312E-02	21.459	23.320	484.22	2.4048E-06
52.6	1.1319E-02	5.8823E-02	21.438	23.365	484.68	2.4094E-06
52.7	1.1638E-02	6.0366E-02	21.417	23.409	485.13	2.4139E-06
52.8	1.1964E-02	6.1943E-02	21.396	23.453	485.58	2.4185E-06
52.9	1.2298E-02	6.3554E-02	21.375	23.497	486.03	2.4231E-06
53.0	1.2640E-02	6.5199E-02	21.354	23.541	486.48	2.4276E-06
53.1	1.2990E-02	6.6880E-02	21.333	23.585	486.94	2.4322E-06
53.2	1.3348E-02	6.8596E-02	21.313	23.629	487.38	2.4368E-06
53.3	1.3714E-02	7.0348E-02	21.292	23.673	487.83	2.4413E-06
53.4	1.4089E-02	7.2136E-02	21.272	23.717	488.28	2.4459E-06
53.5	1.4472E-02	7.3962E-02	21.251	23.762	488.73	2.4505E-06
53.6	1.4864E-02	7.5826E-02	21.231	23.806	489.18	2.4550E-06
53.7	1.5265E-02	7.7728E-02	21.211	23.850	489.62	2.4596E-06
53.8	1.5674E-02	7.9669E-02	21.191	23.894	490.07	2.4642E-06
53.9	1.6094E-02	8.1651E-02	21.171	23.938	490.52	2.4688E-06
54.0	1.6522E-02	8.3672E-02	21.151	23.982	490.96	2.4733E-06
54.1	1.6960E-02	8.5734E-02	21.131	24.026	491.40	2.4779E-06
54.2	1.7408E-02	8.7838E-02	21.112	24.070	491.85	2.4825E-06
54.3	1.7865E-02	8.9984E-02	21.092	24.113	492.29	2.4871E-06
54.4	1.8333E-02	9.2172E-02	21.073	24.157	492.73	2.4917E-06
54.5	1.8810E-02	9.4404E-02	21.053	24.201	493.18	2.4963E-06
54.6	1.9299E-02	9.6680E-02	21.034	24.245	493.62	2.5008E-06
54.7	1.9797E-02	9.9001E-02	21.015	24.289	494.06	2.5054E-06
54.8	2.0307E-02	1.0137E-01	20.996	24.333	494.50	2.5100E-06
54.9	2.0827E-02	1.0378E-01	20.977	24.377	494.94	2.5146E-06

* ENTROPY S EXPRESSED IN DIMENSIONLESS FORM S/R

TABLE 1 (CONT.)

TEMPERATURE °K	PRESSURE ATM	DENSITY AMAGAT	ENTROPY*	ENTHALPY BTU/LBM	SOUND SPEED FT/SEC	VISCOSITY LBM/FT SEC
55.0	2.1359E-02	1.0624E-01	20.958	24.421	495.38	2.5192E-06
55.1	2.1901E-02	1.0874E-01	20.939	24.465	495.81	2.5238E-06
55.2	2.2456E-02	1.1130E-01	20.920	24.508	496.25	2.5284E-06
55.3	2.3021E-02	1.1390E-01	20.902	24.552	496.69	2.5330E-06
55.4	2.3599E-02	1.1655E-01	20.883	24.596	497.13	2.5376E-06
55.5	2.4189E-02	1.1926E-01	20.865	24.640	497.56	2.5421E-06
55.6	2.4791E-02	1.2201E-01	20.846	24.684	498.00	2.5467E-06
55.7	2.5405E-02	1.2482E-01	20.828	24.727	498.43	2.5513E-06
55.8	2.6033E-02	1.2767E-01	20.810	24.771	498.86	2.5559E-06
55.9	2.6672E-02	1.3058E-01	20.792	24.815	499.30	2.5605E-06
56.0	2.7325E-02	1.3355E-01	20.774	24.858	499.73	2.5651E-06
56.1	2.7992E-02	1.3657E-01	20.756	24.902	500.16	2.5697E-06
56.2	2.8671E-02	1.3964E-01	20.738	24.946	500.59	2.5743E-06
56.3	2.9365E-02	1.4277E-01	20.720	24.989	501.03	2.5789E-06
56.4	3.0072E-02	1.4596E-01	20.702	25.033	501.46	2.5835E-06
56.5	3.0793E-02	1.4920E-01	20.685	25.077	501.89	2.5881E-06
56.6	3.1529E-02	1.5250E-01	20.667	25.120	502.31	2.5927E-06
56.7	3.2279E-02	1.5586E-01	20.650	25.164	502.74	2.5974E-06
56.8	3.3044E-02	1.5929E-01	20.633	25.207	503.17	2.6020E-06
56.9	3.3824E-02	1.6277E-01	20.615	25.251	503.60	2.6066E-06
57.0	3.4619E-02	1.6631E-01	20.598	25.294	504.02	2.6112E-06
57.1	3.5430E-02	1.6991E-01	20.581	25.338	504.45	2.6158E-06
57.2	3.6256E-02	1.7358E-01	20.564	25.381	504.87	2.6204E-06
57.3	3.7098E-02	1.7731E-01	20.547	25.425	505.30	2.6250E-06
57.4	3.7956E-02	1.8111E-01	20.530	25.468	505.72	2.6296E-06
57.5	3.8831E-02	1.8497E-01	20.513	25.512	506.15	2.6342E-06
57.6	3.9722E-02	1.8890E-01	20.497	25.555	506.57	2.6388E-06
57.7	4.0630E-02	1.9289E-01	20.480	25.599	506.99	2.6435E-06
57.8	4.1555E-02	1.9696E-01	20.464	25.642	507.41	2.6481E-06
57.9	4.2498E-02	2.0109E-01	20.447	25.685	507.83	2.6527E-06
58.0	4.3458E-02	2.0529E-01	20.431	25.729	508.25	2.6573E-06
58.1	4.4436E-02	2.0956E-01	20.414	25.772	508.67	2.6619E-06
58.2	4.5432E-02	2.1390E-01	20.398	25.815	509.09	2.6666E-06
58.3	4.6446E-02	2.1832E-01	20.382	25.859	509.51	2.6712E-06
58.4	4.7479E-02	2.2280E-01	20.366	25.902	509.92	2.6758E-06
58.5	4.8531E-02	2.2737E-01	20.350	25.945	510.34	2.6804E-06
58.6	4.9602E-02	2.3200E-01	20.334	25.988	510.76	2.6850E-06
58.7	5.0692E-02	2.3671E-01	20.318	26.031	511.17	2.6897E-06
58.8	5.1802E-02	2.4150E-01	20.302	26.075	511.59	2.6943E-06
58.9	5.2932E-02	2.4637E-01	20.286	26.118	512.00	2.6989E-06
59.0	5.4082E-02	2.5131E-01	20.271	26.161	512.42	2.7035E-06
59.1	5.5252E-02	2.5633E-01	20.255	26.204	512.83	2.7082E-06
59.2	5.6443E-02	2.6144E-01	20.239	26.247	513.24	2.7128E-06
59.3	5.7656E-02	2.6662E-01	20.224	26.290	513.65	2.7174E-06
59.4	5.8889E-02	2.7188E-01	20.209	26.333	514.06	2.7220E-06
59.5	6.0144E-02	2.7723E-01	20.193	26.376	514.47	2.7267E-06
59.6	6.1421E-02	2.8266E-01	20.178	26.419	514.88	2.7313E-06
59.7	6.2720E-02	2.8818E-01	20.163	26.462	515.29	2.7359E-06
59.8	6.4042E-02	2.9379E-01	20.148	26.505	515.70	2.7406E-06
59.9	6.5386E-02	2.9947E-01	20.133	26.548	516.10	2.7452E-06

* ENTROPY S EXPRESSED IN DIMENSIONLESS FORM S/R

TABLE 2

NOZZLE SUPPLY AND TEST SECTION CONDITIONS

MACH NUMBER	10	15	20	
SUPPLY				
PRESSURE	430.	2365.	3110.	ATM
TEMPERATURE	1030.	1843.	2800.	°K
	1854.	3317.	5040.	°R
ENTROPY (S/R)	21.44	22.15	23.74	
ENTHALPY	492.4	1016.	1594.	BTU/LBM
DENSITY	7.721	18.68	16.92	LBM/FT^3
TEST SECTION				
PRESSURE X 10^2	1.127	0.448	.0612	ATM
TEMPERATURE	52.58	49.50	44.06	°K
	94.64	89.10	79.31	°R
DENSITY X 10^3	4.567	1.929	0.296	LBM/FT^3
VELOCITY	4846.	7055.	8877.	FT/SEC
REYNOLDS NUMBER PER FOOT X 10^6	9.2	6.0	1.3	

TABLE 3

INTERVALS USED WITH WOOLLEY'S PROGRAM

	FROM	(INTERVAL)	TO
MACH 10	450 ATM	(-1 ATM)	430 ATM
	1029.80 $^{\circ}$K	(-.05 $^{\circ}$K)	1028.50 $^{\circ}$K
	427 ATM	(-1 ATM)	420 ATM
	1020 $^{\circ}$K	(-5 $^{\circ}$K)	890 $^{\circ}$K
	890 $^{\circ}$K	(-1 $^{\circ}$K)	840 $^{\circ}$K
	840 $^{\circ}$K	(-5 $^{\circ}$K)	60. $^{\circ}$K
	60.0 $^{\circ}$K	(-.25 $^{\circ}$K)	53.0 $^{\circ}$K
	53.0 $^{\circ}$K	(-.02 $^{\circ}$K)	52.5 $^{\circ}$K
	52.5 $^{\circ}$K	(-.25 $^{\circ}$K)	40.25 $^{\circ}$K
MACH 15	2380 ATM	(-1 ATM)	2365 ATM
	1842.38 $^{\circ}$K	(-.02 $^{\circ}$K)	1840.92 $^{\circ}$K
	1840 $^{\circ}$K	(-5 $^{\circ}$K)	1600 $^{\circ}$K
	1600 $^{\circ}$K	(-1 $^{\circ}$K)	1520 $^{\circ}$K
	1520 $^{\circ}$K	(-5 $^{\circ}$K)	65.0 $^{\circ}$K
	65.0 $^{\circ}$K	(-.25 $^{\circ}$K)	50.0 $^{\circ}$K
	50.0 $^{\circ}$K	(-.02 $^{\circ}$K)	49.2 $^{\circ}$K
MACH 20	3130 ATM	(-1 ATM)	3110 ATM
	2799.51 $^{\circ}$K	(-.03 $^{\circ}$K)	2798.76 $^{\circ}$K
	3106 ATM	(-1 ATM)	3101 ATM
	2797.6 $^{\circ}$K	(-.3 $^{\circ}$K)	2790.4 $^{\circ}$K
	2790 $^{\circ}$K	(-5 $^{\circ}$K)	2400 $^{\circ}$K
	2400 $^{\circ}$K	(-1 $^{\circ}$K)	2320 $^{\circ}$K
	2320 $^{\circ}$K	(-5 $^{\circ}$K)	70.0 $^{\circ}$K
	70.0 $^{\circ}$K	(-.25 $^{\circ}$K)	45.25 $^{\circ}$K
	44.96 $^{\circ}$K	(-.02 $^{\circ}$K)	43.5 $^{\circ}$K

TABLE 4

SELECTED INVISCID CORE AND NOZZLE WALL COORDINATES

DISTANCE FROM THROAT (FT)	MACH NUMBER = 10		MACH NUMBER = 15		MACH NUMBER = 20	
	RADIUS OF WALL (FT)	RADIUS OF CORE (FT)	RADIUS OF WALL (FT)	RADIUS OF CORE (FT)	RADIUS OF WALL (FT)	RADIUS OF CORE (FT)
-.75	0.33958	0.33924				
-.70	0.33112	0.33077				
-.65	0.31348	0.31317				
-.60	0.29083	0.29057				
-.55	0.26512	0.26490				
-.50	0.23781	0.23764				
-.45	0.21092	0.21078	0.19167	0.19140		
-.40	0.18543	0.18531	0.18130	0.18106	0.16667	0.16657
-.38	0.17567		0.17406	0.17385	0.16416	0.16403
-.36	0.16633		0.16572	0.16554	0.15970	0.15955
-.34	0.15772	0.15761	0.15651	0.15635	0.15329	0.15314
-.32	0.15002	0.14991	0.14666	0.14652	0.14533	0.14519
-.30	0.14285	0.14275	0.13639	0.13627	0.13639	0.13626
-.28	0.13619	0.13608	0.12592	0.12582	0.12660	0.12648
-.26	0.13011	0.13000	0.11545	0.11536	0.11600	
-.24	0.12463	0.12452	0.10492		0.10517	
-.22	0.11975	0.11964	0.09467		0.09417	0.09409
-.20	0.11548	0.11537	0.08508		0.08306	0.08299
-.19	0.11357	0.11346	0.08067		0.07758	0.07751
-.18	0.11181	0.11170	0.07650		0.07217	0.07211
-.17	0.11019	0.11008	0.07225	0.07219	0.06685	0.06680
-.16	0.10872	0.10860	0.06842	0.06837	0.06166	0.06161
-.15	0.10738	0.10726	0.06472	0.06467	0.05662	0.05658
-.14	0.10618	0.10606	0.06124	0.06119	0.05171	0.05167
-.13	0.10511	0.10498	0.05796	0.05791	0.04706	0.04702
-.12	0.10416	0.10403	0.05489	0.05484	0.04261	0.04257
-.11	0.10333	0.10320	0.05205	0.05200	0.03838	0.03835
-.10	0.10262	0.10249	0.04944	0.04940	0.03443	0.03440
-.09	0.10202	0.10188	0.04708	0.04704	0.03075	0.03072
-.08	0.10151	0.10137	0.04497	0.04493	0.02680	0.02678
-.07	0.10110	0.10095	0.04311	0.04307	0.02429	0.02426
-.06	0.10078	0.10062	0.04151	0.04146	0.02161	0.02159
-.05	0.10052	0.10036	0.04016	0.04011	0.01928	0.01926
-.04	0.10036	0.10020	0.03906	0.03901	0.01733	0.01731
-.03	0.10024	0.10007	0.03821	0.03816	0.01578	0.01576
-.02	0.10017	0.09999	0.03761	0.03756	0.01465	0.01463
-.01	0.10014	0.09995	0.03726	0.03721	0.01396	0.01394
0.00	0.10014	0.09994	0.03715	0.03709	0.01373	0.01370
0.01	0.10016	0.09995	0.03727	0.03721	0.01395	0.01392
0.02	0.10019	0.09998	0.03761	0.03754	0.01441	0.01436
0.03	0.10023	0.10001	0.03804	0.03796	0.01517	0.01511
0.04	0.10029	0.10006	0.03859	0.03850	0.01607	0.01600

TABLE 4 (CONT.)

DISTANCE FROM THROAT (FT)	MACH NUMBER = 10		MACH NUMBER = 15		MACH NUMBER = 20	
	RADIUS OF WALL (FT)	RADIUS OF CORE (FT)	RADIUS OF WALL (FT)	RADIUS OF CORE (FT)	RADIUS OF WALL (FT)	RADIUS OF CORE (FT)
0.05	0.10035	0.10011	0.03925	0.03915	0.01716	0.01707
0.06	0.10043	0.10018	0.04000	0.03989	0.01842	0.01831
0.07	0.10052	0.10026	0.04085	0.04072	0.01985	0.01971
0.08	0.10062	0.10035	0.04177	0.04163	0.02143	0.02127
0.09	0.10073	0.10046	0.04278	0.04263	0.02317	0.02297
0.10	0.10085	0.10057	0.04387	0.04370	0.02503	0.02479
0.11	0.10098	0.10069	0.04503	0.04484	0.02699	0.02671
0.12	0.10112	0.10082	0.04626	0.04606	0.02901	0.02869
0.13	0.10127	0.10096	0.04756	0.04734	0.03108	0.03072
0.14	0.10143	0.10111	0.04893	0.04869	0.03318	0.03277
0.15	0.10160	0.10127	0.05037	0.05010	0.03530	0.03484
0.16	0.10178	0.10144	0.05186	0.05158	0.03744	0.03692
0.17	0.10197	0.10162	0.05342	0.05311	0.03959	0.03901
0.18	0.10216	0.10181	0.05503	0.05469	0.04174	0.04110
0.19	0.10237	0.10200	0.05669	0.05632	0.04390	0.04319
0.20	0.10258	0.10221	0.05839	0.05800	0.04606	0.04528
0.30	0.10516	0.10469	0.07699	0.07626	0.06755	0.06595
0.40	0.10847	0.10791	0.09677	0.09559	0.08882	0.08615
0.50	0.11246	0.11179	0.11688	0.11516	0.10996	0.10602
0.60	0.11705	0.11626	0.13709	0.13473	0.13109	0.12571
0.70	0.12221	0.12129	0.15735	0.15425	0.15226	0.14529
0.80	0.12790	0.12683	0.17762	0.17373	0.17349	0.16482
0.90	0.13409	0.13286	0.19792	0.19315	0.19471	0.18429
1.00	0.14077	0.13935	0.21823	0.21255	0.21538	0.20345
1.10	0.14791	0.14630	0.23859	0.23192	0.23559	0.22215
1.20	0.15549	0.15368	0.25897	0.25128	0.25535	0.24039
1.30	0.16352	0.16147	0.27941	0.27064	0.27467	0.25820
1.40	0.17199	0.16967	0.29988	0.28999	0.29357	0.27560
1.50	0.18087	0.17827	0.32039	0.30935	0.31209	0.29259
1.60	0.19015	0.18726	0.34066	0.32861	0.33024	0.30921
1.70	0.19985	0.19663	0.36064	0.34760	0.34803	0.32548
1.80	0.20994	0.20638	0.38033	0.36632	0.36550	0.34140
1.90	0.22041	0.21649	0.39973	0.38475	0.38264	0.35701
2.00	0.23127	0.22696	0.41882	0.40288	0.39949	0.37231
2.10	0.24251	0.23779	0.43764	0.42073	0.41604	0.38731
2.20	0.25411	0.24896	0.45617	0.43830	0.43232	0.40203
2.30	0.26607	0.26046	0.47442	0.45559	0.44834	0.41649
2.40	0.27841	0.27231	0.49242	0.47261	0.46410	0.43068
2.50	0.29107	0.28446	0.51014	0.48936	0.47963	0.44464
2.60	0.30408	0.29694	0.52762	0.50587	0.49492	0.45834
2.70	0.31740	0.30969	0.54483	0.52211	0.51000	0.47183
2.80	0.33105	0.32276	0.56182	0.53812	0.52485	0.48510

TABLE 4 (CONT.)

DISTANCE FROM THROAT (FT)	MACH NUMBER = 10		MACH NUMBER = 15		MACH NUMBER = 20	
	RADIUS OF WALL (FT)	RADIUS OF CORE (FT)	RADIUS OF WALL (FT)	RADIUS OF CORE (FT)	RADIUS OF WALL (FT)	RADIUS OF CORE (FT)
2.90	0.34497	0.33607	0.57857	0.55390	0.53949	0.49815
3.00	0.35921	0.34968	0.59509	0.56943	0.55394	0.51100
3.10	0.37370	0.36351	0.61139	0.58475	0.56819	0.52365
3.20	0.38846	0.37758	0.62748	0.59986	0.58225	0.53611
3.30	0.40345	0.39188	0.64335	0.61474	0.59613	0.54839
3.40	0.41865	0.40635	0.65902	0.62943	0.60984	0.56049
3.50	0.43407	0.42104	0.67450	0.64392	0.62338	0.57241
3.60	0.44966	0.43587	0.68978	0.65820	0.63675	0.58417
3.70	0.46539	0.45083	0.70487	0.67229	0.64997	0.59576
3.80	0.48129	0.46595	0.71979	0.68621	0.66302	0.60719
3.90	0.49730	0.48117	0.73452	0.69995	0.67593	0.61847
4.00	0.51339	0.49646	0.74908	0.71350	0.68870	0.62961
4.10	0.52958	0.51184	0.76346	0.72687	0.70131	0.64059
4.20	0.54583	0.52728	0.77769	0.74009	0.71379	0.65143
4.30	0.56211	0.54274	0.79175	0.75314	0.72614	0.66213
4.40	0.57842	0.55823	0.80564	0.76602	0.73836	0.67271
4.50	0.59476	0.57375	0.81939	0.77875	0.75044	0.68314
4.60	0.61108	0.58924	0.83299	0.79133	0.76240	0.69344
4.70	0.62738	0.60471	0.84644	0.80375	0.77424	0.70363
4.80	0.64366	0.62017	0.85974	0.81602	0.78596	0.71369
4.90	0.65991	0.63559	0.87289	0.82815	0.79757	0.72363
5.00	0.67609	0.65095	0.88592	0.84014	0.80905	0.73345
5.20	0.70829	0.68150	0.91156	0.86371	0.83170	0.75275
5.40	0.74020	0.71177	0.93668	0.88675	0.85392	0.77162
5.60	0.77175	0.74170	0.96130	0.90927	0.87573	0.79006
5.80	0.80296	0.77128	0.98542	0.93129	0.89717	0.80810
6.00	0.83370	0.80043	1.00910	0.95285	0.91821	0.82574
6.20	0.86408	0.82919	1.03234	0.97393	0.93890	0.84302
6.40	0.89398	0.85748	1.05514	0.99458	0.95925	0.85994
6.60	0.92342	0.88533	1.07752	1.01480	0.97925	0.87650
6.80	0.95240	0.91272	1.09948	1.03460	0.99894	0.89274
7.00	0.98088	0.93961	1.12104	1.05401	1.01831	0.90864
7.20	1.00890	0.96605	1.14225	1.07302	1.03739	0.92423
7.40	1.03643	0.99200	1.16309	1.09165	1.05618	0.93952
7.60	1.06348	1.01747	1.18358	1.10992	1.07469	0.95451
7.80	1.09008	1.04248	1.20372	1.12783	1.09293	0.96921
8.00	1.11619	1.06701	1.22353	1.14539	1.11091	0.98365
8.20	1.14186	1.09109	1.24303	1.16263	1.12863	0.99780
8.40	1.16710	1.11473	1.26220	1.17953	1.14610	1.01170
8.60	1.19188	1.13790	1.28106	1.19611	1.16334	1.02534
8.80	1.21625	1.16065	1.29964	1.21239	1.18037	1.03873
9.00	1.24018	1.18297	1.31791	1.22836	1.19714	1.05188

TABLE 4 (CONT.)

DISTANCE FROM THROAT (FT)	MACH NUMBER = 10		MACH NUMBER = 15		MACH NUMBER = 20	
	RADIUS OF WALL (FT)	RADIUS OF CORE (FT)	RADIUS OF WALL (FT)	RADIUS OF CORE (FT)	RADIUS OF WALL (FT)	RADIUS OF CORE (FT)
9.20	1.26369	1.20486	1.33591	1.24404	1.21370	1.06481
9.40	1.28680	1.22634	1.35363	1.25943	1.23003	1.07749
9.60	1.30953	1.24743	1.37108	1.27454	1.24612	1.08996
9.80	1.33184	1.26810	1.38827	1.28937	1.26204	1.10221
10.0	1.35378	1.28839	1.40520	1.30394	1.27777	1.11425
11.0	1.45797	1.38422	1.48624	1.37298	1.35359	1.17141
12.0	1.55363	1.47135	1.56172	1.43618	1.42510	1.22395
13.0	1.64153	1.55056	1.63216	1.49409	1.49273	1.27231
14.0	1.72237	1.62255	1.69805	1.54722	1.55684	1.31690
15.0	1.79674	1.68795	1.75977	1.59597	1.61776	1.35805
16.0	1.86518	1.74730	1.81766	1.64070	1.67574	1.39604
17.0	1.92817	1.80109	1.87200	1.68174	1.73098	1.43112
18.0	1.98614	1.84978	1.92307	1.71937	1.78369	1.46353
19.0	2.03944	1.89373	1.97108	1.75382	1.83402	1.49344
20.0	2.08844	1.93334	2.01621	1.78532	1.88212	1.52103
21.0	2.13341	1.96891	2.05865	1.81408	1.92812	1.54646
22.0	2.17465	2.00074	2.09857	1.84027	1.97212	1.56987
23.0	2.21242	2.02912	2.13608	1.86406	2.01422	1.59139
24.0	2.24693	2.05430	2.17134	1.88560	2.05451	1.61113
25.0	2.27842	2.07652	2.20446	1.90504	2.09307	1.62920
26.0	2.30708	2.09600	2.23554	1.92250	2.12997	1.64571
27.0	2.33309	2.11295	2.26469	1.93812	2.16528	1.66074
28.0	2.35663	2.12757	2.29199	1.95199	2.19905	1.67437
29.0	2.37787	2.14006	2.31754	1.96424	2.23135	1.68670
30.0	2.39696	2.15059	2.34140	1.97496	2.26222	1.69778
31.0	2.41405	2.15935	2.36366	1.98425	2.29170	1.70771
32.0	2.42928	2.16650	2.38437	1.99220	2.31984	1.71653
33.0	2.44279	2.17221	2.40360	1.99891	2.34666	1.72432
34.0	2.45471	2.17664	2.42141	2.00446	2.37222	1.73113
35.0	2.46516	2.17996	2.43784	2.00893	2.39652	1.73703
36.0	2.47428	2.18233	2.45293	2.01242	2.41960	1.74207
37.0	2.48220	2.18391	2.46672	2.01501	2.44148	1.74631
38.0	2.48903	2.18486	2.47921	2.01679	2.46217	1.74980
38.2	2.49028	2.18499	2.48155	2.01706	2.46617	1.75041
38.4	2.49149	2.18510	2.48384	2.01730	2.47012	1.75100
38.6	2.49266	2.18520	2.48607	2.01751	2.47402	1.75155
38.8	2.49380	2.18528	2.48825	2.01770	2.47787	1.75209
39.0	2.49491	2.18535	2.49038	2.01786	2.48168	1.75259
39.2	2.49599	2.18541	2.49244	2.01800	2.48544	1.75307
39.4	2.49703	2.18545	2.49445	2.01812	2.48915	1.75352
39.6	2.49805	2.18549	2.49639	2.01821	2.49282	1.75396
39.8	2.49904	2.18552	2.49825	2.01828	2.49643	1.75436
40.0	2.50000	2.18554	2.50000	2.01834	2.50000	1.75474

TABLE 5

CARD INPUT DATA FOR ACP* AND RGTBLP** PROGRAMS

MACH NUMBER 10 - ACP*

NN	IFTH	LM	LN	KK	EMT	XT	RCT	EMZP
10	0	2	0	100	10.	9.	0.	2.8

GAMA	XZ	DZX	DTX	EPSA	EPSB
1.4E+00	1.0E-03	2.0E-03	2.0E-03	5.0E-06	5.0E-06

MACH NUMBER 10 - RGTBLP**

THETA	REXIT	XPUNCH	XO	RO	OMEGAO	HI
.0003	2.185577	100.	-.75	.33924	-5.	0.

NN	LM	NFS	IP	J	LAWCF
910	2	1	1	2	1

M	TX(2)	TX(3)	TX(4)	TX(5)	TX(6)	TX(8)
2	900.	2.0	700.	10.	400.	300.

DELX	XEND	IP
.01	-.28	
.001	.02	10
.01	0.2	
.05	5.0	2
.2	999.	

MACH NUMBER 15 - ACP*

NN	IFTH	LM	LN	KK	EMT	XT	RCT	EMZP
15		2	0	100	15.	0.	0.	0.

GAMA	XZ	DZX	DTX	EPSA	EPSB
1.4E+00	1.0E-03	2.0E-03	2.0E-03	5.0E-06	5.0E-06

OMEGA	EMB	XER	RCPLUS
11.0	4.134	0.99	12.0

*   AXISYMMETRIC CORE PROGRAM (SEE REFERENCE (15))
**   REAL GAS TURBULENT BOUNDARY LAYER PROGRAM (SEE APPENDIX C)

TABLE 5 (CONT.)

MACH NUMBER 15 - RGTBLP**

THETA	REXIT	XPUNCH	XO	RO	OMEGAO	HI
.0003	2.018408	100.	-.45	.1914	-5.	0.

NN	LM	NFS	IP	J	LAWCF
915	2	1	1	2	1

M	TX(2)	TX(3)	TX(4)	TX(5)	TX(6)	TX(8)
2	1200.	2.0	900.	10.	400.	300.

DELX	XEND	IP
.01	-.28	
.001	.02	10
.01	0.2	
.05	5.0	2
.2	999.	

MACH NUMBER 20 - ACP*

NN	IFTH	LM	LN	KK	EMT	XT	RCT	EMZP
20	2	2	0	100	20.	0.	0.	0.

GAMA	XZ	DZX	DTX	EPSA	EPSB
1.4E+00	1.0E-03	2.0E-03	2.0E-03	5.0E-06	5.0E-06

OMEGA	EMB	XER	RCPLUS
11.0	4.534	0.99	16.0

MACH NUMBER 20 - RGTBLP**

THETA	REXIT	XPUNCH	XO	RO	OMEGAO	HI
.0001	1.758123	100.	-.4	.16657	-5.	0.

NN	LM	NFS	IP	J	LAWCF
920	2	1	1	2	1

M	TX(2)	TX(3)	TX(4)	TX(5)	TX(6)	TX(8)
2	1600.	2.0	1200.	5.0	800.	300.

DELX	XEND	IP
.01	-.28	
.001	.02	10
.01	0.2	
.05	5.0	2
.2	999.	

*   AXISYMMETRIC CORE PROGRAM (SEE REFERENCE (15))
**   REAL GAS TURBULENT BOUNDARY LAYER PROGRAM (SEE APPENDIX C)

TABLE 6

SELECTED NOZZLE DIMENSIONS

MACH NUMBER	10	15	20
LENGTH (FT)			
INLET	0.75	0.45	0.40
EXPANSION	40.00	40.00	40.00
TOTAL	40.75	40.45	40.40
DIAMETER (FT)			
ENTRANCE	0.679	0.383	0.333
THROAT	0.200	0.074	0.028
EXIT	5.000	5.000	5.000
CORE*	4.371	4.037	3.509
USABLE**	4.005	3.752	3.282
AREA (FT^2)			
ENTRANCE	0.3622	0.1154	0.0872
THROAT	0.0315	0.0043	0.0006
EXIT	19.635	19.635	19.635
CORE*	15.006	12.798	9.6729
USABLE**	12.596	11.059	8.4588

* INVISCID CORE MEASURED AT NOZZLE EXIT

** USABLE DIAMETER AT NOZZLE EXIT DEFINED
AS THE NOZZLE EXIT DIAMETER MINUS TWICE
THE BOUNDARY LAYER THICKNESS AT THE EXIT

TABLE 7

CORRECTED WALL RADII IN SUBSONIC INLETS

| MACH NUMBER	POINT NUMBER	DISTANCE FROM THROAT (FEET)	DISTANCE FROM THROAT (INCHES)	RADIUS OF WALL (INCHES)	RADIUS OF WALL (FEET)
10	37	-0.39	-4.68	2.166	0.18050
	38	-0.38	-4.56	2.108	0.17567
	39	-0.37	-4.44	2.052	0.17100
	40	-0.36	-4.32	1.996	0.16633
15	58	-0.24	-2.88	1.259	0.10492
	68	-0.23	-2.76	1.196	0.09967
	78	-0.22	-2.64	1.136	0.09467
	88	-0.21	-2.52	1.077	0.08975
	98	-0.20	-2.40	1.021	0.08508
	108	-0.19	-2.28	0.968	0.08067
	118	-0.18	-2.16	0.918	0.07650
20	33	-0.26	-3.12	1.392	0.11600
	43	-0.25	-3.00	1.327	0.11058
	53	-0.24	-2.88	1.262	0.10517
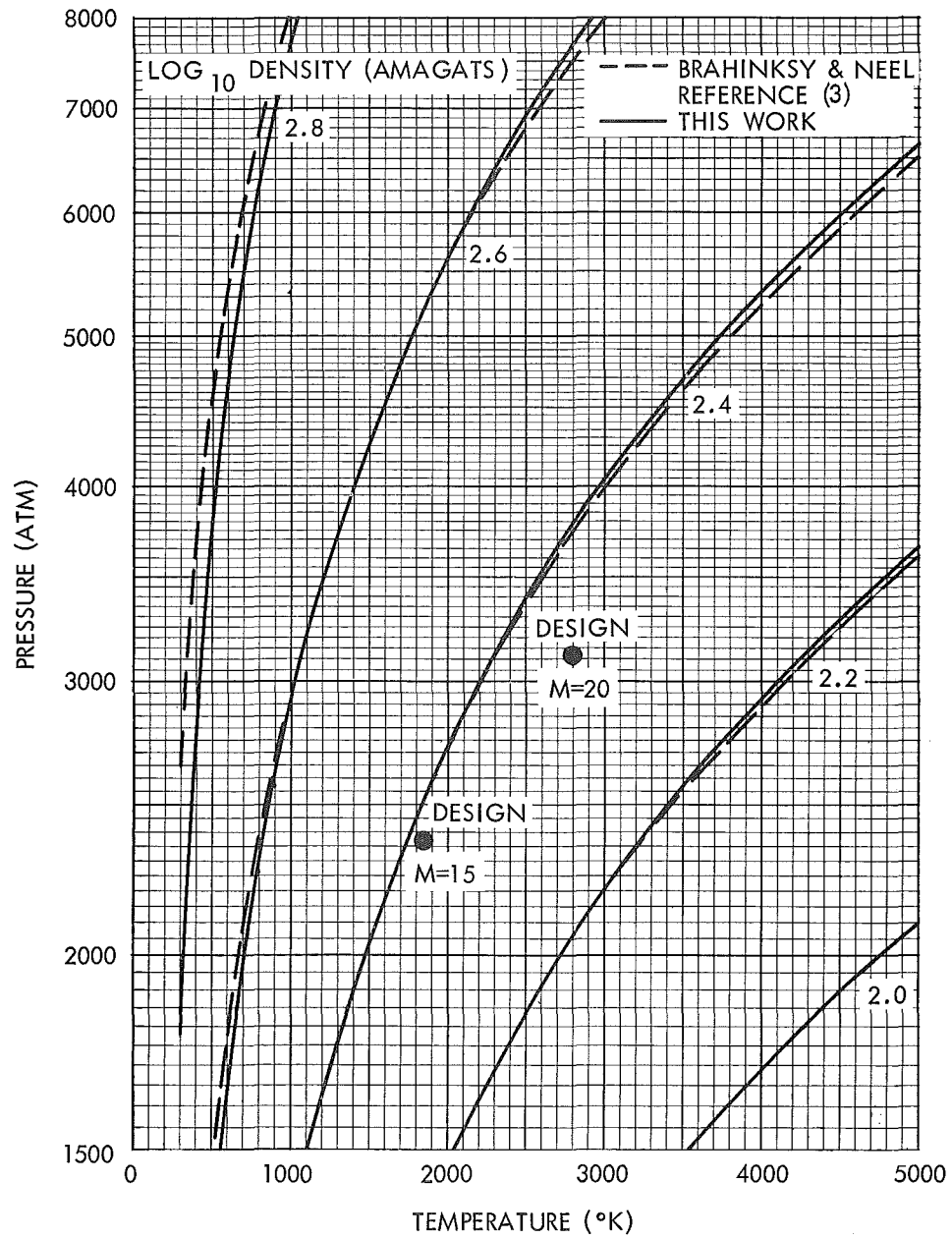
FIG. 1 COMPARISON OF PRESSURE-TEMPERATURE VARIATIONS AT HIGH DENSITIES WITH AEDC DATA TABULATIONS
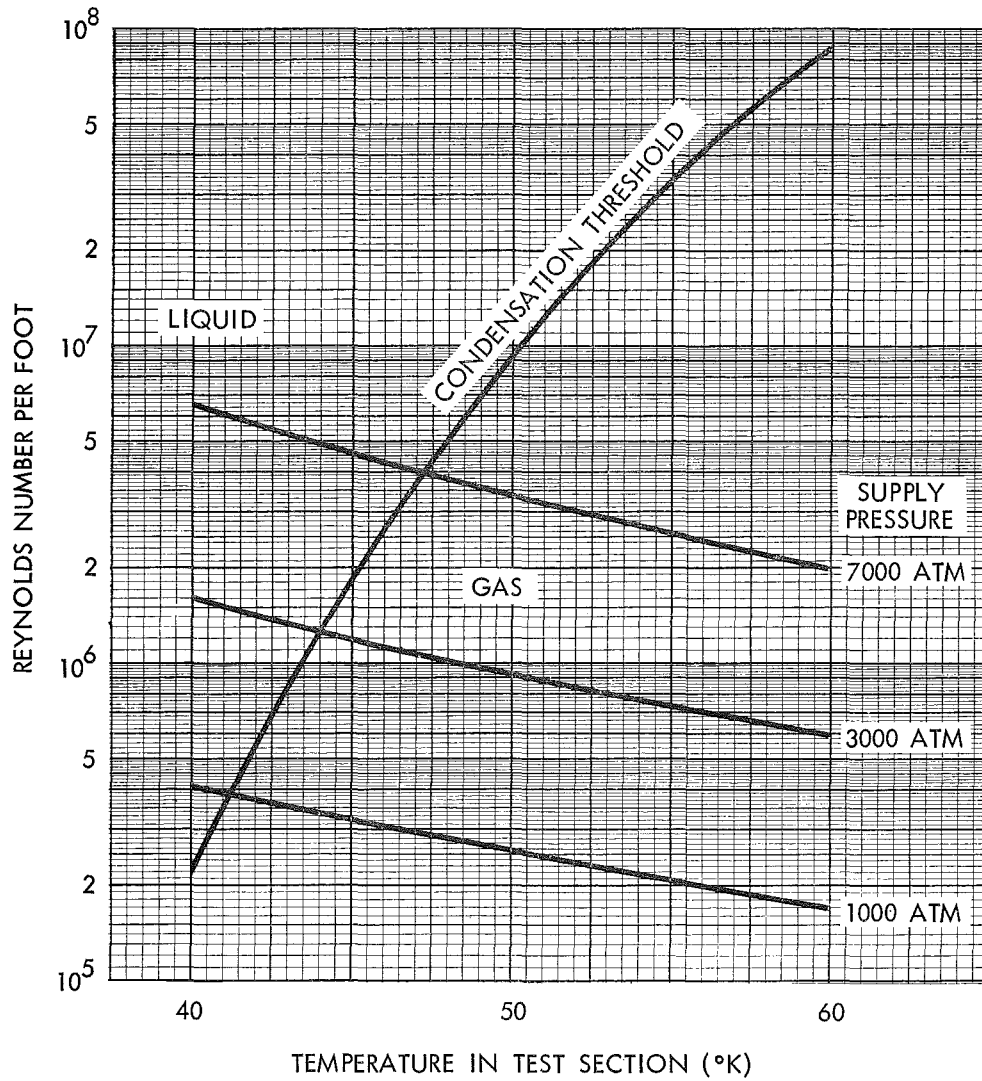
FIG. 2   VARIATION OF REYNOLDS NUMBER IN TEST SECTION WITH TEMPERATURE FOR
CONSTANT PRESSURE OR CONDENSATION THRESHOLD OPERATION AT MACH 20

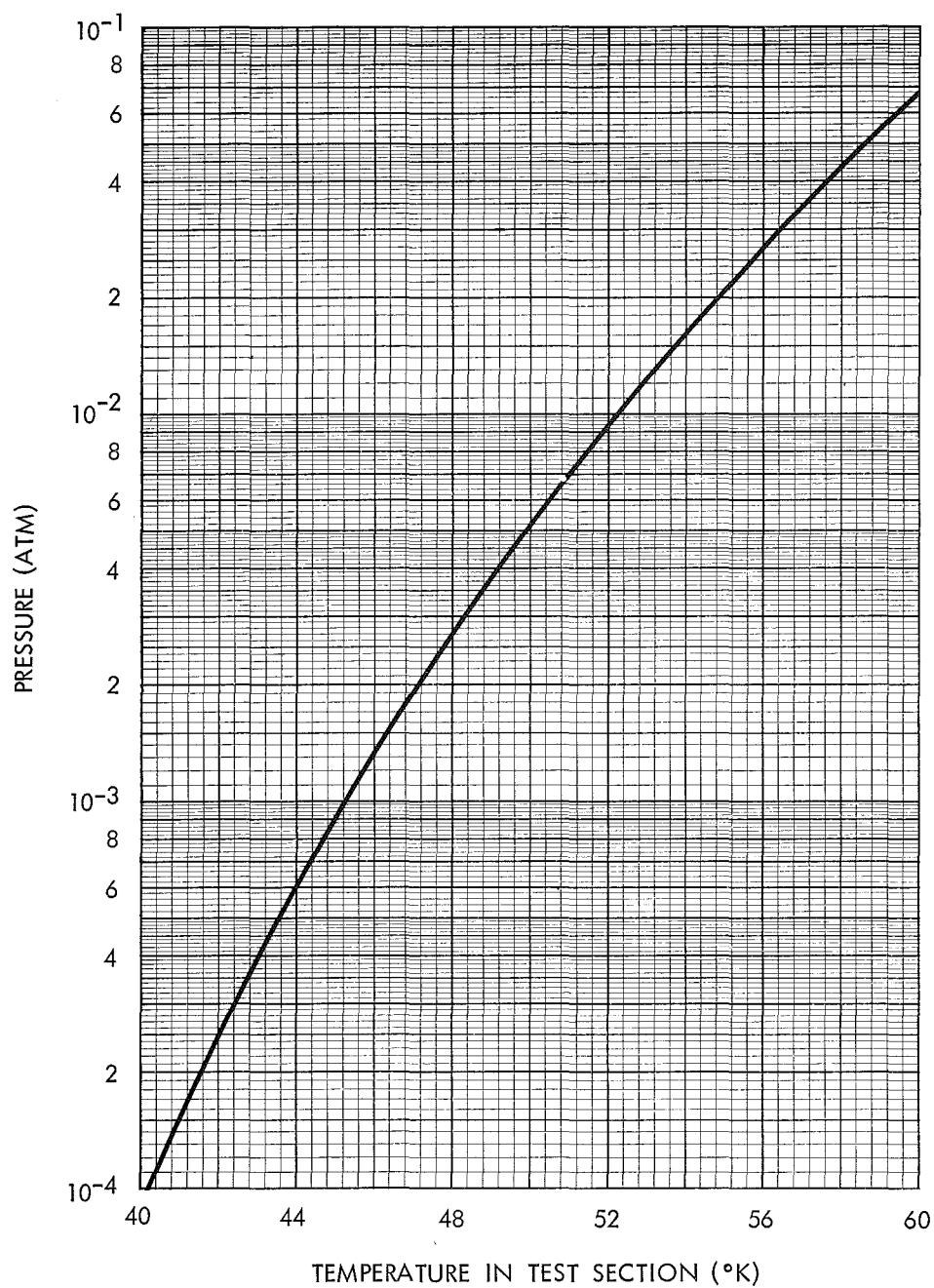FIG. 3   VARIATION OF PRESSURE IN TEST SECTION WITH TEMPERATURE FOR
CONDENSATION THRESHOLD OPERATION
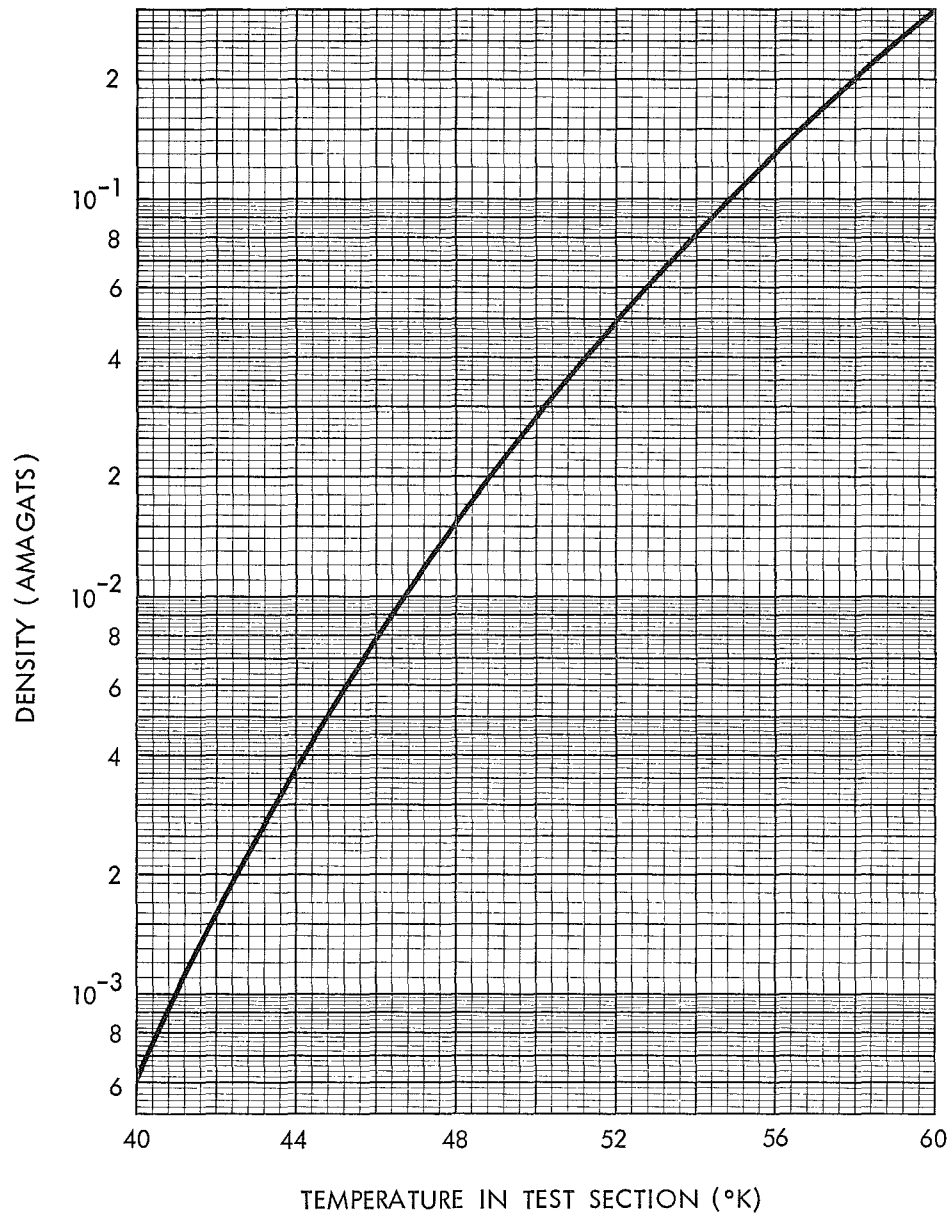
FIG. 4   VARIATION OF DENSITY IN TEST SECTION WITH TEMPERATURE FOR
CONDENSATION THRESHOLD OPERATION

FIG. 5 VARIATION OF ENTROPY IN TEST SECTION WITH TEMPERATURE FOR
CONDENSATION THRESHOLD OPERATION
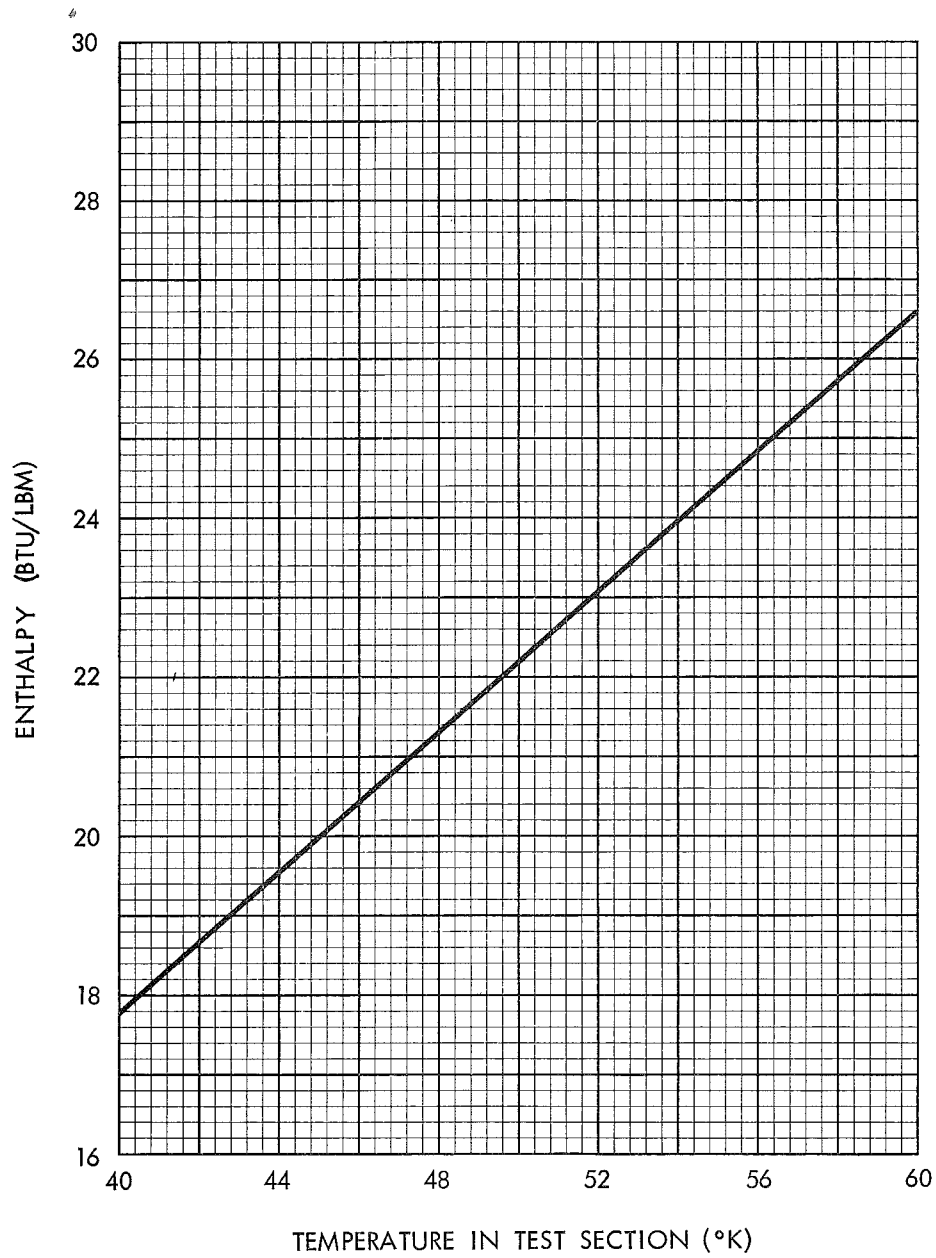
FIG. 6 VARIATION OF ENTHALPY IN TEST SECTION WITH TEMPERATURE FOR
CONDENSATION THRESHOLD OPERATION
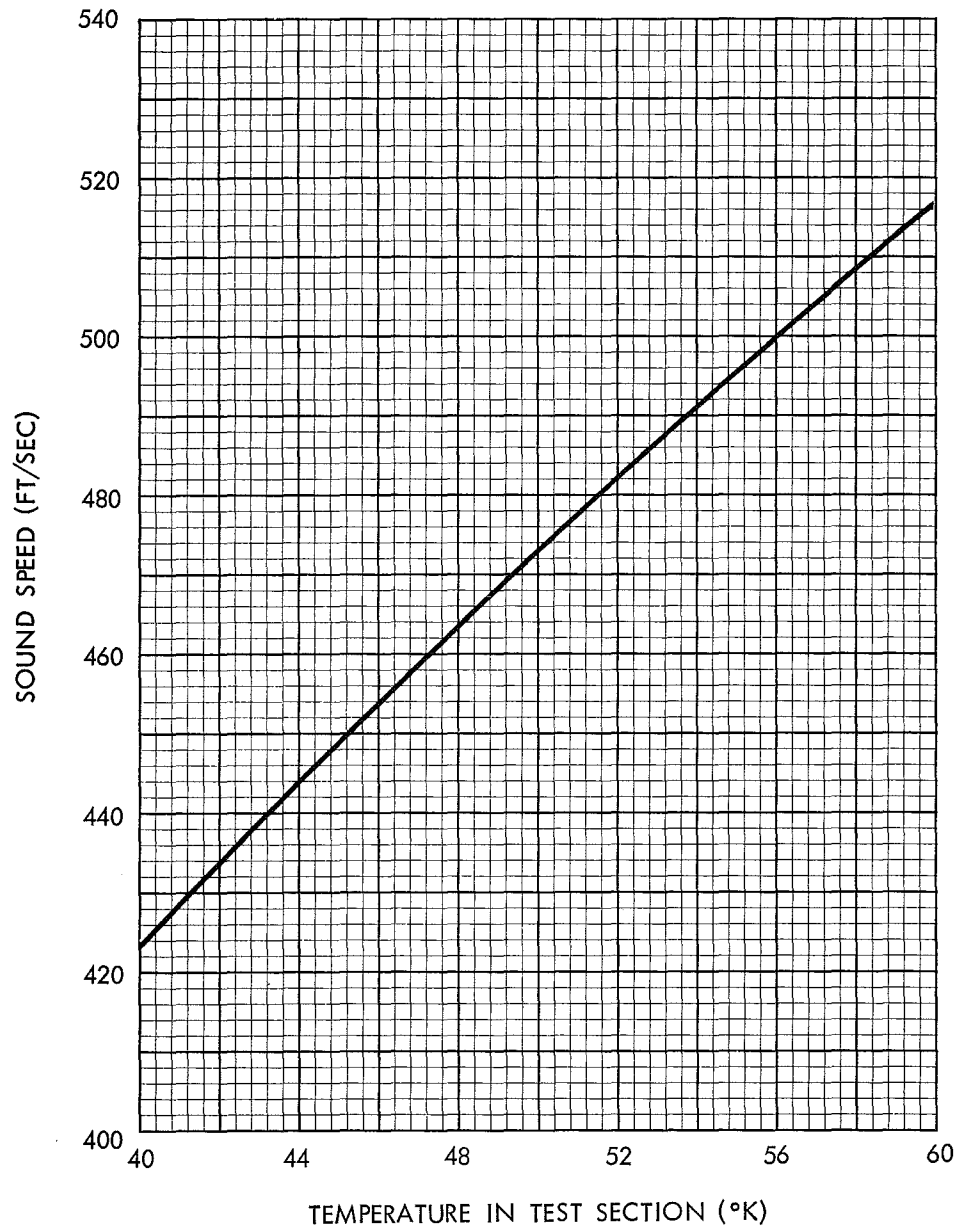
FIG. 7 VARIATION OF SOUND SPEED IN TEST SECTION WITH TEMPERATURE FOR CONDENSATION THRESHOLD OPERATION
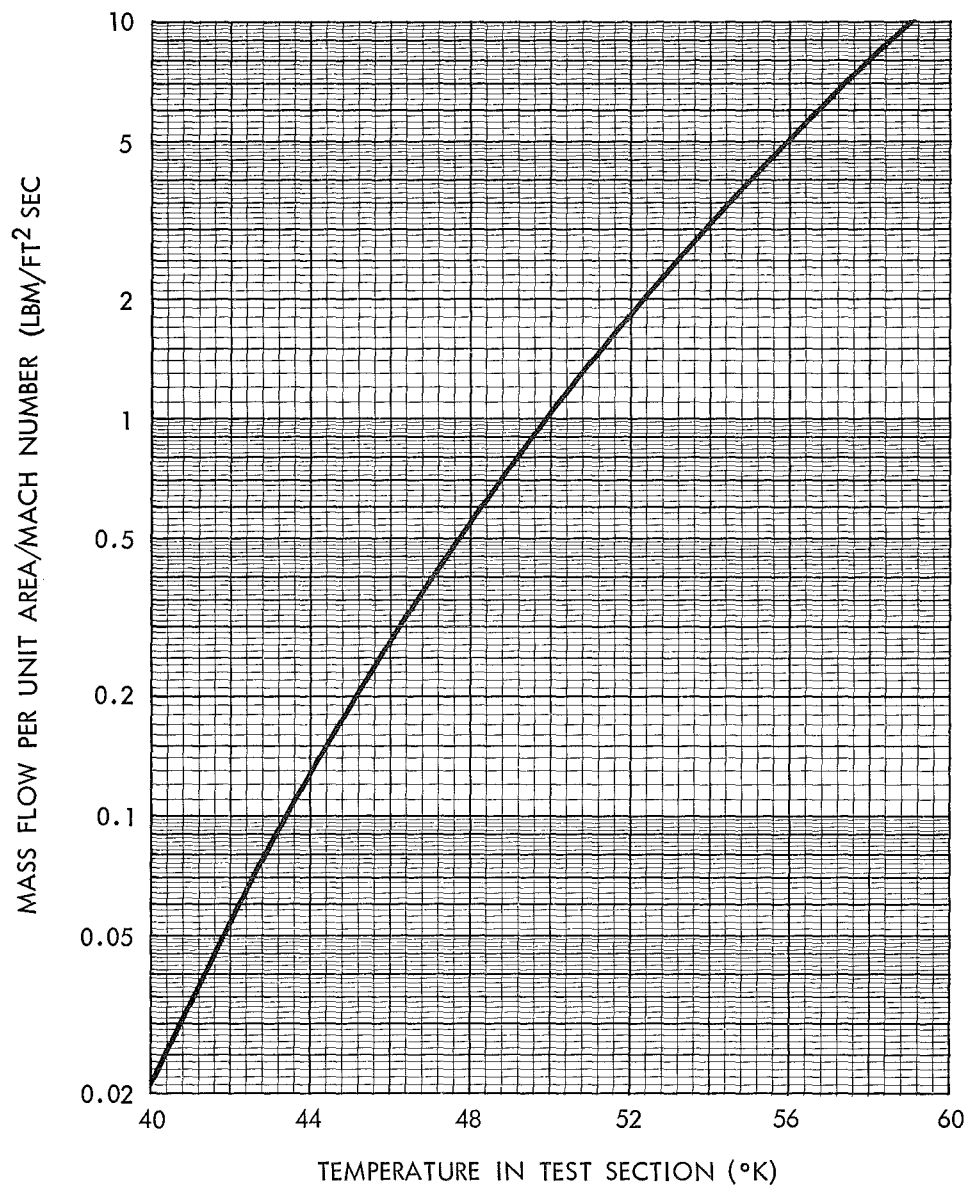
FIG. 8 VARIATION OF MASS FLOW IN TEST SECTION WITH TEMPERATURE FOR CONDENSATION THRESHOLD OPERATION
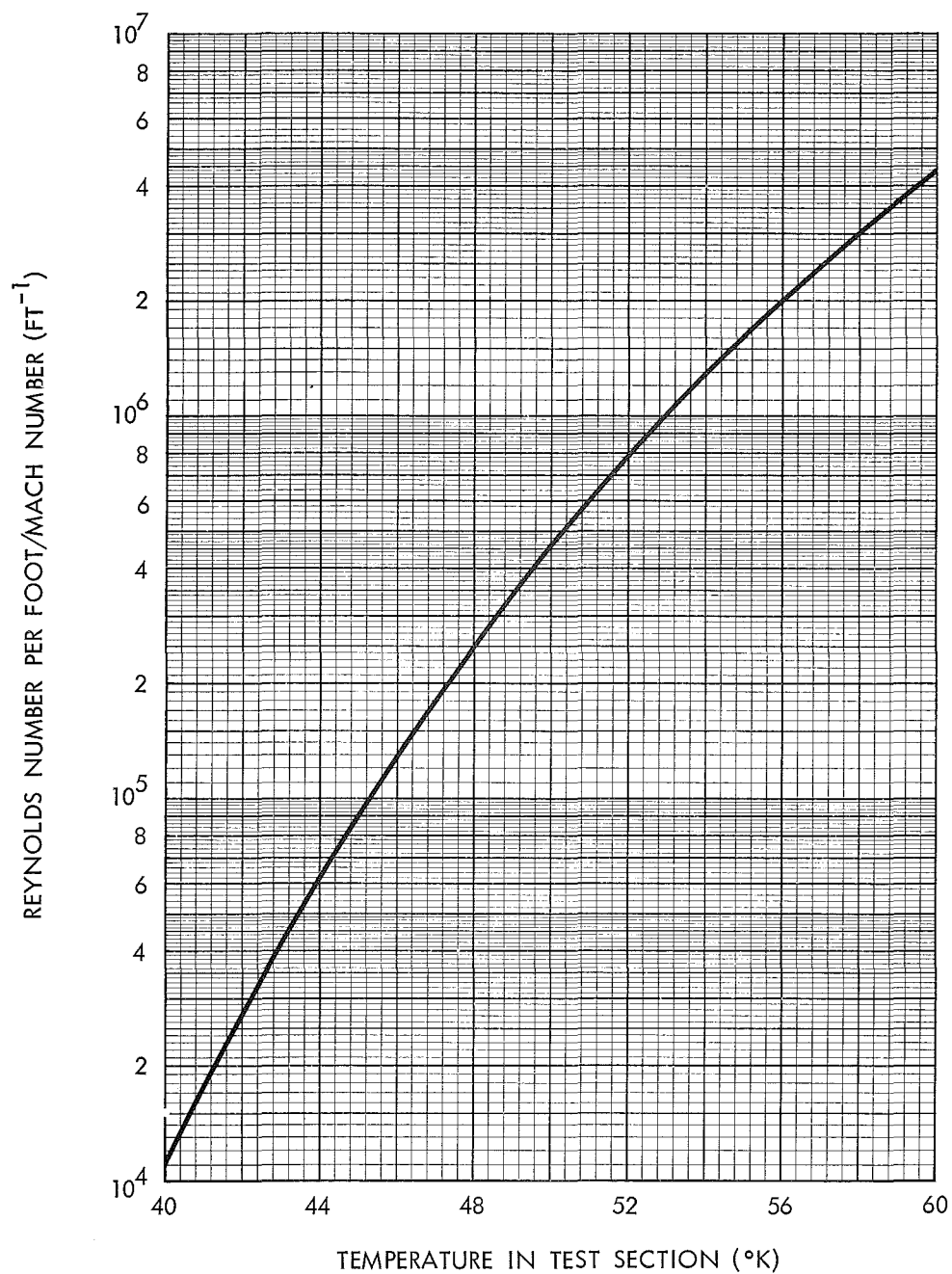
FIG. 9 VARIATION OF REYNOLDS NUMBER IN TEST SECTION WITH TEMPERATURE FOR CONDENSATION THRESHOLD OPERATION
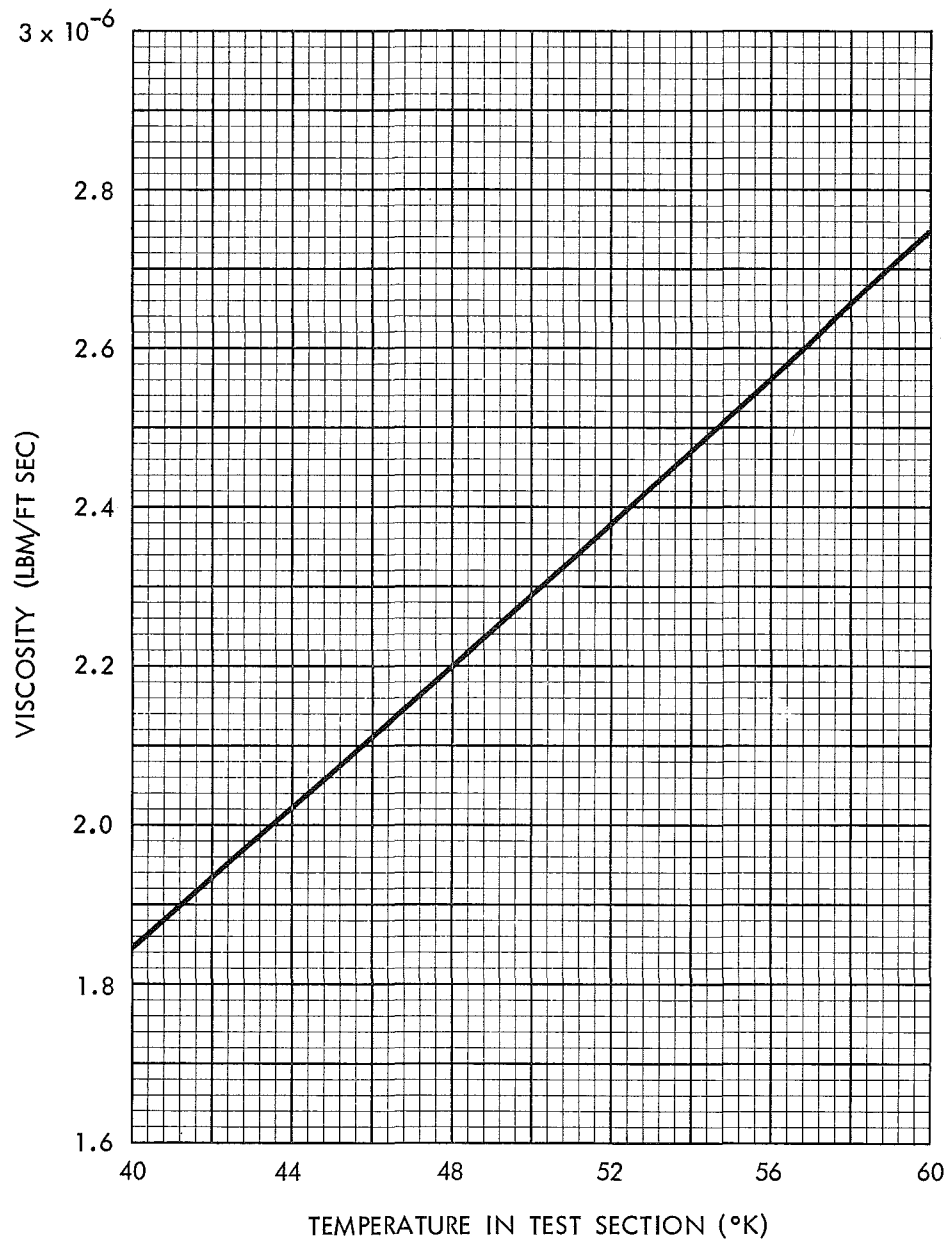
FIG. 10 VARIATION OF VISCOSITY IN TEST SECTION WITH TEMPERATURE
FOR CONDENSATION THRESHOLD OPERATION

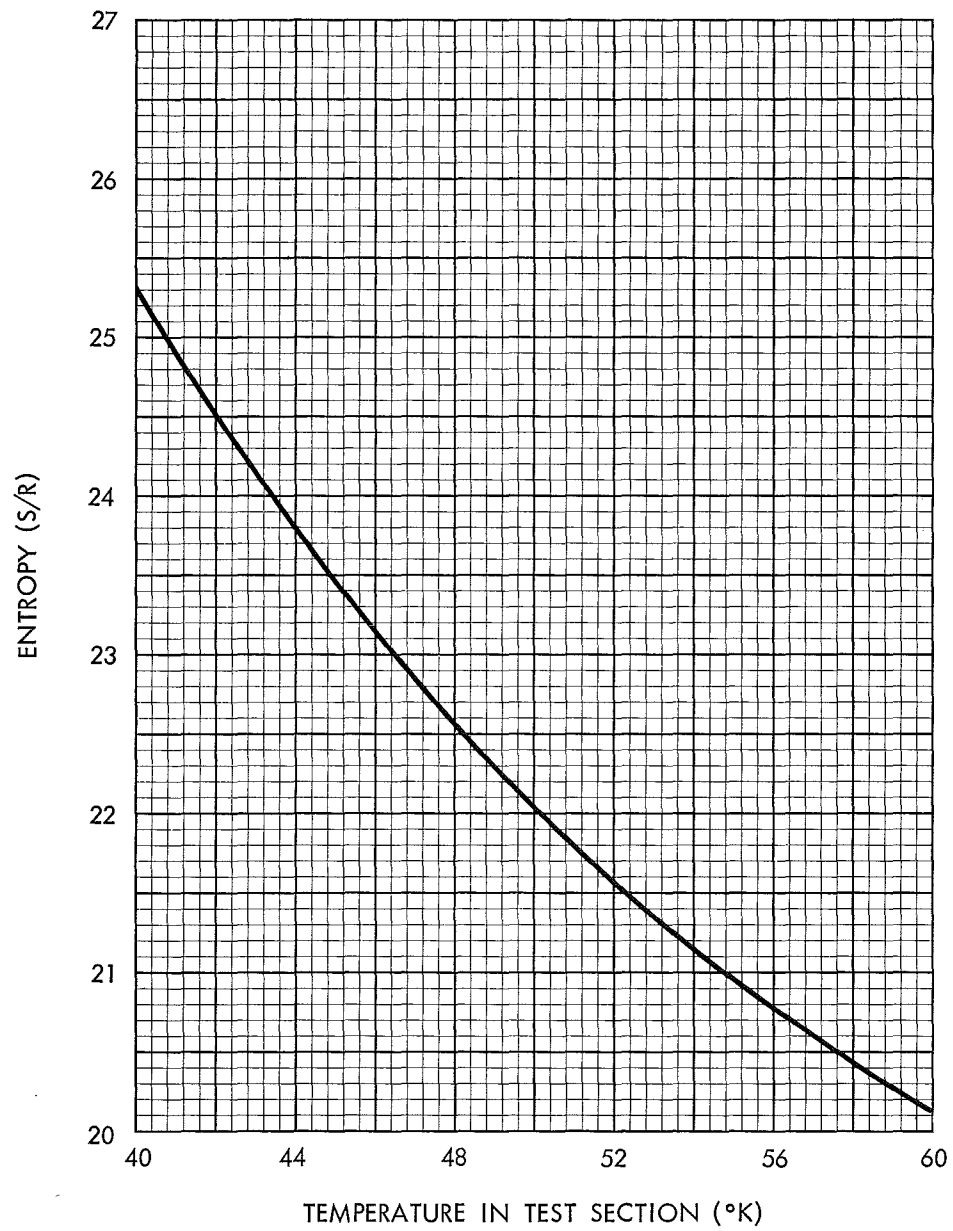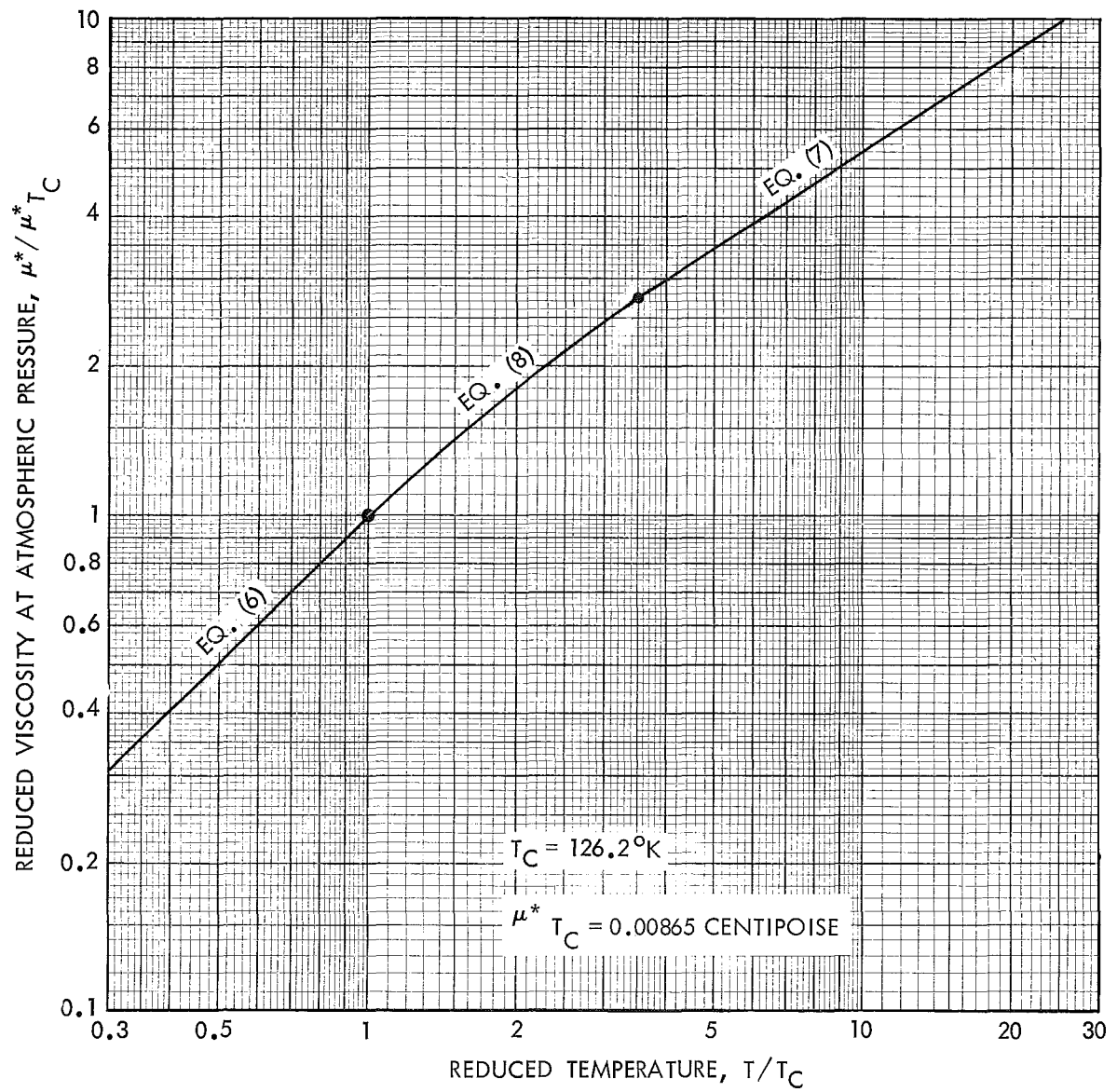FIG. 11 VISCOSITY—TEMPERATURE VARIATION USED IN BOUNDARY
LAYER CALCULATIONS
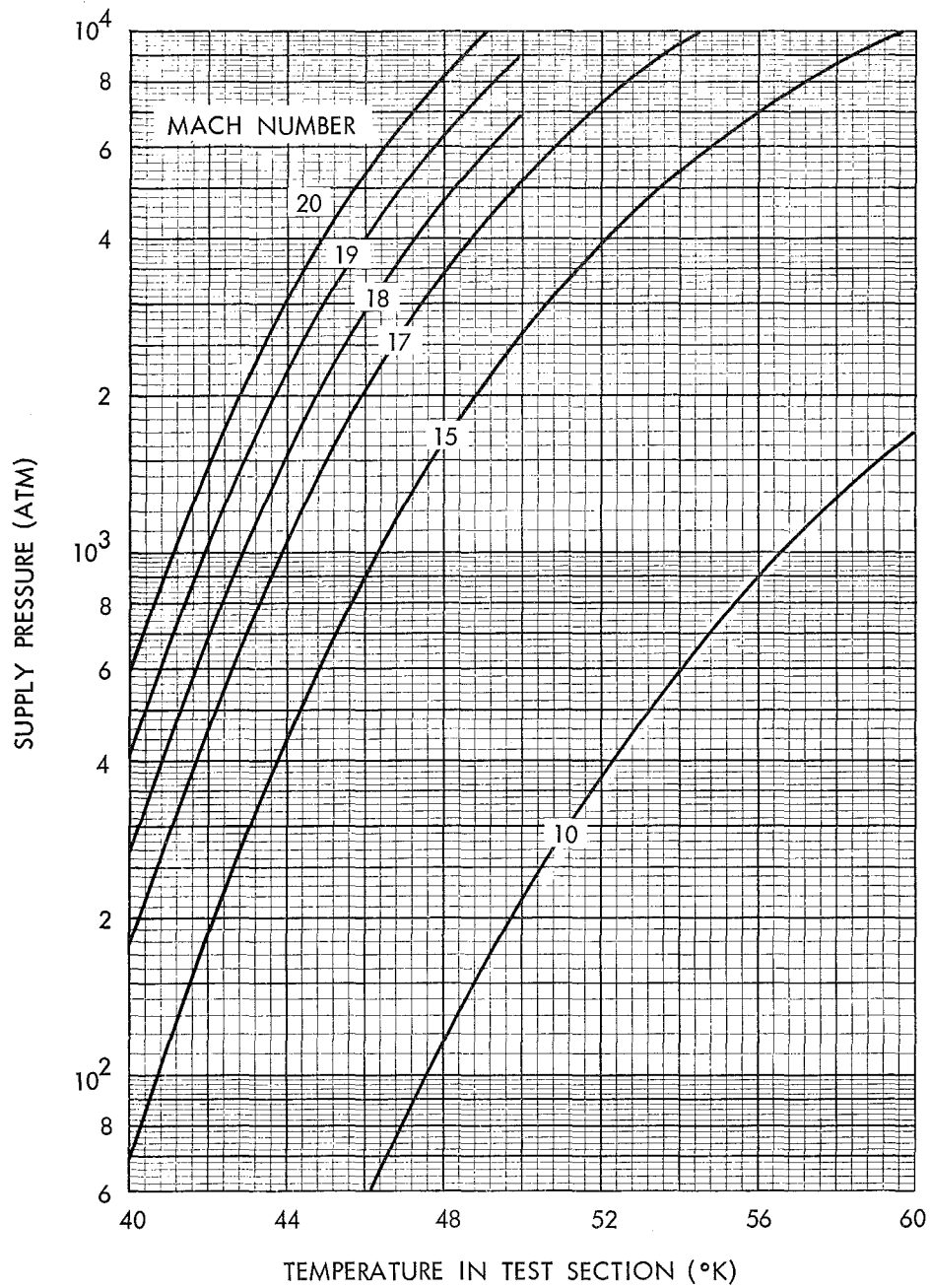
FIG. 12 VARIATION OF SUPPLY PRESSURE REQUIRED FOR CONDENSATION THRESHOLD
OPERATION WITH TEST SECTION TEMPERATURE AND MACH NUMBER
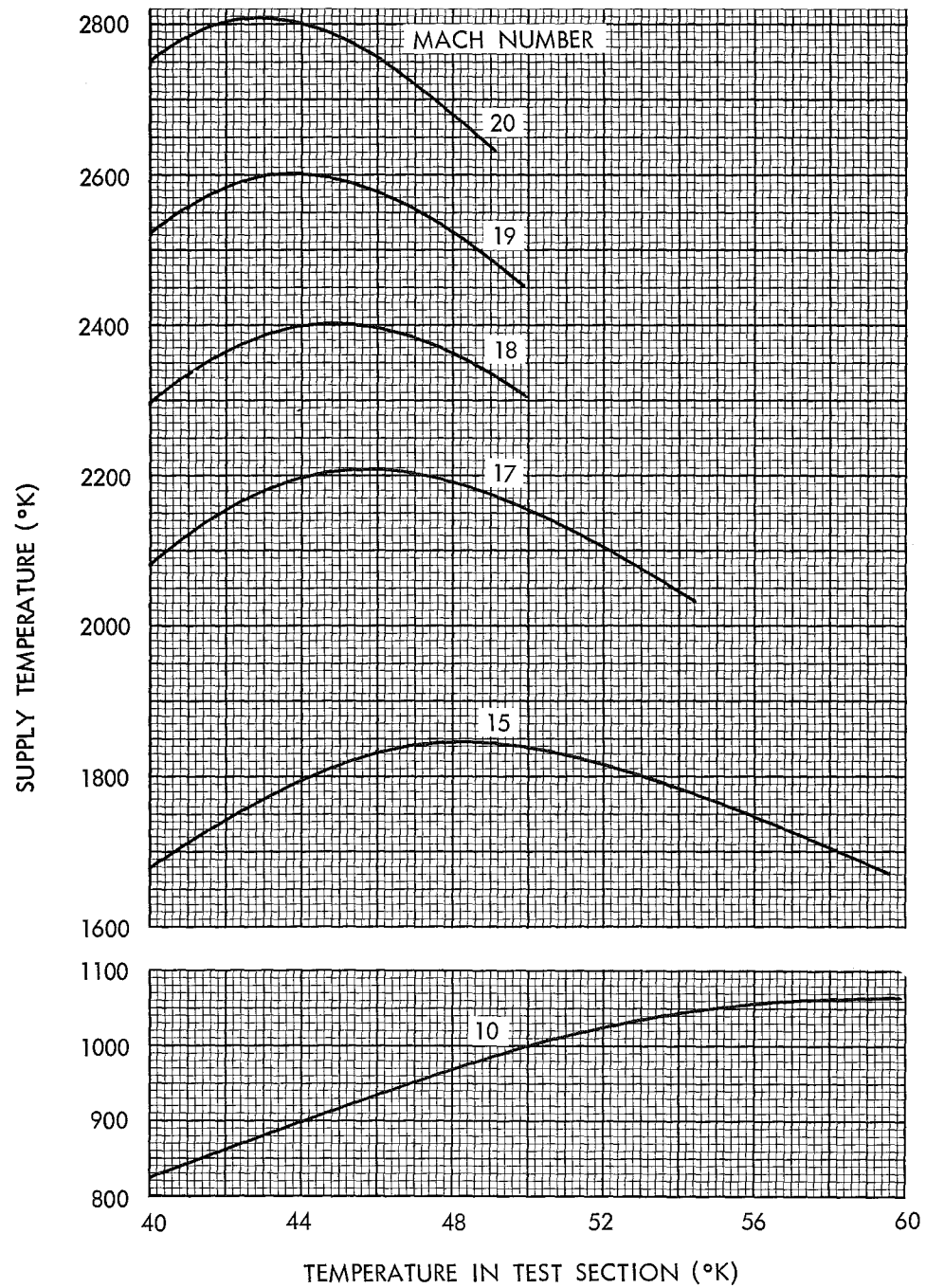
FIG. 13 VARIATION OF SUPPLY TEMPERATURE REQUIRED FOR CONDENSATION THRESHOLD
OPERATION WITH TEST SECTION TEMPERATURE AND MACH NUMBER
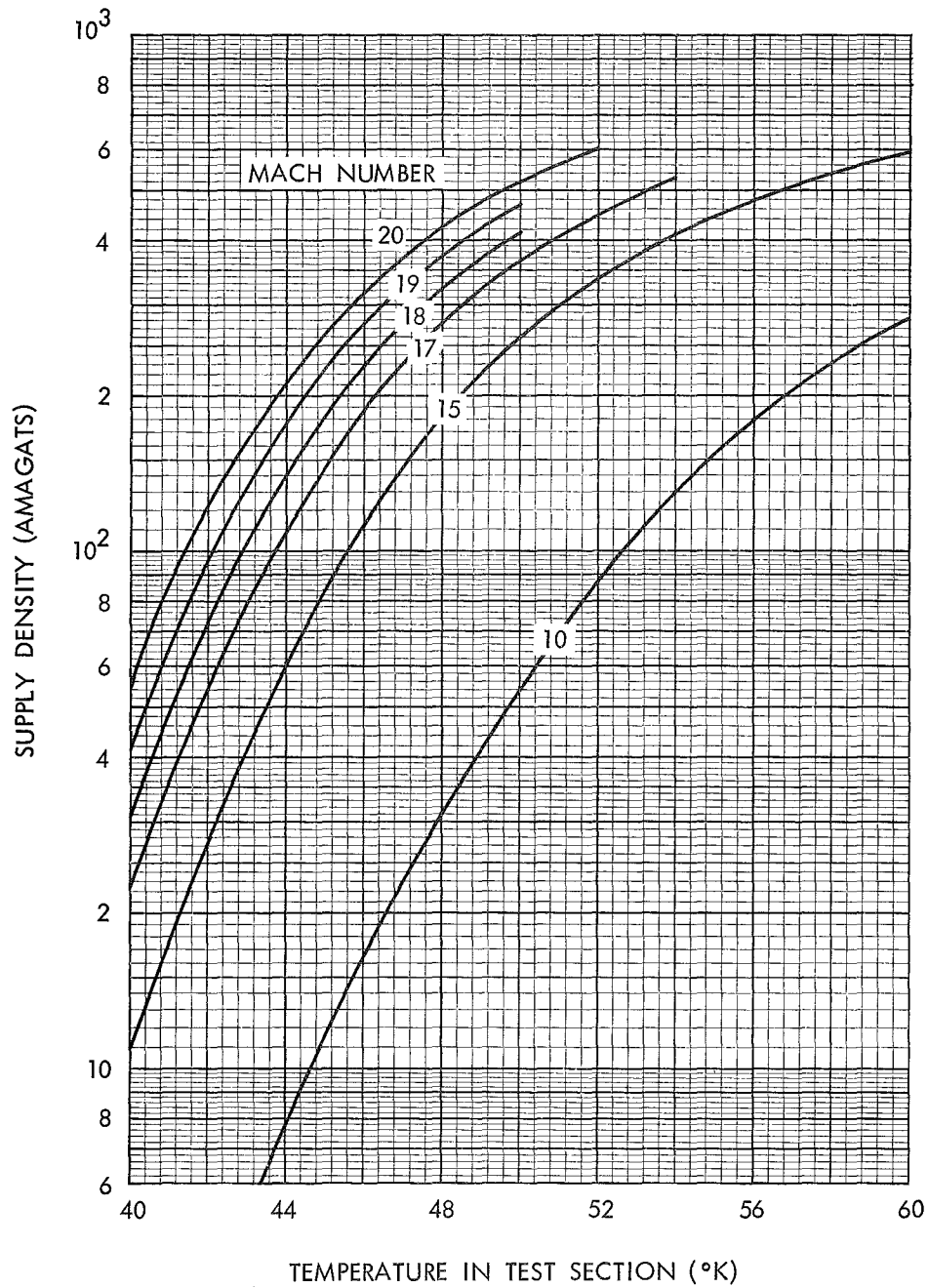
FIG. 14 VARIATION OF SUPPLY DENSITY REQUIRED FOR CONDENSATION THRESHOLD OPERATION WITH TEST SECTION TEMPERATURE AND MACH NUMBER
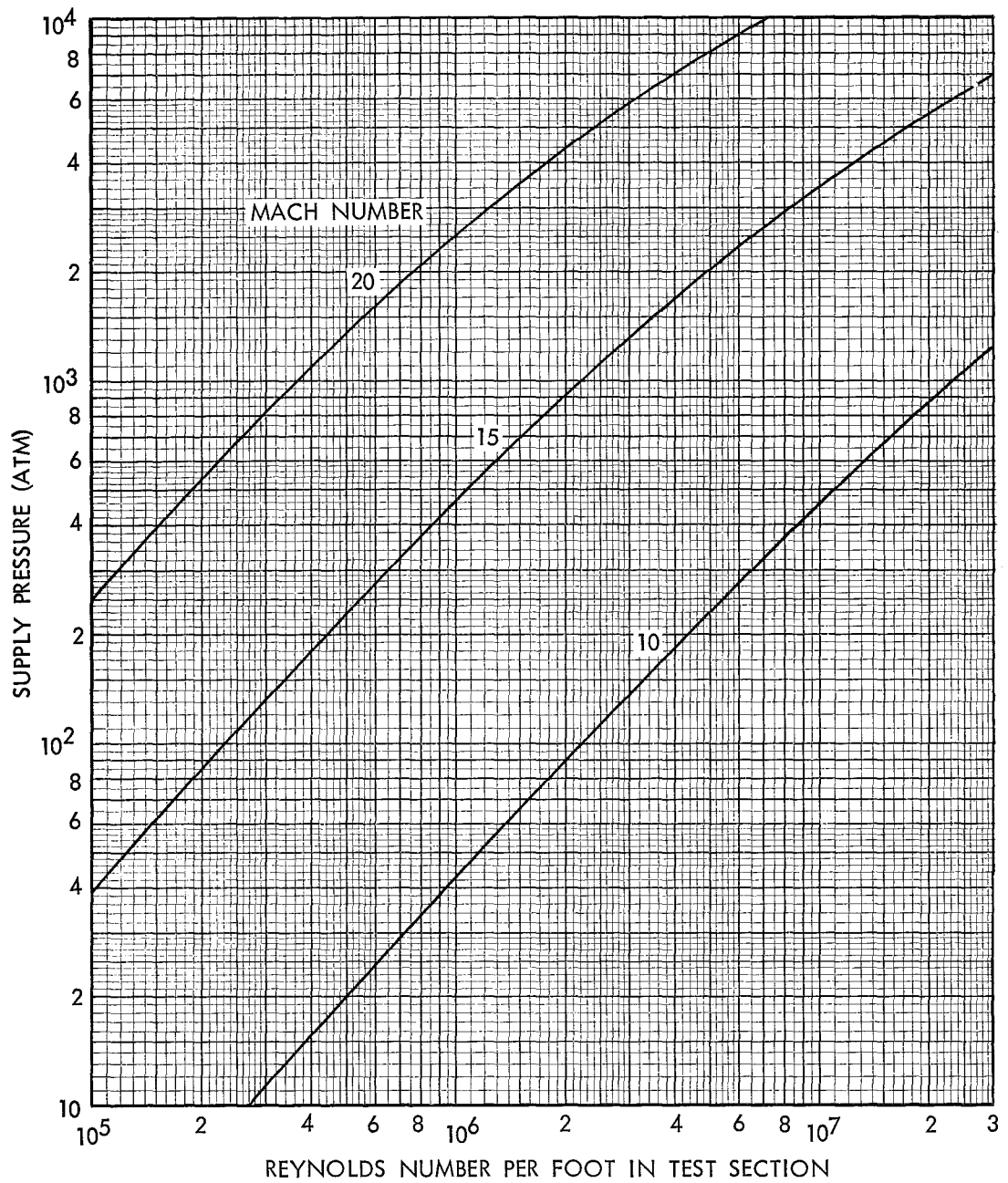
FIG. 15 VARIATION OF SUPPLY PRESSURE REQUIRED FOR CONDENSATION THRESHOLD
OPERATION WITH TEST SECTION REYNOLDS NUMBER PER FOOT AND MACH NUMBER
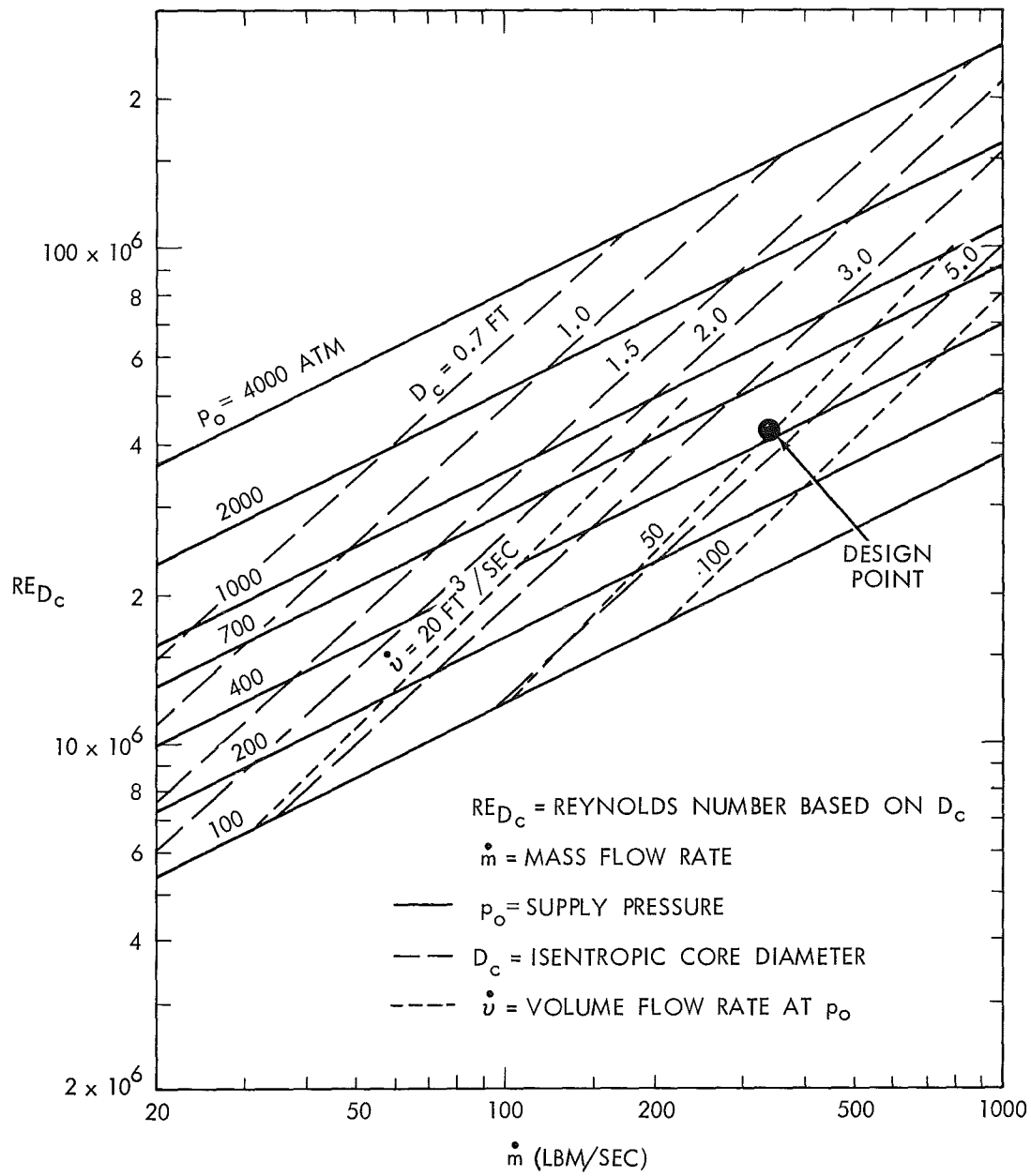
FIG. 16   REQUIRED SUPPLY PRESSURE, CORE DIAMETER, AND VOLUME FLOW RATE FOR GIVEN
RE_{D_c} AND MASS FLOW RATE (MACH 10)
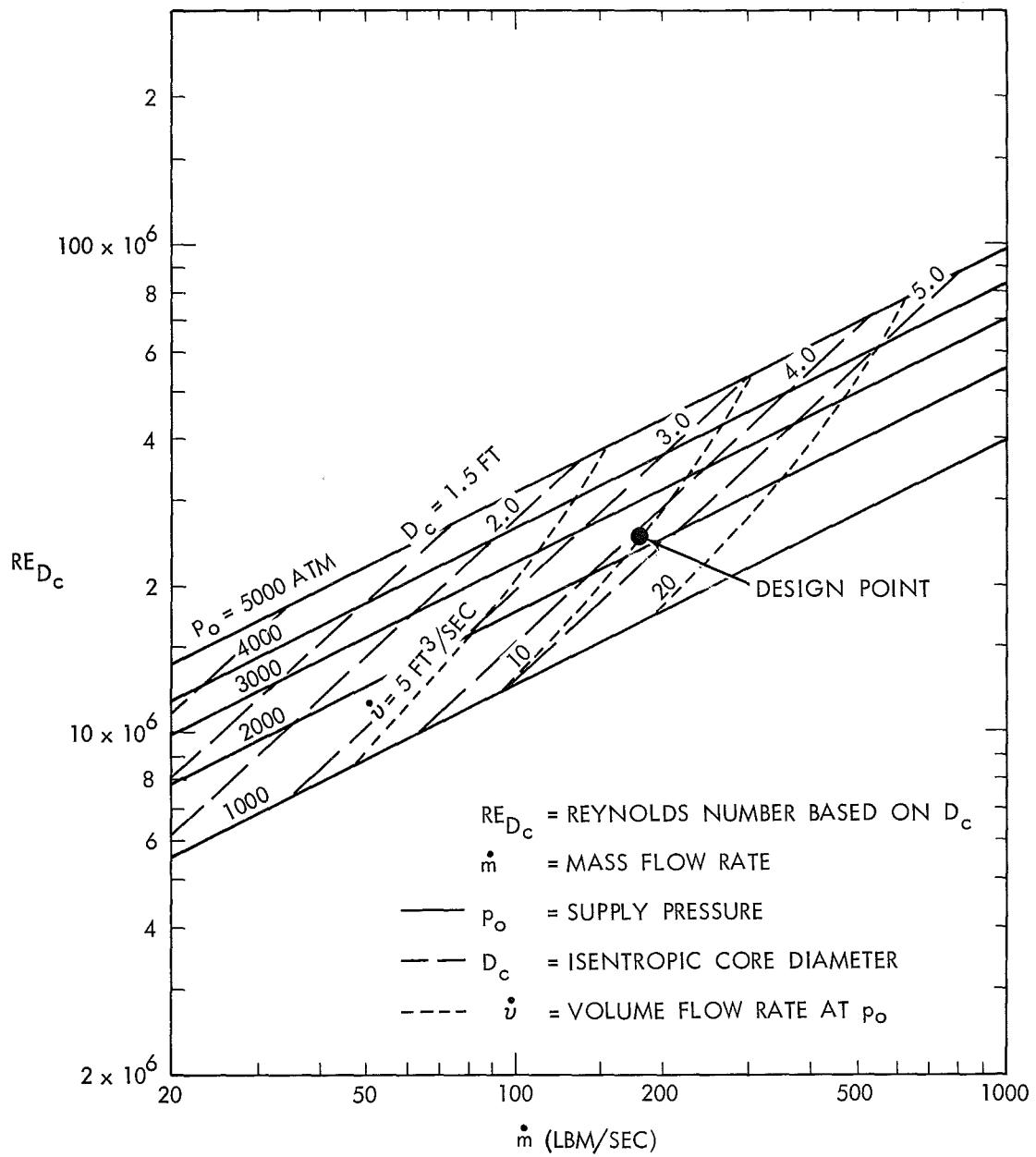
FIG. 17   REQUIRED SUPPLY PRESSURE, CORE DIAMETER, AND VOLUME FLOW RATE FOR GIVEN RE_{D_c} AND MASS FLOW RATE (MACH 15)
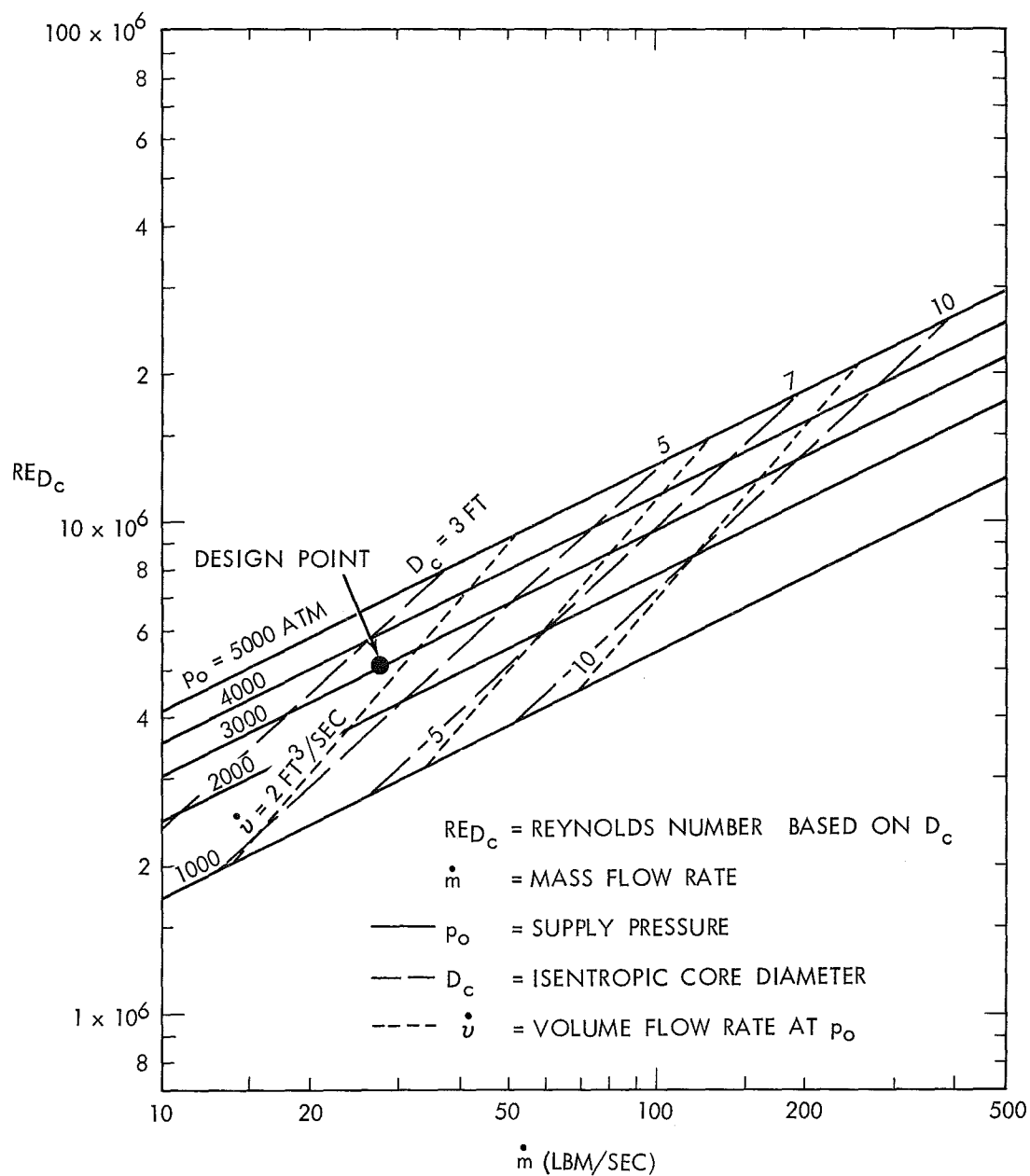
FIG. 18   REQUIRED SUPPLY PRESSURE, CORE DIAMETER, AND VOLUME FLOW RATE FOR GIVEN RE_{D_c} AND MASS FLOW RATE (MACH 20)
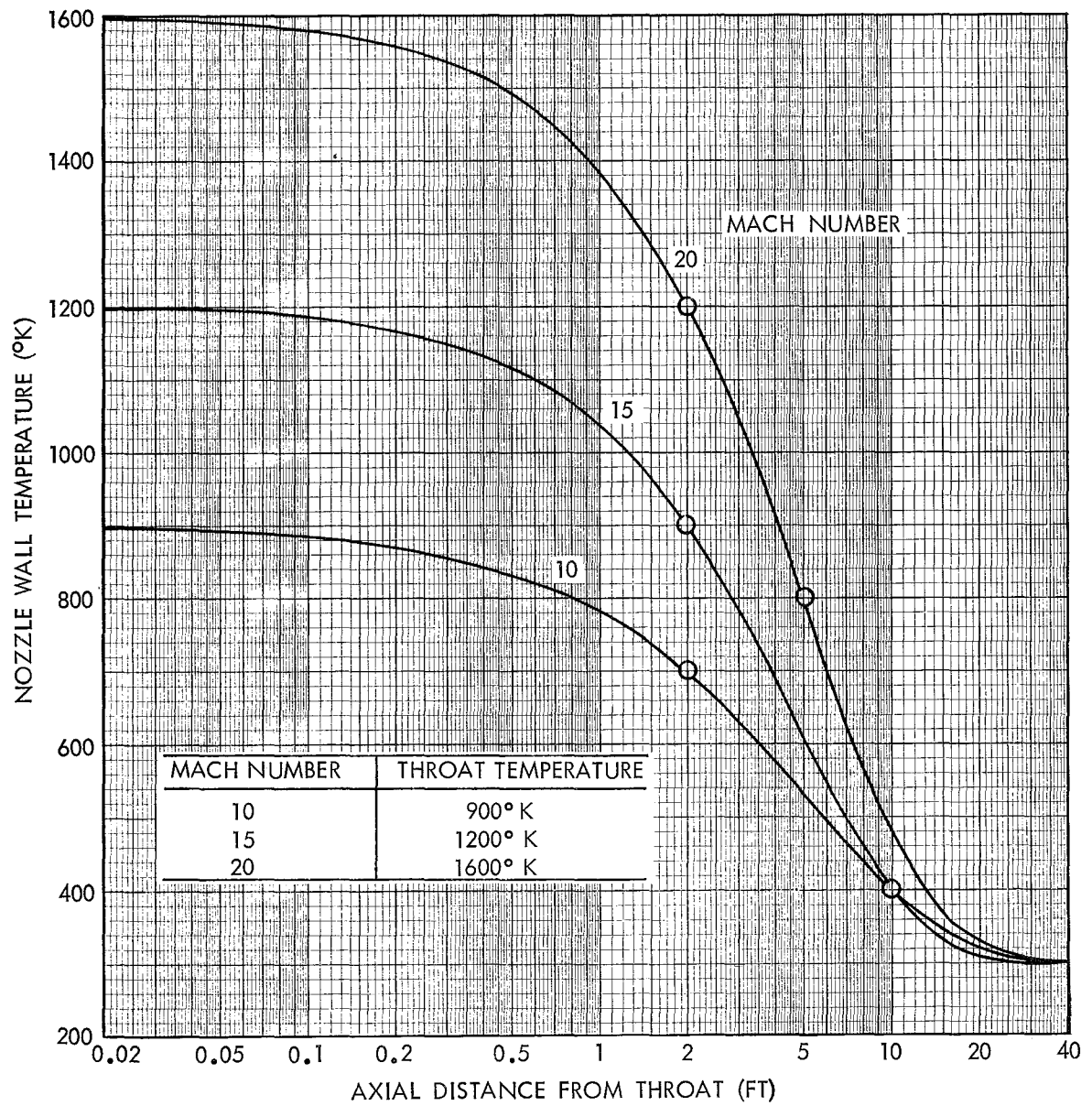
FIG. 19 ASSUMED VARIATION OF NOZZLE WALL TEMPERATURE WITH AXIAL DISTANCE
DOWNSTREAM OF THROAT
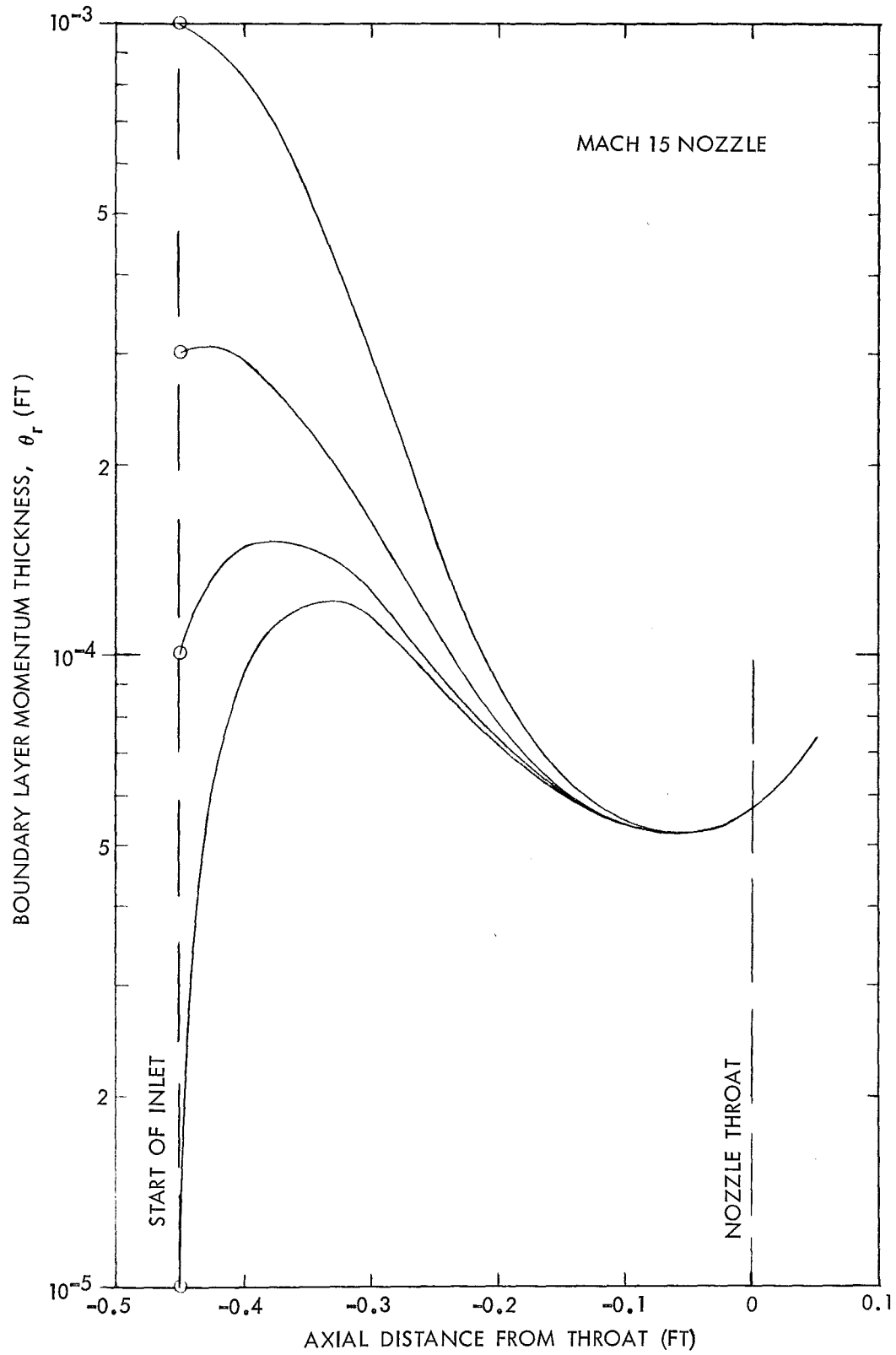
FIG. 20 DEPENDENCE OF θ_r IN SUBSONIC INLET ON INITIAL VALUE USED
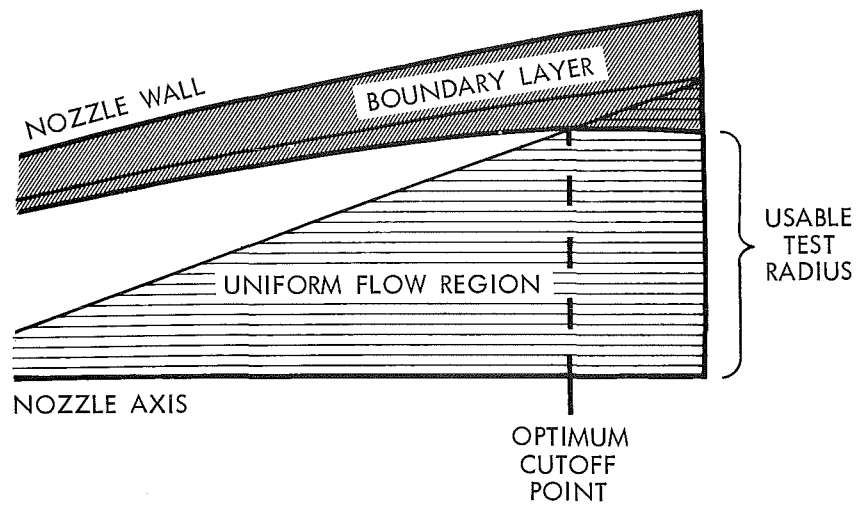
FIG. 21   SCHEMATIC DIAGRAM OF NOZZLE EXIT SHOWING DEFINITION AND LOCATION OF OPTIMUM CUTOFF POINT
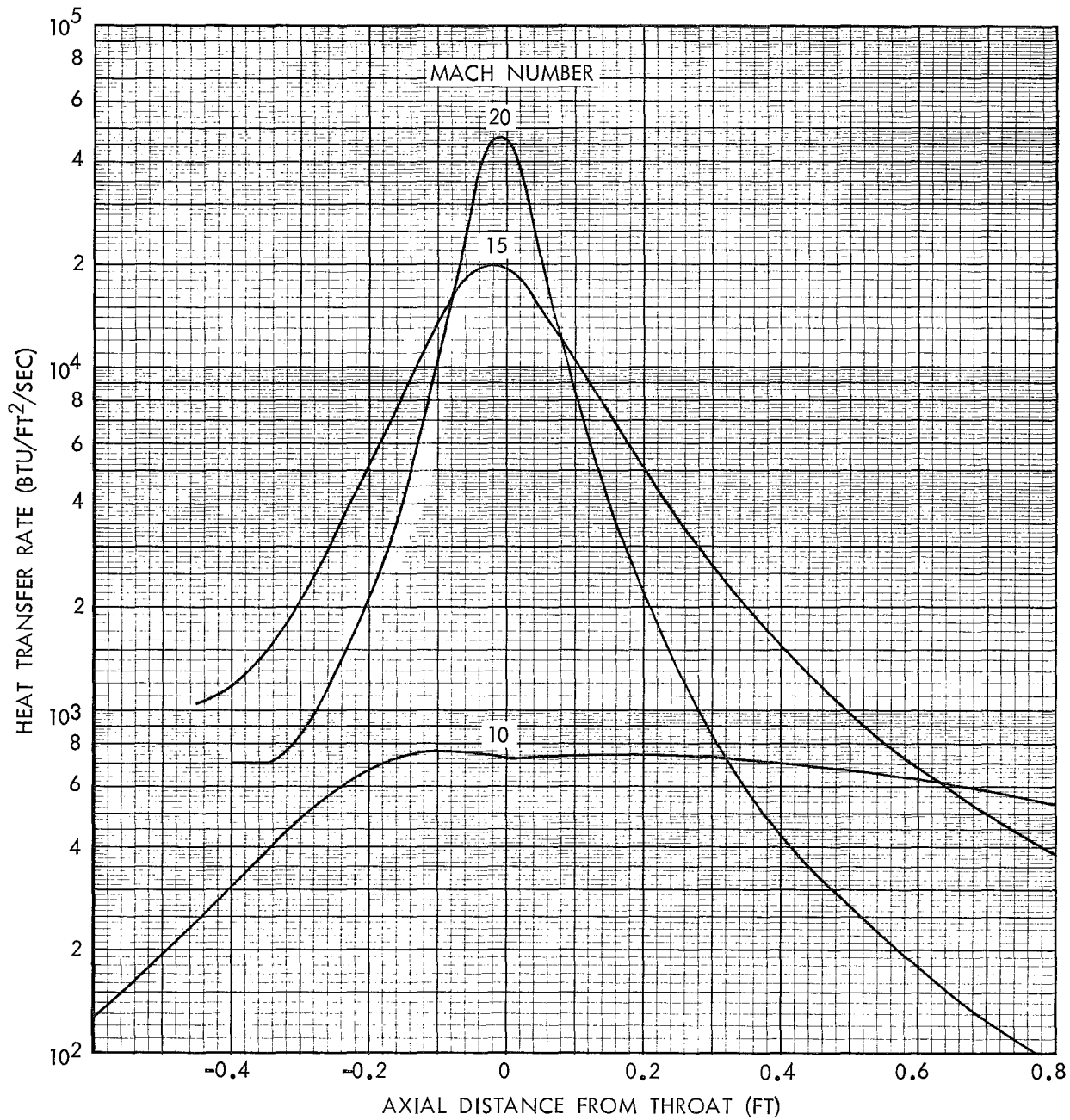
FIG. 22 VARIATION OF SURFACE HEAT TRANSFER RATE WITH AXIAL DISTANCE IN
THROAT REGION FOR ASSUMED TEMPERATURE DISTRIBUTIONS
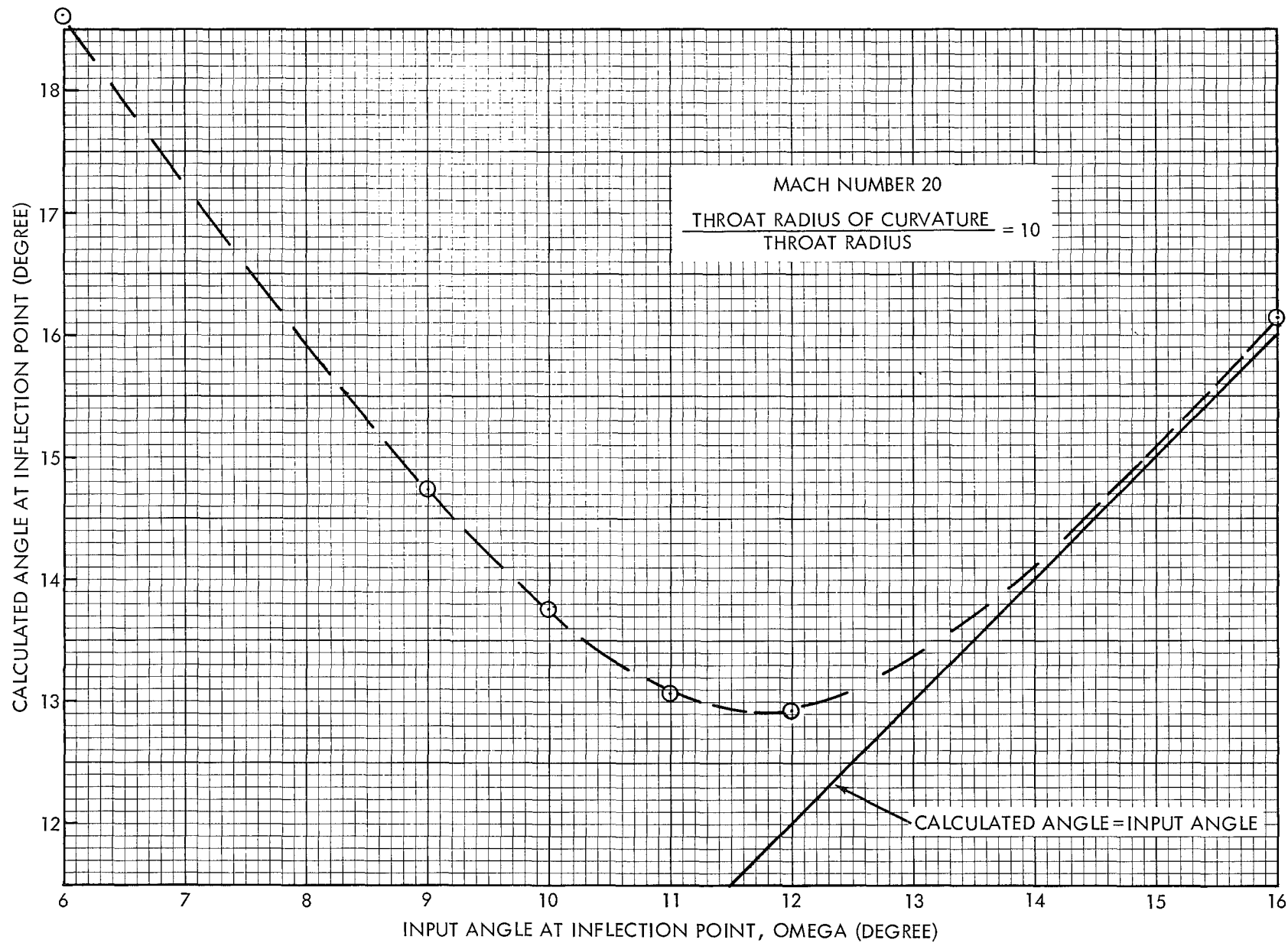
FIG. 23 VARIATION OF CALCULATED ANGLE AT INFLECTION POINT WITH INPUT VALUE

MACH NUMBER 20

$$\frac{\text{THROAT RADIUS OF CURVATURE}}{\text{THROAT RADIUS}} = 10$$

CALCULATED ANGLE AT INFLECTION POINT (DEGREE)

INPUT ANGLE AT INFLECTION POINT, OMEGA (DEGREE)

CALCULATED ANGLE = INPUT ANGLE

NOLTR 71-6
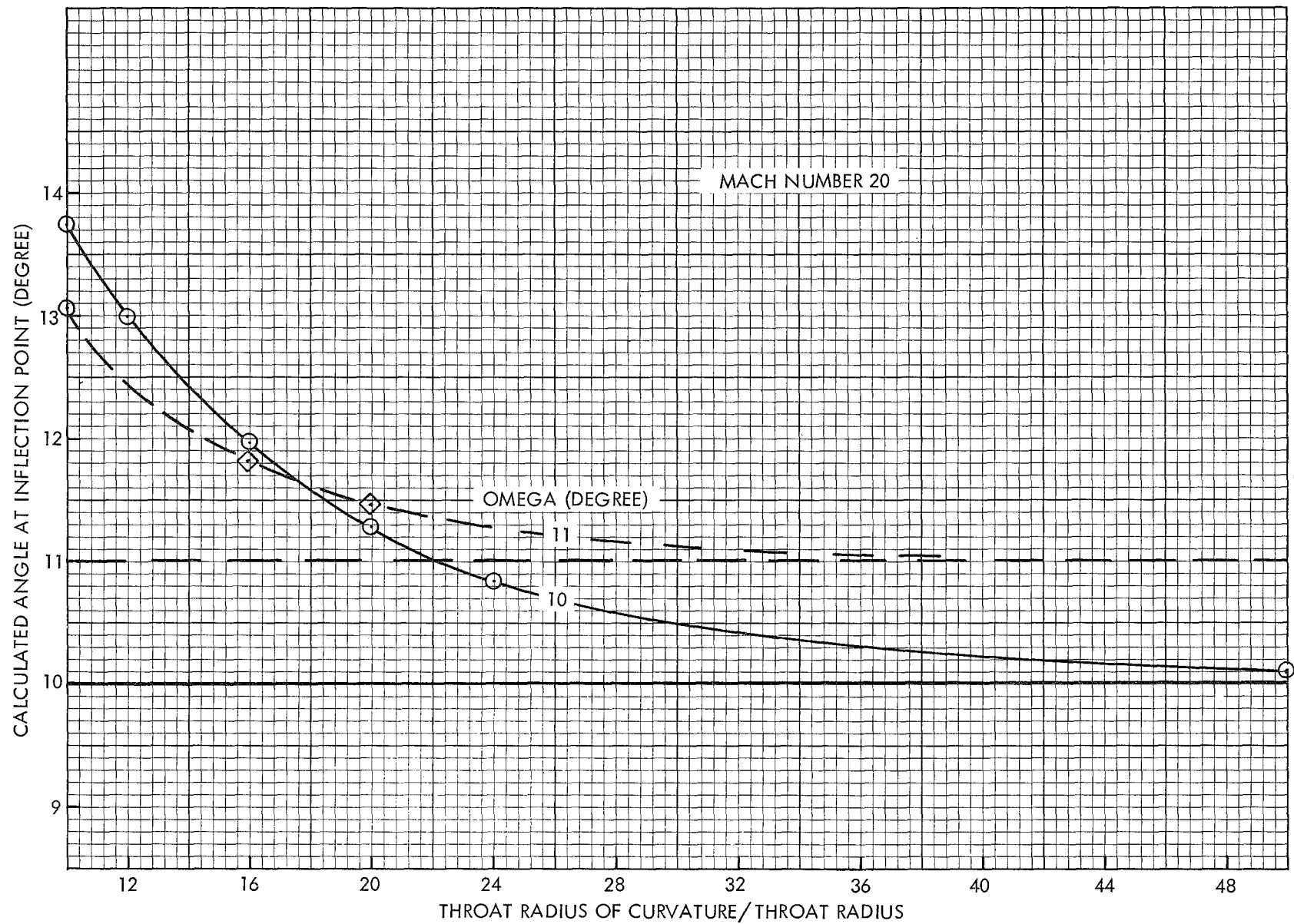
FIG. 24   VARIATION OF CALCULATED ANGLE AT INFLECTION POINT WITH THROAT
RADIUS OF CURVATURE/THROAT RADIUS

APPENDIX A

MODIFIED CENTERLINE MACH NUMBER DISTRIBUTION

The Axisymmetric Core Program (ACP) has been used to compute
the inviscid core flow in the supersonic portion of the nozzle. This
program has been modified from the form presented in reference (15)
in order to incorporate a third centerline Mach number distribution.
For high Mach numbers where throat diameters are typically small, the
cubic and exponential distributions contained in the ACP program lead
to large radii of curvature at the nozzle throat. Since such nozzles
are difficult to manufacture and can lead to throat heating problems,
a third centerline Mach number distribution has been added to the
program.

In this third distribution, a quadratic Mach number variation in
the region of the nozzle throat is matched to one corresponding to a
region of radial flow further downstream.* However, the Mach number
in this radial flow region does not reach the exit Mach number with
the desired zero gradient. To smooth this transition, a section of
variable length is inserted between the radial flow region and the
uniform flow region. In this section, the Mach number is given by
the expression

$$M = M_e \, e^{-a(x_t - x)^2} \qquad\qquad (A\text{-}1)$$

where M_e is the exit Mach number and a and x_t are determined by
matching the Mach number and its gradient at some arbitrary point to
the values obtained from the radial flow region distribution. This
match point then becomes the boundary between the radial flow region
and the transition region. The match point is chosen by specifying
*See the derivation of the Mach number distribution on pages A-3 to A-7.

its location as some fraction (XER) of the distance from the throat
at which the exit Mach number would be reached if no transition
section were inserted. The quantity x_t is the location at which the
transition section ends and the uniform flow region begins.

The use of this multiple-section distribution will decrease the
radius of curvature at the nozzle throat while allowing the Mach
number to vary smoothly along the nozzle axis. It has been incorporated
into the program and identified as the Harris centerline Mach number
distribution to distinguish it from the Schaaf (exponential) and
Thickstun (cubic) distributions. The Harris centerline is used if the
input quantity IFTH equals 2. In order that the instructions given in
reference (15) for running this program with the Schaaf and Thickstun
centerline distributions remain valid, the input quantities required
for defining the Harris distribution are read from a third data card
(when IFTH equals 2) with the statements

> 45 READ (5, 46) OMEGA, EMB, XER, RCPLUS
> 46 FORMAT (4F10.5)

The required input quantities are defined as follows (see sketch below):

OMEGA   angle at the inflection point measured with respect
to the nozzle centerline (see next section),

EMB   Mach number at point B,

XER   location of the match point between the radial flow
region and the transition section expressed as a
fraction of the distance from the throat at which the
exit Mach number would be reached if no transition
section were inserted,

RCPLUS   desired ratio of throat radius of curvature to throat
radius

The values of XT, RCT, and EMZP (defined in reference (15)) are
calculated in subroutine CLP. Therefore, dummy values (or blanks) can
be used for these three quantities on the first data card. The values
of XT, RCT, and EMZP written in the output heading are the calculated

ones. The input quantities OMEGA, EMB, and XER are written in the
output as PA, PB, and PC, respectively, while the coefficient a in the
transition region Mach number distribution (equation A-1) is written
as PD. The value input for the quantity RCPLUS is not written in the
output but can be obtained by dividing the output values of RCT and
THROAT RADIUS.

DERIVATION OF MACH NUMBER DISTRIBUTION
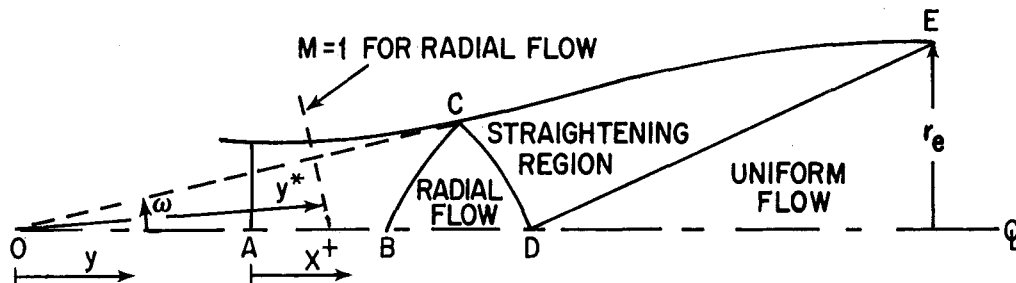
The derivation which follows is strictly valid only when the ratio
of specific heats γ is constant with a value of 1.4 throughout the
flow. Thus, for flows with other constant or variable specific heats,
the flow will not be completely radial in the region BCD shown in the
above sketch. However, this will not cause any real difficulty,
because the flow in the region BCD is calculated from the resulting
centerline Mach number distribution using the method of characteristics
rather than from the radial flow equations. In other words, the radial
flow region BCD exists formally only in the following derivation. It
does not exist formally in the nozzle calculation. As the gas departs
from perfect gas behavior, not only does the flow in region BCD depart
somewhat from strictly radial flow, but also the calculated angle at
the inflection point departs from the input quantity OMEGA used to
determine the centerline Mach number distribution. Figure 23 shows
that for a given RCPLUS (ratio of throat radius of curvature to throat
radius), the calculated inflection point angle matches the input value
OMEGA fairly well at larger values of OMEGA, but departs more and more
as OMEGA decreases. Moreover, for the case shown in Figure 23, the

minimum value obtained for the calculated angle is above the desirable 10°-12° range. Figure 24 shows that by increasing RCPLUS the calculated angle can be made to agree more closely with the input value OMEGA and (as was also shown in Figure 23) the agreement is better at the larger values of OMEGA. However, it is not necessary to make the two angles agree closely. The important thing is that the calculated angle be kept within the desired range. As the two figures have shown, this may require the use of a value of OMEGA substantially smaller than the desired angle at the inflection point. At the present time, these figures are about the only guide to selecting the value of OMEGA. Until more such results are available, the process of obtaining the desired angle will be a trial and error one.

In the following derivation, the sonic line is assumed to be straight, perpendicular to the nozzle axis, and located at point A. The Mach number distribution from A to B is quadratic in distance with the same slope at B as that calculated for point B using the radial flow assumptions for region BCD. The following notation is used.

r_e radius of inviscid core at exit

x $(=x^+ r_e)$ distance from throat

y $(=y^+ r_e)$ distance from apparent source of radial flow (point 0)

M_D Mach number at point D

M_B' Mach number gradient $\dfrac{dM}{dx^+}$ at point B

From A to B
_____

$$M(x^+) = \frac{M_B' - M_A'}{2} \; x_B^+ \left(\frac{x^+}{x_B^+}\right)^2 + M_A' \; x_B^+ \left(\frac{x^+}{x_B^+}\right) + M_A \tag{A-2}$$

$$M'(x^+) = (M'_B - M'_A) \frac{x^+}{x_B^+} + M'_A \tag{A-3}$$

where

$$x_B^+ = 2 \frac{M_B - M_A}{M'_B + M'_A} \tag{A-4}$$

Since point A is the position of the sonic line, M_A equals 1. The gradient M'_A at the sonic point is found from the throat radius r_* ($=r_*^+ r_e$) and the input quantity RCPLUS ($=\frac{R_c}{r_*} = \frac{R_c^+}{r_*^+}$) using the perfect gas relation

$$M'_A = M'\Big|_{M=1} = \sqrt{\frac{\frac{\gamma+1}{2}}{r_*^+ R_c^+}} = \frac{1}{r_*^+} \sqrt{\frac{1.2}{RCPLUS}} \tag{A-5}$$

From B to D

For the radial flow region BCD, the flow angle ω at the inflection point C is related to the Mach numbers at points B and D. The relationship is

$$\nu(M_B) + 4\omega = \nu(M_D) \tag{A-6}$$

where $\nu(M)$ is the Prandtl-Meyer angle tabulated for two-dimensional flow. (For table of $\nu(M)$, see reference (27)). Thus, the Mach number at point B (input quantity EMB) is obtained from the Mach number at point D (= design Mach number) and the desired maximum expansion angle ω (input quantity OMEGA). Typically, ω is in the range 10° - 12°.

In this radial flow region, the distance y from the source (point 0) is related to the Mach number by the one-dimensional relation for the area ratio $\frac{A}{A_*}$,

$$\left(\frac{y}{y_*}\right)^2 = \frac{A}{A_*} = \frac{1}{M}\ [\frac{2}{\gamma+1}\ (1 + \frac{\gamma-1}{2}\ M^2)]^{\frac{\gamma+1}{2(\gamma-1)}} \tag{A-7}$$

where y_* is the value of y for which M = 1. For $\gamma = 1.4$, this can be written as

$$\frac{y}{y_*} = [K(M)]^{1/2} \tag{A-8}$$

where

$$K(M) \equiv \frac{1}{M}\ [\frac{1 + 0.2M^2}{1.2}]^3 \tag{A-9}$$

Also

$$\frac{y_*}{r_e} = g(\omega,\ M_D) \tag{A-10}$$

where

$$\frac{1}{g(\omega,M_D)} = 2(\sin \frac{\omega}{2})\ [K(M_D)]^{1/2} \tag{A-11}$$

Noting that

$$x = y - \overline{OA} = y - (y_B - x_B)$$

we find

$$x^+ \equiv \frac{x}{r_e} = g(\omega,M_D)\ \{[K(M)]^{\frac{1}{2}} - [K(M_B)]^{\frac{1}{2}}\} + \frac{x_B}{r_e} \tag{A-12}$$

and by differentiation

$$M' = \frac{dM}{dx^+} = \frac{2.4M}{g(\omega,M_D)\ (M^2-1)}\ \left[\frac{1.2M}{1+0.2M^2}\right]^{\frac{1}{2}} \tag{A-13}$$

A-6

SOLUTION PROCEDURE

The procedure to be used in setting up this centerline Mach number distribution is now as follows. First, the nozzle design Mach number M_D and the desired maximum expansion angle ω are chosen. Then using equation (A-6) and tables such as in reference (27), the Mach number at point B ($=M_B$) is calculated. The three quantities M_D, ω, M_B and the desired ratio of the throat radius of curvature to throat radius $\dfrac{R_C}{r_*}$ are read into the program as the input quantities EMT, OMEGA, EMB, and RCPLUS, respectively. In the program, using the throat radius r_*^+ obtained from the area ratio – Mach number relationship for one-dimensional flow, equations (A-5), (A-4), (A-9)*, (A-11), and (A-13) are used in the order given to calculate the quantities M_A', x_B^+, $K(M_B)$, $K(M_D)$, $g(\omega,M_D)$, and M_B', respectively. With these quantities, M and M' can be determined from

$$0 < x \leq x_B \qquad \text{equations (A-2) and (A-3)}$$

$$x_B \leq x \leq XER*x_D \qquad \text{equations (A-12) and (A-13)}$$

$$XER*x_D < x_t \qquad \text{equation (A-1)}$$

Since equation (A-12) can not be solved explicitly for M, a Newton-Raphson iterative procedure is used. Beginning with M at the previous station as a first guess, the value of M is corrected in successive iterations until two consecutive values agree to within 0.002 percent.

---

*Equation (A-9) is used twice, once for $K(M_B)$, once for $K(M_D)$.

LISTING OF MODIFIED SUBROUTINES

```
      SUBROUTINE CLP (EMZP,PA,PB,PC,PD,EMT,XT,RCT,IFTH,RSTAR,EPSB,GAMA)
C     ACP     1/30/71    WJG
      COMMON HSTAG,SSTAG,PSTAG,RHOSTG,ASTAR,TA,TB,TC,TD,TE,TF,TG
      IF (IFTH-1) 1,1,45
    1 IF(EMZP) 5,5,10
    5 EMZP=SQRT (((GAMA+1.)/2.)/RSTAR/RCT)
   10 IF(RCT) 15,15,20
   15 RCT=((GAMA+1.)/2.)/(RSTAR*EMZP**2)
   20 IF(IFTH) 30,30,25
C     THICKSTUN CENTER LINE
   25 PA=(EMT-1.)/XT**2
      PB=2./XT-EMZP/(EMT-1.)
      PC=0.0
      PD=0.0
      IF(PB+1./XT) 30,30,75
C     SCHAAF CENTER LINE
   30 IFTH=0
      PB=0.1
      DO 35 L=1,25
      PT = PB*XT
      EBX = EXP (PT*XT)
      EMX = EMZP/(2.*PT)
      PC = EMX*(1.-EBX) +EBX*(EMT - 1.)
      PCP = EMX*(EBX-1.)/PB + EBX*XT**2*(EMT-1.-EMX)
      HB = PC/PCP
      PB = PB - HB
      PD = L
      IF(ABS (HB) - EPSB) 40,40,35
   35 CONTINUE
   40 PA = EMZP/(2.*XT*PB) + 1. - EMT
      GO TO 75
C     HARRIS CENTER LINE
   45 READ (5,46) OMEGA,EMB,XER,RCPLUS
   46 FORMAT (4F10.5)
      TE=((1.+.2*EMT**2)/1.2)**3/EMT
      TD=((1.+.2*EMB**2)/1.2)**3/EMB
      TC=1./(2.*SIN(OMEGA/114.5916)*SQRT(TE))
      TB=2.4*EMB*SQRT(1.2*EMB/(1.+.2*EMB**2))/(TC*(EMB**2-1.))
      RCT=RCPLUS*RSTAR
      EMZP=SQRT (((GAMA+1.)/2.)/RSTAR/RCT)
      AXB=(TB-EMZP)/2.
      XB=(EMB-1.)/(AXB+EMZP)
      TA=XB
      PA=OMEGA
      PB=EMB
      PC=XER
      XT=TC*(SQRT(TE)-SQRT(TD))+TA
      XE=XER*XT
      TF=((XE-TA)/TC+SQRT(TD))**2
      EM=EMT-1.5*(XT-XE)
      I=0
   50 I=I+1
      EMSQ=EM**2
      FM=(5.+EMSQ)/6.
      DM=(EM*FM-TF*EMSQ/FM**2)/(FM-EMSQ)
      EM=EM+DM
      IF (ABS(DM)/EM-2.0E-05) 70,70,55
   55 IF (I-25) 50,50,60
```

```
   60 WRITE (6,65) EM,DM
   65 FORMAT (26H0   NO CONVERGENCE IN CLP    1P2E15.6//)
   70 EME=EM
      EMPE=3.456*SQRT(TF)*(EM/(1.+.2*EM**2))**2/(TC*(EM**2-1.))
      ADX=0.5*EMPE/EME
      ADXSQ=ALOG(EMT/EME)
      DX=ADXSQ/ADX
      A=ADX/DX
      XT=DX+XE
      PD=A
      TG=XE
      TE=AXB/XB
      TF=EMZP
   75 RETURN
      END




      SUBROUTINE CL (EMT,XT,PA,PB,PC,PD,EM,EMP,X,IFTH)
C     ACP     1/30/71    WJG
      COMMON HSTAG,SSTAG,PSTAG,RHOSTG,ASTAR,TA,TB,TC,TD,TE,TF,TG
      IF (IFTH-1) 10,5,15
C     THICKSTUN CENTER LINE
    5 EM=EMT-PA*(1.+PB*X)*(X-XT)**2
      EMP=-PA*(X-XT)*(PB*(3.*X-XT)+2.)
      GO TO 60
C     SCHAAF CENTER LINE
   10 EBX = EXP (PB*(X-XT)**2)
      EM = EMT - PA*(EBX-1.)
      EMP = -2.*PA*PB*(X-XT)*EBX
      GO TO 60
C     HARRIS CENTER LINE
   15 I=0
      EMZP=TF
      IF (X-TA) 20,20,25
   20 EM=1.+X*(EMZP+TE*X)
      EMP=EMZP+2.*TE*X
      GO TO 55
   25 IF (X-TG) 30,50,50
   30 FKM=((X-TA)/TC+SQRT(TD))**2
      EM=EM1
   35 I=I+1
      EMSQ=EM**2
      FM=(5.+EMSQ)/6.
      DM=(EM*FM-FKM*EMSQ/FM**2)/(FM-EMSQ)
      EM=EM+DM
      IF (ABS(DM)/EM-2.0E-05) 45,45,40
   40 IF (I-25) 35,35,45
   45 EMP=3.456*SQRT(FKM)*(EM/(1.+.2*EM**2))**2/(TC*(EM**2-1.))
      GO TO 55
   50 DX=XT-X
      EM=EMT*EXP(-PD*DX**2)
      EMP=2.*PD*DX*EM
   55 EM1=EM
   60 RETURN
      END
```

APPENDIX B

UTILITY PROGRAM FOR PREPARING
BOUNDARY LAYER INPUT DATA CARDS

In order to calculate the subsonic inlet contour using the option available in the boundary layer program, the gas properties for Mach numbers less than one must be supplied to the program. These properties are read into the boundary layer program from cards to avoid modifying the tape from the Axisymmetric Core Program which contains the gas properties only for the supersonic Mach numbers. If the Mach number at the beginning of the inlet is not too low, then the gas properties calculated during the isentropic expansion calculation may be sufficient to give the desired accuracy in the required interpolations. If not, the isentropic expansion can be recalculated and more subsonic data generated. In either case, the subsonic gas property data present on the isentropic expansion tape can be transferred to cards in the form required for the boundary layer program by using the utility program SUBSON listed below.

The only input to the program is the isentropic expansion tape which is mounted on unit 17. The program will read a set of subsonic data from the tape, convert it to the correct form, and punch the results into cards, repeating this procedure until the area ratio decreases below 1.0001. The data for area ratio equal to one (throat or sonic conditions) is then punched into the final card.

PROGRAM LISTING

```
 1 READ(17,2) NN,PSTAG,TT,RHOSTG,HSTAG,TZ,SSTAG,TAR,TSTAR,ASTAR,
   1PROSTR,RHOSTR,RHOQST,EMMAX,DELTAP
 2 FORMAT(37H1  ISENTROPIC EXPANSION TABLE NUMBER I4//18H SUPPLY COND
   1ITIONS/9H P(ATM.)=1PE14.7,11H T(KELVIN)=1PE14.7,22H RHO(SLUGS/CUBI
   2C FT.)=1PE14.7/23H ENTHALPY(BTU/LB.MASS)=1PE14.7,4H  Z=1PE14.7,
   36H  S/R=1PE14.7,10H A/ASTAR=1PE14.7//18H THROAT CONDITIONS/11H T(
   4KELVIN)=1PE14.7,18H  ASTAR(FT./SEC.)=1PE14.7,10H  P(ATM.)=1PE14.7/
   522H RHO(SLUGS/CUBIC FT.)=1PE14.7,30H  MASS FLOW(SLUGS/SQ.FT.SEC.)=
   61PE14.7//8H M MAX.=1PE14.7,9H  DELTAP=1PE14.7////120H      LOG10(P/
   7PT)         LOG10(RHO/RHOT)    H/HT            Z              A/ASTA
   8R(SNDSPD)  M             AREA/AREA STAR)
   DO 15 J=1,800
   READ (17,7) PRTL,RHORTL,HRT,Z,AR,EM,AREAR
 7 FORMAT (1P7E17.7)
   RVRSTR=SQRT(AREAR)
   PRT=10.**PRTL
   RHORT=10.**RHORTL
   Q=1.-HRT
   PUNCH 10,EM,RVRSTR,Q,PRT,RHORT
10 FORMAT (5F14.8)
   IF (AREAR-1.0001) 20,20,15
15 CONTINUE
20 PRT=PROSTR/PSTAG
   RHORT=RHOSTR/RHOSTG
   EM=1.
   RVRSTR=1.0
   Q=ASTAR**2/(50060.*HSTAG)
   PUNCH 10, EM,RVRSTR,Q,PRT,RHORT
   STOP
    END
```

APPENDIX C

COMPUTER PROGRAM FOR TURBULENT
BOUNDARY LAYER CALCULATIONS

The Real Gas Turbulent Boundary Layer Program (RGTBLP) presented
here has been developed for the calculation of turbulent boundary
layers in axisymmetric nozzles using air or nitrogen under conditions
where the gas no longer behaves like a perfect gas. The program,
valid for thick or thin boundary layers, is based on the method
developed by Tetervin (reference (16)) and uses the auxiliary
relations and the air and nitrogen properties discussed earlier in
this report. The air properties are valid for pressures up to 100
atmospheres and temperatures up to 5000°K. The nitrogen properties
are valid up to 1000 atmospheres and 3000°K. Above these values, the
program should be used with some caution.

The computer program has been set up to allow the calculation of
multiple cases using the same non-dimensionalized inviscid core
contour. Thus, the gas properties and coordinates for the inviscid
core are read only once, during the first case. This eliminates the
need for tape switching and (if the subsonic inlet option is being
used) large quantities of data cards. The supersonic inviscid core
data is input from the tape generated by the Axisymmetric Core
Program (ACP). The inviscid core data for the subsonic inlet and
throat regions is input from punched cards. These cards are required
only if the subsonic inlet is to be calculated. A utility program
for punching these cards from the isentropic expansion tape used as
input to the ACP program is given in Appendix B.

For very low Mach numbers at the beginning of the subsonic inlet,
it might be necessary to generate additional data for the subsonic
inlet calculation to ensure that the interpolation scheme used in the
program does not lead to large inaccuracies near the start of the

inlet. If required, additional data at very low Mach numbers can be
obtained by recalculating the isentropic expansion or by interpolating
the available data. For the nozzles discussed in this report,
additional data was obtained by rerunning Woolley's program with
finer temperature steps near the supply temperature. For the Mach
number 20 nozzle, it was also necessary to use linear interpolation
to generate even more data between the supply values and those at the
lowest Mach number calculated using Woolley's program. The total
number of inviscid core data cards was 85, 163, and 155 (18 by linear
interpolation) for the Mach number 10, 15, and 20 nozzles, respectively.
Except for the 18 points obtained by linear interpolation for the Mach
20 case, the temperatures used in rerunning Woolley's program to
generate the additional data for the subsonic inlet calculation have
been included in Table 3. Because of the large number of cards
involved, the inviscid core data are not included in the listing of data
input given in Table 5.

In order to maintain control over the interval of integration
used throughout the calculation (and to prevent errors caused by
backing up toward the starting point during the calculation), the
program-controlled variable interval of integration option available
in the utility integration package FNOL2 was not used. Instead, FNOL2
is used in its constant interval of integration mode. However, the
interval can be varied in a practical sense by dividing the nozzle
into sections of arbitrary length and integrating over each successive
section with the desired (constant) interval for that section. The
interval can be increased or decreased in successive sections, as
preferred. As indicated below, the interval DELX and the X coordinate
XEND (distance from the nozzle throat) at which the nozzle section
ends are read from a data card. The boundary layer is computed using
the interval DELX until X equals XEND. Then, another card with
values of DELX and XEND for the next nozzle section is read and the
process repeated. Each successive value of XEND must be greater than
the previous one, so that the calculation proceeds continuously toward
the nozzle exit. The last value of XEND must be equal to or greater
than the length of the supersonic portion of the nozzle (XEXIT) in

order that the program will terminate properly (and proceed to the
next case, if any). If the value of XEND given is greater than
XEXIT, then the calculation will stop at XEXIT. Therefore, to simplify
the choice of the last XEND, it is convenient to use some excessively
large value for XEND such as 999. (Units of XEND are feet).

PROGRAM INPUT

The data for this program are input from magnetic tape and from
punched cards. The tape input consists of the inviscid core contour
tape generated by the Axisymmetric Core Program (ACP). This tape is
mounted on tape unit 26. The card input consists of the following
six card groups, each consisting of one or more cards.

Group 1 Required for each case. This group consists of one card
identifying the gas to be used. Either AIR or NITROGEN
should be punched beginning in column 1. Since this program
is set up to calculate multiple cases (if desired), it will
automatically return to this READ after completing each case.
Therefore, a blank card is used after the last data set to
stop the program normally.

Group 2 Required for each case. This group is used to label the
beginning of the output with 0 - 50 lines of Hollerith
information, as desired. Card 1 controls the reading of the
Hollerith information from 0-50 cards following card 1. If
multiple cases are being run, lines 1 through LIN (see below)
plus up to 10 additional lines (arbitrarily distributed
among the 50 allowed) used for the previous case can be
replaced by new lines input from cards. This permits
replacement of some of the lines each run without the need
of re-entering lines which stay the same.

Card Number	Card Columns	Format Used	Variable Name	Definition
1	1-5	I5	LIN	Number of cards (lines) of labeling to be read in. Do not include replacement cards covered by LREPLC (see below).
	6-10	I5	LOUT	Total number of lines of labeling to be written out.

Card Number	Card Columns	Format Used	Variable Name	Definition
	11-60	10I5	LREPLC	Line numbers of 0-10 lines from previous case to be replaced for this case.
2-51	1-72	12A6	TITLE	Hollerith labeling, 72 characters per card. Number of cards (0-50) equal to LIN plus one for each non-zero value read for LREPLC.

Group 3 Required for each case. Two cards in this group contain most of the required initial values and control numbers. Several of the control numbers have default values, such that if the value read from the card is zero, a particular value is assigned in the program. This eliminates the need to punch control numbers for the most used options.

Card Number	Card Columns	Format Used	Variable Name	Definition
1	1-10	F10.5	THETA	Momentum thickness (ft) at initial station
	11-20	F10.5	REXIT	Radius (ft) of inviscid core at nozzle exit
	21-30	F10.5	XPUNCH	Axial distance (ft) from throat at which punching of nozzle coordinates into cards is to begin
	31-40	F10.5	XO	Axial distance (ft) from throat at which calculation begins. XO<0 for subsonic inlet calculation.
	41-50	F10.5	RO	Radius (ft) of subsonic inlet at XO. Ignored if XO≥0.
	51-60	F10.5	OMEGAO	Angle (degrees) of subsonic inlet at X0. OMEGAO <0 for converging wall at XO. Ignored if XO≥0.
	61-70	F10.5	HI	Shape parameter at initial station. If HI=0, program calculates starting value using THETA.

Card Number	Card Columns	Format Used	Variable Name	Definition
2	1-5	I5	NN	Identification number.
	6-10	I5	LM	Tape output control. If LM>0, output will be on tape 16 as well as on system tape.
	11-15	I5	NFS	Number of files to be skipped before reading inviscid core contour data from tape 26.
	16-20	I5	IP	Overridden by Group 6. Can be left blank.
	21-25	I5	J	Integration mode control. If 1, Runga-Kutta only. If 2, Runga-Kutta for first four and last intervals, Adams-Moulton for others. If 3, Runga-Kutta repeated for each step. (See reference (26) for details). The Adams-Moulton mode (J=2) is normally used.
	26-30	I5	LAWCF	Skin friction law control. If 1, Spalding-Chi law. If 2, Ludwieg-Tillmann law with reference enthalpy.

Group 4   Required only for the first case and even then only if the subsonic inlet option is to be used in one of the cases. This group of cards contains the inviscid core properties required for the subsonic inlet calculation. The form used for these properties is the same non-dimensionalized form used in the Axisymmetric Core Program (ACP) for the supersonic portion of the inviscid core. A utility routine for obtaining these cards from the isentropic expansion tape used as input to the ACP program is given in Appendix B. The last card of this group must correspond to the throat conditions, i.e. the Mach number must be one.

Card Number	Card Columns	Format Used	Variable Name	Definition
EACH	1-14	F14.8	EMW	Mach number
	15-28	F14.8	RVRSTR	Radius/throat radius (i.e. square root of area ratio)
	29-42	F14.8	QW	Ratio of square of flow velocity to twice the supply enthalpy
	43-56	F14.8	PW	Ratio of pressure to supply pressure
	57-70	F14.8	RORSTG	Ratio of density to supply density

Group 5 Required for each case. This card defines the wall temperature distribution to be used in the calculation. The three options available are: constant temperature wall, adiabatic wall, and prescribed temperature distribution based on equation (25). Variables TX(3), TX(4), TX(5), TX(6), TX(8) are ignored if prescribed temperature distribution is not used.

Card Number	Card Columns	Format Used	Variable Name	Definition
1	1-5	I5	M	Wall temperature option control. If 1, constant wall temperature. If 2, prescribed wall temperature distribution. If 3, adiabatic wall conditions
	6-15	F10.5	TX(2)	Constant wall temperature (°K) if M=1. Throat wall temperature (°K) if M=2. Starting guess for wall temperature (°K) at initial station if M=3.
	16-25	F10.5	TX(3)	Distance (ft) from throat of first intermediate temperature point for prescribed distribution.
	26-35	F10.5	TX(4)	Wall temperature (°K) at TX(3).

Card Number	Card Columns	Format Used	Variable Name	Definition
	36-45	F10.5	TX(5)	Distance (ft) from throat of second intermediate temperature point for prescribed distribution.
	46-55	F10.5	TX(6)	Wall temperature (°K) at TX(5).
	56-65	F10.5	TX(8)	Wall temperature (°K) at nozzle exit.

Group 6 Required for each case. These cards control the interval of integration (see discussion above) and the frequency of output for each section of the nozzle.

Card Number	Card Columns	Format Used	Variable Name	Definition
EACH	1-10	F10.5	DELX	Interval of integration (ft).
	11-20	F10.5	XEND	Distance (ft) from throat to downstream end of section in which DELX will be used. If XEND is greater than length of supersonic portion of nozzle (XEXIT), calculation will terminate at XEXIT.
	21-25	I5	IP	Output write frequency, e.g. output at every other step if IP=2. Regardless of value of IP, output will be written for first and last steps. If zero, program sets IP=1.

PROGRAM OUTPUT

Output written on the system tape will include all pertinent identification from the axisymmetric core contour tape used as input

plus nearly all the card input quantities listed in the previous
section. In addition, for each step of the integration at which
output is written (see IP in input card Group 6), a table of forty-
eight quantities is written. This table includes the gas properties
at the edge of the boundary layer, the various boundary layer thick-
nesses, heat transfer parameters and other quantities of interest.
Each page of tables is labeled with headings for easy identification
of the various quantities and the headings are defined at the
beginning of the output.* If a permanent copy of the output is
desired, the input quantity LM should be made greater than zero. In
this case, output identical to that written on the system tape will
be written on tape 16. In addition to the output written on tape,
the user can obtain the wall and core coordinates on punched cards.
This card output, governed by the two card input quantities IP and
XPUNCH, consists of the five quantities X, RW, R, XINCH, RWINCH, defined
as follows:

X	distance (ft) from nozzle throat along centerline
RW	radius (ft) of nozzle wall at X
R	radius (ft) of inviscid core at X
XINCH	X expressed in inches
RWINCH	RW expressed in inches

---

*The reader can identify the forty-eight quantities tabulated by
comparing the WRITE statement in subroutine OUT with the list of
definitions contained in subroutine LABEL3.

PROGRAM LISTING

```
C      REAL GAS TURBULENT BOUNDARY LAYER PROGRAM
C      RGTBLP ------ 1/30/71 ------ W.J.GLOWACKI
C
       COMMON EX,R,EM,RHOE,PE,UE,HE,REXIT,XEXIT,XT,HO,
      1       DXDX,DRDX,DEMDX,DRHODX,DPEDX,DUEDX,DHEDX,
      2       CF,COEFF,DELSTR,DELTA,DHIDX,DH1,DH2,DRWDX,
      3       DSVDEL,DSVTH,DSWDX,DTHDX,EMUE,GAS,HAD,HFI,
      4       HI,HJ,HK,HW,IP,IP1,LAWCF,LM,M,N,PAGE,PR,Q,
      5       RE,RECVRY,RETH,REYANL,RHOW,ROE,RW,ST,SUM1,
      6       SUM2,TE,THETA,THVDEL,TW,TX(8),XEND,XPUNCH,
      7       XTRA1,XTRA2,XTRA3,ZE
       DIMENSION Z(5),D(5)
       DATA AIR/6HAIR   /, GAS2 /6HNITROG/,BLANK/6H
C
C      PRANDTL NUMBER ASSUMED CONSTANT AT .72
       PR=.72
C      RECVRY = PRANDTL NUMBER TO 1/3 POWER
       RECVRY=.89628
C      REYANL = PRANDTL NUMBER TO -2/3 POWER
       REYANL=1.2448
C
   10 READ (5,20) GAS
   20 FORMAT (A6)
       IF (GAS.EQ.BLANK) GO TO 100
       IF (GAS.EQ.AIR)  GO TO 40
       IF (GAS.EQ.GAS2) GO TO 40
       WRITE (6,30) GAS
   30 FORMAT (1H1 A6,22H IS NOT AN ALLOWED GAS   )
       GO TO 100
C
   40 CALL LABEL1 (GAS)
C
       READ (5,50)THETA,REXIT,XPUNCH,X0,R0,OMEGA0,HI,NN,LM,NFS,IP,J,LAWCF
   50 FORMAT (7F10.5/6I5)
       IF (J.EQ.0) J=2
       IF (IP.EQ.0) IP=1
       IF (LAWCF.EQ.0) LAWCF=1
       IF (NFS.EQ.0) GO TO 70
       DO 60 NF=1,NFS
       EXTERNAL UN26
       CALL FSFILE (UN26)
   60 CONTINUE
   70 X=X0
       R=R0
       DRDX=TAN (OMEGA0/57.29578)
       IP1=1-IP
       PAGE=0.
C
       CALL CORE (X,LM,1)
       M=4
       CALL WALL (X)
       CALL LABEL2 (X0,R0,OMEGA0,NN,J)
       CALL CORE (X,LM,2)
       CALL LABEL3 (LM)
C
       IF (HI.GT.0.) GO TO 80
       CALL RHOTZE
       IF (GAS.EQ.AIR) CALL EMUAIR (HE,PE,EMUE)
       IF (GAS.NE.AIR) CALL EMUN2 (TE,RHOE,EMUE)
       RETH=UE*RHOE*THETA/EMUE
       RETHLG=ALOG10(RETH)
       HFI=10.**(0.599-RETHLG*(0.198-0.0189*RETHLG))
```

```
      HI=HFI
   80 Z(1)=THETA
      Z(2)=HI
      CF=0.
C
   90 READ (5,91) DELX,XEND,IP
   91 FORMAT (2F10.5,I5)
      IF (IP.EQ.0) IP=1
      EXTERNAL DER,TERM,OUT
      CALL FNOL2 (J,2,DELX,0,IP, 0,X,Z,D,DER,TERM,OUT)
      IF (XEND.LT.XEXIT) GO TO 90
C
   95 END FILE 16
      GO TO 10
C
  100 REWIND 16
      REWIND 26
      STOP
      END




      FUNCTION COMP(U,X)
C
C     REAL GAS TURBULENT BOUNDARY LAYER PROGRAM
C     RGTBLP ------ 1/30/71 ------ W.J.GLOWACKI
C
C     THIS SUBROUTINE EVALUATES Z FROM LOG10 P AND LOG10 RHO
C     AND IS IDENTICAL TO COMP USED IN AIETP DATED 7/01/65
C
      IF(U-0.5)10,5,5
    5 Y=-1.0
      GO TO 15
   10 Y=1.0
   15 AO=1.042+U*(1.069+U*(6.354E-3+U*(-3.3E-3+U*(-9.155E-4+U*(5.952E-4
     1+U*(2.866E-4+U*(4.287E-5+2.18E-6*U)))))))
      A1=-44.71+U*(8.358+U*(-.2318+U*(-.107+U*(-.1176+U*(1.642E-2+U*(
     12.461E-2+U*(5.21E-3+3.362E-4*U)))))))
      CO=1.137+U*(1.063+U*(2.836E-2+U*(1.698E-2+U*(-2.23E-4+U*(-2.836E-3
     1+U*(-8.384E-4+U*(-9.259E-5-3.451E-6*U))))))))
      C2=.1805+U*(-9.217E-2+U*(1.075E-2+U*(3.633E-3+U*(-1.602E-4+U*(
     1-4.084E-4+U*(-9.916E-5+U*(-8.743E-6-2.119E-7*U)))))))
      EO=1.435+U*(1.1+U*(3.016E-2+U*(1.447E-3+U*(-6.107E-3+U*(-2.075E-3
     1+U*(-1.37E-4+U*(2.689E-5+3.088E-6*U)))))))
      ZO=-15.*(U-.5)
      IF(ZO-10.)21,20,20
   20 E1=-22.0
      GO TO 30
   21 IF(ZO+8.)22,22,23
   22 E1=-56.6+9.8*U
      GO TO 30
   23 E1=-22.0+(9.8*U-34.6)/(1.+EXP (ZO))
   30 E2=-.2476+U*(-4.858E-2+U*(1.217E-2+U*(3.934E-3+U*(-3.705E-4+U*(
     1-5.415E-4+U*(-1.095E-4+U*(-5.681E-6+1.694E-7*U)))))))
      E3=.3904+U*(.3021+U*(4.053E-2+U*(-1.283E-2+U*(-1.935E-3+U*(
     15.477E-4+U*(2.667E-4+U*(4.022E-5+2.142E-6*U)))))))
      GO=1.87016+U*(1.08549+U*(2.39061E-2+U*(2.06972E-2+U*(1.71414E-2+U
     1*(6.45427E-3+U*(1.05835E-3+6.27306E-5*U))))))
      G1=-13.9930+U*(2.33941+U*(.431717+U*(.162394+U*(5.00809E-2+U*(
     17.94148E-3+4.80406E-4*U)))))
      G2=.408955+U*(-1.83205E-2+U*(-9.92156E-3+U*(5.94758E-3+U*(
     14.30655E-3+U*(9.39536E-4+U*(8.33593E-5+2.33120E-6*U)))))))
      G3=-.718311+U*(-.423658+U*(2.64678E-2+U*(1.17670E-2+U*(
     11.67085E-3+U*(5.85089E-5-2.21499E-6*U)))))
      FIO=2.462+U*(1.035+U*(-7.083E-3+U*(6.893E-3+U*(3.469E-3+U*(
```

```
      1-1.743E-4+U*(-4.025E-4+U*(-8.534E-5-5.571E-6*U)))))))
       FI1=-16.37+U*(1.561+U*(-.2057+U*(-5.558E-2+U*(4.067E-2+U*(1.993E-2
      1+U*(-2.783E-3+U*(-1.926E-3-1.952E-4*U)))))))
       FI2=.1986+U*(-8.448E-2+U*(-6.44E-4+U*(2.533E-4+U*(-6.545E-4+U*(
      1-5.846E-5+U*(8.109E-5+U*(2.085E-5+1.431E-6*U)))))))
   40 Z1=A1*(X-AO)
      IF(Z1-10.)42,41,41
   41 F1=0.0
      GO TO 51
   42 IF(Z1+8.)43,43,44
   43 F1=.3468*(X-AO)
      GO TO 50
   44 IF(ABS (Z1)-.01)45,45,46
   45 F1=-.3468/A1
      GO TO 51
   46 F1=.3468*(X-AO)/(1.-EXP (Z1))
   50 Z2=-100.*(X-CO)
      IF(Z2-10.)52,51,51
   51 F2=0.0
      GO TO 61
   52 IF(Z2+8.)53,53,54
   53 F2=C2*(X-CO)
      GO TO 60
   54 IF(ABS (Z2)-.01)55,55,56
   55 F2=.01*C2
      GO TO 61
   56 F2=C2*(X-CO)/(1.-EXP (Z2))
   60 Z3=E1*(X-EO)
      IF(Z3-10.)62,61,61
   61 F3=0.0
      GO TO 81
   62 IF(Z3+8.)63,63,64
   63 F3=E2*X+E3
      GO TO 80
   64 IF(Y) 65,70,70
   65 IF(ABS (Z3)-.01) 66,66,67
   66 F3=-E2/E1
      GO TO 81
   67 F3=E2*(X-EO)/(1.-EXP (Z3))
      GO TO 80
   70 F3=(E2*X+E3)/(1.+EXP (Z3))
   80 Z4=G1*(X-GO)
      IF(Z4-10.)82,81,81
   81 F4=0.0
      GO TO 91
   82 IF(Z4+8.)83,83,84
   83 F4=G2*X+G3
      GO TO 90
   84 F4=(G2*X+G3)/(1.+EXP (Z4))
   90 Z5=FI1*(X-FIO)
      IF(Z5-10.)92,91,91
   91 F5=0.0
      GO TO 100
   92 IF(Z5+8.)93,93,94
   93 F5=FI2*(X-FIO)
      GO TO 100
   94 IF(ABS (Z5)-.01)95,95,96
   95 F5=-FI2/FI1
      GO TO 100
   96 F5=FI2*(X-FIO)/(1.-EXP (Z5))
  100 RECIP=1.-F1-F2+F3+F4+F5
      COMP=1./RECIP
      RETURN
       END
```

```
      SUBROUTINE CORE (X,LM,L1)
C
C     REAL GAS TURBULENT BOUNDARY LAYER PROGRAM
C     RGTBLP ------ 1/30/71 ------ W.J.GLOWACKI
C
      COMMON QP,REXIT,XEXIT,XTRE,HSTAG,DQPDX
      DIMENSION Q(7), Q1(7), Q2(7), Q3(7), QP(7), DQPDX(7), A(7), B(7),
     1KP(999),XW(999),YW(999),EMW(999),PW(999),QW(999),RORSTG(999)
      DATA NCASE/0/
C
C     Q(1)=X, Q(2)=R, Q(3)=EM, Q(4)=RHOE, Q(5)=PE, Q(6)=UE, Q(7)=HE
C
      GO TO (10,200,390), L1
C
C     READ CORE PROPERTIES DURING FIRST CASE ONLY
   10 NCASE=NCASE+1
      IF (NCASE.GT.1) GO TO 40
C
C     READ HEADINGS IDENTIFYING EXPANSION AND CORE PROGRAM CALCULATIONS
      READ(26,20)NN,PSTAG,TT,RHOSTG,HSTAG,TZ,SSTAG,TAR,TSTAR,ASTAR,
     1PROSTR,RHOSTR,RHOQST,EMMAX,DELTAP
   20 FORMAT(37H1  ISENTROPIC EXPANSION TABLE NUMBER I4//18H SUPPLY COND
     1ITIONS/9H P(ATM.)=1PE14.7,11H T(KELVIN)=1PE14.7,22H RHO(SLUGS/CUBI
     2C FT.)=1PE14.7,23H ENTHALPY(BTU/LB.MASS)=1PE14.7,4H  Z=1PE14.7,
     36H  S/R=1PE14.7,10H  A/ASTAR=1PE14.7//18H THROAT CONDITIONS/11H T(
     4KELVIN)=1PE14.7,18H  ASTAR(FT./SEC.)=1PE14.7,10H  P(ATM.)=1PE14.7/
     522H RHO(SLUGS/CUBIC FT.)=1PE14.7,30H  MASS FLOW(SLUGS/SQ.FT.SEC.)=
     61PE14.7//8H M MAX.=1PE14.7,9H  DELTAP=1PE14.7////120H * * * * * *
     7* * * * * * * * * * * * * * * * * * * * * * * * * * * * * * * * * *
     8* * * * * * * * * * * * * * * * * * * * *)
      READ(26,30)NNN,EMT,RSTAR,XT,RCT,EMZP,IFTH,PA,PB,PC,PD,KT,KK,GAMA,
     1XZ,DZX,DTX,EPSA,EPSB
   30 FORMAT(46H0AXIALLY SYMMETRIC NOZZLE WALL CONTOUR NUMBER I3///23H T
     1ERMINAL MACH NUMBER =F10.6,16H THROAT RADIUS =1PE14.7//5H XT =1PE1
     24.7,10H    RCT =1PE14.7,11H    EMZP =1PE14.7//6H IFTH=I2,7H      P
     3A=1PE14.7,7H      PB=1PE14.7,7H      PC=1PE14.7,7H      PD=1PE14.7,7H
     4 KT=I3,4X,3HKK=I3//6H GAMA=1PE10.3,4X,3HXZ=1PE10.3,4X,4HDZX=1PE10.
     53,4X,4HDTX=1PE10.3,4X,5HEPSA=1PE10.3,4X,5HEPSB=1PE10.3/13H1 NN   K
     6   XW 14X,2HYW 14X,6HTHETAW 10X,2HMW 14X,9HPW/P STAG 7X,2HQW 14X,
     712HRHO/RHO STAG)
C
   40 WRITE(6,20)NN,PSTAG,TT,RHOSTG,HSTAG,TZ,SSTAG,TAR,TSTAR,ASTAR,
     1PROSTR,RHOSTR,RHOQST,EMMAX,DELTAP
      WRITE(6,50)NNN,EMT,RSTAR,XT,RCT,EMZP,IFTH,PA,PB,PC,PD,KT,KK,GAMA,
     1XZ,DZX,DTX,EPSA,EPSB
   50 FORMAT(46H0AXIALLY SYMMETRIC NOZZLE WALL CONTOUR NUMBER I3///23H T
     1ERMINAL MACH NUMBER =F10.6,16H THROAT RADIUS =1PE14.7//5H XT =1PE1
     24.7,10H    RCT =1PE14.7,11H    EMZP =1PE14.7//6H IFTH=I2,7H      P
     3A=1PE14.7,7H      PB=1PE14.7,7H      PC=1PE14.7,7H      PD=1PE14.7,7H
     4 KT=I3,4X,3HKK=I3//6H GAMA=1PE10.3,4X,3HXZ=1PE10.3,4X,4HDZX=1PE10.
     53,4X,4HDTX=1PE10.3,4X,5HEPSA=1PE10.3,4X,5HEPSB=1PE10.3/120H * * *
     6* * * * * * * * * * * * * * * * * * * * * * * * * * * * * * * * * *
     7* * * * * * * * * * * * * * * * * * * * * *)
      IF (LM.EQ.0) GO TO 60
      WRITE(16,20)NN,PSTAG,TT,RHOSTG,HSTAG,TZ,SSTAG,TAR,TSTAR,ASTAR,
     1PROSTR,RHOSTR,RHOQST,EMMAX,DELTAP
      WRITE(16,50)NNN,EMT,RSTAR,XT,RCT,EMZP,IFTH,PA,PB,PC,PD,KT,KK,
     1GAMA,XZ,DZX,DTX,EPSA,EPSB
   60 IF (NCASE.GT.1) GO TO 120
C
      STAGH=50060.*HSTAG
      STAGP=2116.*PSTAG
      XW(1)=0.
      YW(1)=RSTAR
      EMW(1)=1.
      PW(1)=PROSTR/PSTAG
```

```
      QW(1)=ASTAR**2/STAGH
      RORSTG(1)=RHOSTR/RHOSTG
      I=1
C
      IF (X.GE.0.)GO TO 100
C     READ INLET CORE PROPERTIES FROM CARDS
      I=0
   70 I=I+1
      READ (5,80) EMW(I),RVRSTR,QW(I),PW(I),RORSTG(I)
   80 FORMAT (5F14.8)
      YW(I)=RVRSTR*RSTAR
      IF (EMW(I).LT.1.) GO TO 70
      I2=I
C
C     READ CHARACTERISTIC CORE CONTOUR AND PROPERTIES FROM TAPE
  100 IF (I.EQ.999) GO TO 500
      I=I+1
      READ(26,110)NN,KP(I),XW(I),YW(I),THETAW,EMW(I),PW(I),QW(I),
     1RORSTG(I)
  110 FORMAT (2I4,7E16.7)
      IF (KP(I).LT.KT) GO TO 100
      XWLAST=XW(I)
  120 XEXIT=XWLAST*REXIT
      XTRE=XT*REXIT
      J=0
      L=1
      IF (X.GE.0.) GO TO 300
C
C     INTERP WILL INTERPOLATE TO FIND VALUES AT BEGINNING OF INLET
  130 XWO=X/REXIT
      YWO=QP(2)/REXIT
      DYDXO=DQPDX(2)
      JMAX=999
      CALL INTERP (3,JMAX,YW,EMW,YWO,EMWO,J)
      CALL INTERP (3,JMAX,YW,QW,YWO,QWO,J1)
      CALL INTERP (3,JMAX,YW,PW,YWO,PWO,J1)
      CALL INTERP (3,JMAX,YW,RORSTG,YWO,RORSTO,J1)
C
C     SUBROUTINE SHAPE WILL DETERMINE SHAPE OF INLET CORE CONTOUR
      CALL SHAPE (XWO,YWO,DYDXO,XW,YW,JMAX,J,I2)
C
C     START INTERPOLATIONS AT BEGINNING OF INLET
      Q(1)=REXIT*XWO
      Q(2)=REXIT*YWO
      Q(3)=EMWO
      Q(4)=RHOSTG*RORSTO
      Q(5)=STAGP*PWO
      Q(6)=SQRT(STAGH*QWO)
      Q(7)=HSTAG*(1.0-QWO)
      J=J+1
      GO TO 310
C
C     WRITE INLET CORE CONTOUR AND PROPERTIES INPUT FROM CARDS
  200 IF(X.GE.0.) GO TO 600
      WRITE(6,210)
  210 FORMAT (1H1 13X,85HSUBSONIC INVISCID CORE DATA REQUIRED FOR CALCUL
     *ATING BOUNDARY LAYER IN SUBSONIC INLET /1H0 13X,85H(FORM USED IS S
     *AME NON-DIMENSIONALIZED FORM USED IN ACP FOR SUPERSONIC INVISCID C
     *ORE)   //1H0 8X,1HI 8X,2HXW 14X,2HYW 14X,2HMW 11X,9HPW/P STAG 10X,
     1 2HQW 9X,13HRHOW/RHO STAG)
      IF (LM.GT.0) WRITE (16,210)
      DO 230 I1=1,I2
      WRITE (6,220)I1,XW(I1),YW(I1),EMW(I1),PW(I1),QW(I1),RORSTG(I1)
  220 FORMAT (I10,1P6E16.7)
      IF (LM.EQ.0) GO TO 230
      WRITE (16,220)I1,XW(I1),YW(I1),EMW(I1),PW(I1),QW(I1),RORSTG(I1)
```

```
    230 CONTINUE
        GO TO 600
C
    300 J=J+1
        Q(1)=REXIT*XW(J)
        Q(2)=REXIT*YW(J)
        Q(3)=EMW(J)
        Q(4)=RHOSTG*RORSTG(J)
        Q(5)=STAGP*PW(J)
        Q(6)=SQRT (STAGH*QW(J))
        Q(7)=HSTAG*(1.0-QW(J))
        GO TO (310,330,350),L
    310 DO 320 I=1,7
    320 Q1(I)=Q(I)
        L=2
        GO TO 300
    330 DO 340 I=1,7
    340 Q2(I)=Q(I)
        L=3
        GO TO 300
    350 DO 360 I=1,7
    360 Q3(I)=Q(I)
C       QP(I)=A(I)*R**2+B(I)*R+Q1(I)
    370 A1=Q2(1)-Q3(1)
        A2=Q1(1)-Q3(1)
        A3=Q1(1)-Q2(1)
        DEN=A1*A2*A3
        DO 380 I=2,7
        A(I)=((Q3(I)-Q1(I))*A3-(Q2(I)-Q1(I))*A2)/DEN
    380 B(I)=(Q1(I)-Q2(I))/A3+A(I)*A3
    390 QP(1)=X
        IF(QP(1)-Q3(1)) 400,400,420
    400 R=QP(1)-Q1(1)
        DO 410 I=2,7
        QP(I)=Q1(I)+R*(B(I)+R*A(I))
    410 DQPDX(I)=2.0*A(I)*R+B(I)
        GO TO 600
    420 IF(KT.LE.KP(J)) GO TO 400
        J=J+1
        Q(1)=REXIT*XW(J)
        Q(2)=REXIT*YW(J)
        Q(3)=EMW(J)
        Q(4)=RHOSTG*RORSTG(J)
        Q(5)=STAGP*PW(J)
        Q(6)=SQRT (STAGH*QW(J))
        Q(7)=HSTAG*(1.0-QW(J))
        DO 430 I=1,7
        Q1(I)=Q2(I)
        Q2(I)=Q3(I)
    430 Q3(I)=Q(I)
        IF(QP(1)-Q3(1))370,370,420
    500 WRITE(6,510)
    510 FORMAT (54H  STORAGE REQUIRED BY INPUT DATA EXCEEDS THAT ASSIGNED)
    600 RETURN
        END




        SUBROUTINE DER(X,Z,D)
C
C       REAL GAS TURBULENT BOUNDARY LAYER PROGRAM
C       RGTBLP ------ 1/30/71 ------ W.J.GLOWACKI
C
        COMMON EX,R,EM,RHOE,PE,UE,HE,REXIT,XEXIT,XT,HO,
       1        DXDX,DRDX,DEMDX,DRHODX,DPEDX,DUEDX,DHEDX,
```

```
      2          CF,COEFF,DELSTR,DELTA,DHIDX,DH1,DH2,DRWDX,
      3          DSVDEL,DSVTH,DSWDX,DTHDX,EMUE,GAS,HAD,HFI,
      4          HI,HJ,HK,HW,IP,IP1,LAWCF,LM,M,N,PAGE,PR,Q,
      5          RE,RECVRY,RETH,REYANL,RHOW,ROE,RW,ST,SUM1,
      6          SUM2,TE,THETA,THVDEL,TW,TX(8),XEND,XPUNCH,
      7          XTRA1,XTRA2,XTRA3,ZE
      8          ,CDLSTR,DLSTRR,THETAR,DTHRDX
      DIMENSION Z(5),D(5)
      DATA XPREV/-100./, AIR/6HAIR    /, APREV/-1./
C
C
C     COMPUTE FUNCTIONS OF X ON FIRST PASS ONLY
   10 IF (X.EQ.XPREV) GO TO 20
      XPREV=X
      Z(3)=X
      CALL CORE (X,0,3)
      RHOEUE=RHOE*UE
      DLNUE=DUEDX/UE
      DLNRHO=DRHODX/RHOE
      HEVHO=HE/HO
      DH2=RECVRY*(HO-HE)
      HAD=HE+DH2
      CALL WALL (X)
      DH1=HAD-HW
      FOFX=(0.5*DHEDX/HE-DLNUE)*HEVHO
      GOFX=32.174*RHOEUE*DH1
      CALL RHOTZE
      IF (GAS.EQ.AIR) CALL EMUAIR (HE,PE,EMUE)
      IF (GAS.NE.AIR) CALL EMUN2 (TE,RHOE,EMUE)
      RE=RHOEUE/EMUE
      N=1
C
C     COMPUTE FUNCTIONS DEPENDING ON THETA AND HI
   20 THETAR=Z(1)
      HI=Z(2)
      HJ=HI+1.
      HK=(HI-1.)/2.
      CALL GAUSS
      A=0.
      DO 30 I=1,20
      IF (THETA.NE.THETAR) A=DELTA/RW/DSWDX
      THRVDL=THVDEL-A*(2.*XTRA2/HJ-XTRA3/HI)
      DELTA=THETAR/THRVDL
      THETA=THVDEL*DELTA
      DELSTR=DSVDEL*DELTA
      DSRVDL=DSVDEL-A*(.5-2.*XTRA2/HJ)
      DLSTRR=DSRVDL*DELTA
      CDLSTR=RW*DSWDX*(1.-SQRT(1.-2.*A*DSRVDL))
      IF (CDLSTR.LE.0.) CDLSTR=DELSTR
      CALL SLOPE (X,CDLSTR,DRDX,DRWDX)
      DSWDX=SQRT(1.+DRWDX**2)
      RW=R+CDLSTR/DSWDX
      CONTRL=1.
      IF (A .NE. 0.) CONTRL=ABS(1.-APREV/A)
      IF (CONTRL .LE..0001.AND.I.GT.2) GO TO 40
      APREV=A
   30 CONTINUE
   40 RETH=RE*THETA
      RETHLG=ALOG10(RETH)
      HFI=10.**(0.599-RETHLG*(0.198-0.0189*RETHLG))
      CALL SKIN
      HALFCF=CF/2.
      ST=HALFCF*REYANL
      Q=ST*GOFX
      N=2
C
```

```
C       EVALUATE REQUIRED DERIVATIVES OF THETAR AND HI
        DTHRDX=HALFCF*DSWDX-THETAR*(DLNUE*(2.+DSVTH)+DLNRHO+DRWDX/RW)
        DHIDX=FOFX*HI*HJ**2*(HK+HI*SUM1-HJ*SUM2)-HALFCF*(HI+HFI)
       1     *(HI-HFI)*DSWDX/THETA
        D(1)=DTHRDX
        D(2)=DHIDX
        RETURN
         END




        SUBROUTINE EMUAIR (H,P,EMU)
C
C       REAL GAS TURBULENT BOUNDARY LAYER PROGRAM
C       RGTBLP ------ 1/30/71 ------ W.J.GLOWACKI
C
C
C       THIS SUBROUTINE EVALUATES THE VISCOSITY OF AIR USING
C       FITS TO THE DATA OF HANSEN  (NACA TN 4150, MAR 1968)
C
     11 EMUSTR=(4.654E-08*SQRT (H))/(1.0+48.47/H)
     12 IF(H-100.0)13,13,15
     13 EMU=EMUSTR
     14 GO TO 100
     15 IF(H-600.0)16,16,19
     16 X=ALOG10(H)-2.0
     17 EMU=EMUSTR*(1.0-0.066*X*X)
     18 GO TO 100
     19 Y=ALOG10(P/2116.0)+4.0
     20 Y2=Y*Y
     21 Y3=Y2*Y
     22 IF(H-2500.0)23,23,32
     23 X=ALOG10(H)-2.77815
     24 X2=X*X
     25 X3=X2*X
     26 A=2.9345-0.018506*Y3+0.34156*Y2-1.8930*Y
     27 B=-3.0797+0.012489*Y3-0.24747*Y2+1.5311*Y
     28 C=0.26833-0.0016713*Y3+0.032455*Y2-0.19542*Y
     29 D=0.960
     30 GO TO 99
     32 IF(H-5000.0)33,33,41
     33 X=ALOG10(H)-3.39794
     34 X2=X*X
     35 X3=X2*X
     36 A=-15.510-0.31453*Y3+2.9963*Y2-4.3024*Y
     37 B=6.1722+0.13513*Y3-1.3980*Y2+2.6807*Y
     38 C=-0.59538-0.010095*Y3+0.13061*Y2-0.38801*Y
     39 D=0.642-0.00058325*Y3+0.005875*Y2+0.017082*Y
     40 GO TO 99
     41 IF(H-15000.0)44,44,42
     42 WRITE(6,43)
     43 FORMAT(55H   H EXCEEDS 15000 BTU/LB, SUBROUTINE EMUAIR IS INVALID)
     44 X=ALOG10(H)-3.69897
     45 X2=X*X
     46 X3=X2*X
     47 A=0.69954+0.0214412*Y3-0.21721*Y2+0.65378*Y
     48 B=-0.12931-0.0056775*Y3+0.057196*Y2-0.25586*Y
     49 C=-0.42031-0.001909*Y3+0.024503*Y2-0.013625*Y
     50 D=0.599+4.175E-05*Y3+2.500E-04*Y2+2.5833E-02*Y
     99 EMU=EMUSTR*(A*X3+B*X2+C*X+D)
    100 RETURN
         END
```

```
      SUBROUTINE EMUN2 (TE,ROE,EMUE)
C
C     REAL GAS TURBULENT BOUNDARY LAYER PROGRAM
C     RGTBLP ------ 1/30/71 ------ W.J.GLOWACKI
C
C     THIS SUBROUTINE EVALUATES THE VISCOSITY OF NITROGEN USING THE
C     BREBACH-THODOS REDUCED-STATE CORRELATION FOR DIATOMIC GASES
C     REF.  INDUSTRIAL AND ENGINEERING CHEMISTRY   JULY 1958
C
      DATA J/0/
C
C     TC = TEMPERATURE AT CRITICAL POINT   (DEG.KELVIN)
C     EMUTC = VISCOSITY AT 1 ATM. AND TC   (CENTIPOISES)
C     A0 = CONVERSION FROM CENTIPOISES TO LBF SEC/FT**2
C     A1 = CONVERSION FROM G/CC TO SLUG/FT**3
C
C     EVALUATE CONSTANTS AT FIRST ENTRY OF ROUTINE ONLY
      IF (J.GT.0) GO TO 20
C     TC AND EMUTC FOR NITROGEN
   10 TC=126.2
      EMUTC=8.65E-03
      A0=2.08854E-05
      A1=1.94032
      A2=A0*EMUTC/TC**.979
      A3=1.7884*A0*EMUTC/SQRT(TC)
      A4=0.7884*TC
      A5=1.196*A0*EMUTC/TC**.659
      A6=.01198*A0/A1
      A7=.06410*A0/A1/A1
      T1=TC
      T2=3.5*TC
      J=1
C
C
C     COMPUTATION OF VISCOSITY WITHOUT DENSITY CORRECTION
C
C     BREBACH-THODOS CORRELATON FOR T/TC LESS THAN 1
   20 IF (TE.GT.T1) GO TO 30
      EMUE=A2*TE**.979
      GO TO 50
C
C     SUTHERLAND-TYPE LINK FOR T/TC BETWEEN 1 AND 3.5
   30 IF (TE.GT.T2) GO TO 40
      EMUE=A3*SQRT(TE)/(1.+A4/TE)
      GO TO 50
C
C     BREBACH-THODOS CORRELATON FOR T/TC GREATER THAN 3.5
   40 EMUE=A5*TE**.659
C
C
C     COMPUTATION OF DENSITY CORRECTION TO VISCOSITY
C     (NON-NEGATIVE FIT TO BREBACH-THODOS NITROGEN DATA)
   50 TR=TE/TC
      D1=EMUE/A0
      D2=D1/EMUTC
      DMUE=0.
      IF (ROE.LE..0194) GO TO 60
      DMUE=ROE*(A6+A7*ROE)
      EMUE=EMUE+DMUE
   60 D3=ROE/A1
      D4=DMUE/A0
      RETURN
       END
```

```
      FUNCTION ENTHLP(U,X)
C
C     REAL GAS TURBULENT BOUNDARY LAYER PROGRAM
C     RGTBLP ------ 1/30/71 ------ W.J.GLOWACKI
C
C     THIS SUBROUTINE EVALUATES H FROM LOG10 P AND LOG10 RHO
C     AND DIFFERS FROM ENTHLP USED IN AIETP DATED 7/01/65
C     ONLY IN THAT THE ERROR CORRECTIONS ARE NEGLECTED
C
      AA1=2.4876733E-2+U*(-8.2553890E-3+U*(9.3531968E-4+U*(-6.9802146E-4
     1+U*(-7.0256556E-5+U*(1.1449208E-4+U*(3.5362594E-5+U*(3.4741999E-6
     2+8.9880020E-8*U)))))))
      AA2=3.4894155+U*(-2.9193911E-2+U*(1.0481798E-2+U*(-2.6714733E-4
     1+U*(-2.6951449E-4+U*(-2.3151119E-4+U*(-6.2749893E-5+U*(-
     27.5707012E-6-3.6330450E-7*U)))))))
      AO=.36547857+U*(1.0189210+U*(-5.4844838E-3+U*(-2.7426243E-2+U*(
     1-7.7107391E-3+U*(2.4202901E-3+U*(1.4256573E-3+U*(2.2860249E-4+
     21.2352353E-5*U)))))))
      A1=-23.014062+U*(.46035662+U*(3.0044637E-2+U*(2.8921658E-2+U*(
     1-4.4337102E-3+U*(1.8974229E-4+U*(2.8921472E-3+U*(8.1853124E-4+
     26.2730577E-5*U)))))))
      A2=.71774971+U*(-6.9915246E-2+U*(-4.7677628E-2+U*(-7.2328367E-3
     1+U*(4.6877100E-3+U*(2.1195796E-3+U*(2.6545771E-4+U*(-4.6416051E-7
     2-1.4305115E-6*U)))))))
      CO=.94993342+U*(1.0187300+U*(-2.7831274E-2+U*(-3.3968208E-2+U*(
     1-7.5758964E-3+U*(4.3377145E-3+U*(2.3585523E-3+U*(3.9680529E-4+
     22.2767082E-5*U)))))))
      C1=-56.5+44.6/(1.+EXP (-U-1.75))
      C2=4.2598137+U*(-1.8016141+U*(.28493805+U*(2.5524034E-2+U*(
     1-2.806944CE-4+U*(-1.8133469E-3+U*(-9.7441476E-4+U*(-1.8356511E-4
     2-1.1383541E-5*U)))))))
      EO=1.374+1.046*U
      E1=-20.616464+U*(.99527941+U*(.36318074+U*(7.4026954E-2+U*(
     1-9.5602994E-3+U*(-6.8683405E-3+U*(-8.0744407E-4+U*(2.9434846E-5+
     27.0238870E-6*U)))))))
      E2=-.22188469+U*(-5.5351400E-2+U*(-8.3290583E-3+U*(-6.5111980E-4
     1+U*(1.3836166E-3+U*(8.2097136E-4+U*(1.9030699E-4+U*(2.0702239E-5+
     28.9265052E-7*U)))))))
      E3=.48990558+U*(.30389535+U*(7.2574817E-2+U*(-6.9748615E-3+U*(
     1-6.4693200E-3+U*(-5.8788707E-4+U*(7.7232629E-5+U*(5.3091414E-6-
     26.6747741E-7*U)))))))
      GO=1.835+1.043*U
      G1=-11.591952+U*(1.8211028+U*(1.8682006E-2+U*(3.8627552E-2+U*(
     11.7205973E-2+U*(-3.7323972E-3+U*(-2.2956386E-3+U*(-3.0764239E-4-
     21.2352353E-5*U)))))))
      G2=1.3480705+U*(.21904060+U*(-6.7552429E-3+U*(1.6563452E-2+U*(
     19.1140456E-3+U*(-2.3675397E-3+U*(-1.7376722E-3+U*(-2.9616734E-4-
     21.6477373E-5*U)))))))
      G3=-2.2628366+U*(-1.8824979+U*(-.28388494+U*(1.2905525E-2+U*(
     11.4367226E-2+U*(6.8502795E-6+U*(-9.3289221E-4+U*(-1.7551892E-4
     2-1.0293628E-5*U)))))))
      HO=2.376+1.046*U
      H1=-28.86+.507*U
      H2=.95+.38/(1.+EXP (2.5*(U+4.2)))
      Z1=E1*(X-EO)
      IF(Z1-10.)11,10,10
   10 FX1=0.0
      GO TO 21
   11 IF(Z1+8.)12,12,13
   12 FX1=E2*X+E3
      GO TO 20
   13 FX1=(E2*X+E3)/(1.+EXP (Z1))
   20 Z2=G1*(X-GO)
      IF(Z2-10.)22,21,21
   21 FX2=0.0
      GO TO 31
```

```
22 IF(Z2+8.)23,23,24
23 FX2=G2*X+G3
   GO TO 30
24 FX2=(G2*X+G3)/(1.+EXP (Z2))
30 Z3=H1*(X-HO)
   IF(Z3-10.)32,31,31
31 FX3=0.0
   GO TO 40
32 IF(Z3+8.)33,33,34
33 FX3=H2*(X-HO)
   GO TO 40
34 IF(ABS (Z3)-.01)35,35,36
35 FX3=-H2/H1
   GO TO 40
36 FX3=H2*(X-HO)/(1.-EXP (Z3))
40 XX=X-FX1-FX2-FX3
50 Z4=A1*(XX-AO)
   IF(74-10.)52,51,51
51 F1=0.0
   GO TO 61
52 IF(Z4+8.)53,53,54
53 F1=A2*(XX-AO)
   GO TO 60
54 IF(ABS (Z4)-.01)55,55,56
55 F1=-A2/A1
   GO TO 61
56 F1=A2*(XX-AO)/(1.-EXP (Z4))
60 Z5=C1*(XX-CO)
   IF(Z5-10.)62,61,61
61 F2=0.0
   GO TO 70
62 IF(Z5+8.)63,63,64
63 F2=C2*(XX-CO)
   GO TO 70
64 IF(ABS (Z5)-.01)65,65,66
65 F2=-C2/C1
   GO TO 70
66 F2=C2*(XX-CO)/(1.-EXP (Z5))
70 HRHOVP=AA1*XX+AA2+F1+F2
75 ENTHLP=33.687746*HRHOVP*10.**(X-U)
   RETURN
    END




      SUBROUTINE GAUSS
C
C     REAL GAS TURBULENT BOUNDARY LAYER PROGRAM
C     RGTBLP ------ 1/30/71 ------ W.J.GLOWACKI
C
C
C     THIS SUBROUTINE EVALUATES DELSTR/THETA AND DELTA/THETA BY
C     16 POINT GAUSSIAN INTEGRATION
C
      COMMON EX,R,EM,RHOE,PE,UE,HE,REXIT,XEXIT,XT,HO,
     1       DXDX,DRDX,DEMDX,DRHODX,DPEDX,DUEDX,DHEDX,
     2       CF,COEFF,DELSTR,DELTA,DHIDX,DH1,DH2,DRWDX,
     3       DSVDEL,DSVTH,DSWDX,DTHDX,EMUE,GAS,HAD,HFI,
     4       HI,HJ,HK,HW,IP,IP1,LAWCF,LM,M,N,PAGE,PR,Q,
     5       RE,RECVRY,RETH,REYANL,RHOW,ROE,RW,ST,SUM1,
     6       SUM2,TE,THETA,THVDEL,TW,TX(8),XEND,XPUNCH,
     7       XTRA1,XTRA2,XTRA3,ZE
      DIMENSION C(16),Z(16)
C
```

```
C     COEFFICIENTS FOR 16 POINT GAUSSIAN INTEGRATION
      DATA C/ .01357623, .031126762, .047579256, .062314485, .074797995,
     1         .08457826, .091301710, .094725305, .094725305, .091301710,
     2         .08457826, .074797995, .062314485, .047579256, .031126762,
     3         .01357623/         ,Z/ .005299535, .027712490, .067184400,
     4         .12229780, .191061880, .270991610, .359198220, .452493740,
     5         .54750626, .640801780, .729008390, .808938120, .877702200,
     6         .93281560, .972287510, .994700460/
C
      SUM1=0.0
      SUM2=0.0
      SUM3=0.
      SUM4=0.
      RO=ROE
      DO 10 J=1,16
      I=17-J
      UVUE=Z(I)**HK
      H=HW+UVUE*(DH1-UVUE*DH2)
      CALL RHOTZ (GAS,PE,H,RO,T,ZEE)
      TERM=(ROE/RO-1.)*C(I)
      TERM3=UVUE*Z(I)*(ROE/RO)*C(I)
      SUM1=SUM1+TERM
      SUM2=SUM2+TERM*Z(I)
      SUM3=SUM3+TERM3
      SUM4=SUM4+TERM3*UVUE
   10 CONTINUE
      A=SUM1+1.
      XTRA2=(1.-SUM3/A)/A
      XTRA3=(1.-SUM4/A)/A
      COEFF=(HI+1.)*HI/(HI-1.)
      DSVTH=COEFF*SUM1+HI
      DELVTH=COEFF*(SUM1+1.)
      THVDEL=1./DELVTH
      DSVDEL=DSVTH*THVDEL
      RETURN
       END




      SUBROUTINE HWALL (GAS,P,T,H,RHO)
C
C     REAL GAS TURBULENT BOUNDARY LAYER PROGRAM
C     RGTBLP ------ 1/30/71 ------ W.J.GLOWACKI
C
C     THIS SUBROUTINE COMPUTES HW FOR A GIVEN PE AND TW
C
      DATA C/2.3025851/, RHO0/2.423516E-03/, AIR/6HAIR
C
      IF (GAS.NE.AIR) GO TO 10
C
C     AIR CALCULATION
C     FOR AIR, WE ASSUME PRESSURE IS LOW ENOUGH SO HW = HW(T) ONLY
      DT=T-499.17
      H=.123406*T*(3.48+.00033175*DT/(1.-EXP(-.012287*DT)))
      GO TO 60
C
C     NITROGEN CALCULATION
   10 Z=1.
      RHOZ=P/(3196.8*T)
      IF (RHOZ.LE.RHO0) GO TO 40
      DO 20 I=1,50
      X=ALOG10(RHO/RHO0)
      Y=.00482*X*EXP(X)
      IF (X.LE.0.) Y=0.
      Z=1.+Y*X
```

```
      F=RHO*Z-RHOZ
      F1=Z+Y*(X+2.)/C
      RHO=RHO-F/F1
      Q=ABS(-F/F1/RHO)
      IF (Q.LE..000001) GO TO 50
   20 CONTINUE
      WRITE (6,30)
   30 FORMAT (28H0  NO CONVERGENCE IN HWALL    )
   40 RHO=RHOZ
   50 H=.12772*T*(Z+2.5)
      IF (T.LE.500.) GO TO 60
      B=EXP(-3390./T)
      H=H+432.971*B/(1.-B)
C
   60 RETURN
      END




      SUBROUTINE INTERP (J1,JMAX,X,Y,X0,Y0,JJ)
C
C     REAL GAS TURBULENT BOUNDARY LAYER PROGRAM
C     RGTBLP ------ 1/30/71 ------ W.J.GLOWACKI
C
C     THIS SUBROUTINE PERFORMS THREE POINT INTERPOLATION IN A TABLE
C     OF X AND Y TO FIND Y0 FOR A GIVEN X0.  THE SEARCH IS IN ONE
C     DIRECTION ONLY, BEGINNING AT J1 AND ENDING AT END OF TABLE.
C
      DIMENSION X(JMAX),Y(JMAX)
      DATA K/1/
C
      GO TO (10,20), K
   10 K=2
      SIGN=+1.
      IF (X(J1).GT.X(J1-1)) GO TO 20
      SIGN=-1.
   20 SX0=SIGN*X0
      DO 30 J=J1,JMAX
      SXAV=SIGN*(X(J-1)+X(J))/2.
      IF (SX0.LT.SXAV) GO TO 40
   30 CONTINUE
   40 DX01=X0-X(J-2)
      DX21=X(J-1)-X(J-2)
      DX31=X(J)-X(J-2)
      DY21=Y(J-1)-Y(J-2)
      DY31=Y(J)-Y(J-2)
      B=(DY31/DX31-DY21/DX21)/(DX31-DX21)
      A=DY21/DX21-B*DX21
      Y0=Y(J-2)+DX01*(A+B*DX01)
      JJ=J-2
      RETURN
      END




      SUBROUTINE LABEL1 (GAS)
C
C     REAL GAS TURBULENT BOUNDARY LAYER PROGRAM
C     RGTBLP ------ 1/30/71 ------ W.J.GLOWACKI
C
C     THIS SUBROUTINE READS A MAXIMUM OF 50 CARDS CONTAINING HOLLORITH
C     INFORMATION WHICH IS PRINTED AT BEGINNING OF OUTPUT.  FOR CASES
C     AFTER THE FIRST CASE, THIS ROUTINE PERMITS LINES 1 THROUGH LIN
C     PLUS UP TO 10 ADDITIONAL LINES (ARBITRARILY DISTRIBUTED AMONG
```

```
C       THE FIFTY ALLOWED) TO BE REPLACED BY NEW LINES INPUT FROM CARDS.
C
        DIMENSION LREPLC(10),TITLE(600)
        DATA AIR/6HAIR
C
C
C       READ IDENTIFYING AND DESCRIPTIVE TITLING (50 LINES MAXIMUM)
   10   READ (5,20) LIN,LOUT,(LREPLC(L),L=1,10)
   20   FORMAT (12I5)
        IIN=12*LIN
        IOUT=12*LOUT
        IF (LIN.EQ.0) GO TO 40
        READ (5,30) (TITLE(I),I=1,IIN)
   30   FORMAT (12A6)
   40   DO 50 L=1,10
        IF (LREPLC(L).EQ.0) GO TO 50
        I12=12*LREPLC(L)
        I1=I12-11
        READ (5,30) (TITLE(I),I=I1,I12)
   50   CONTINUE
C
C
C       WRITE IDENTIFYING AND DESCRIPTIVE TITLING (50 LINES MAXIMUM)
   60   IF (GAS.EQ.AIR) GO TO 80
        WRITE (6,70)
        WRITE (16,70)
   70   FORMAT (1H1 27X,45HNITROGEN TURBULENT BOUNDARY LAYER CALCULATION
      *         /28X,45H---------------------------------------------/////)
        GO TO 100
   80   WRITE (6,90)
        WRITE (16,90)
   90   FORMAT (1H1 27X,40HAIR TURBULENT BOUNDARY LAYER CALCULATION
      *         /28X,40H----------------------------------------  /////)
  100   IF (IOUT.EQ.0) GO TO 130
        WRITE (6,110) (TITLE(I),I=1,IOUT)
        WRITE (16,110) (TITLE(I),I=1,IOUT)
  110   FORMAT (1H 27X,12A6)
        WRITE (6,120)
        WRITE (16,120)
  120   FORMAT (1H0 // 43X,43H(THE NEXT PAGE IS A DUPLICATE OF THIS PAGE))
  130   IF (GAS.EQ.AIR) GO TO 140
        WRITE (6,70)
        WRITE (16,70)
        GO TO 150
  140   WRITE (6,90)
        WRITE (16,90)
  150   IF (IOUT.EQ.0) GO TO 200
        WRITE (6,110) (TITLE(I),I=1,IOUT)
        WRITE (16,110) (TITLE(I),I=1,IOUT)
C
  200   RETURN
        END




        SUBROUTINE LABEL2 (X0,R0,OMEGA0,NN,J)
C
C       REAL GAS TURBULENT BOUNDARY LAYER PROGRAM
C       RGTBLP ------ 1/30/71 ------ W.J.GLOWACKI
C
C       THIS SUBROUTINE WRITES AND IDENTIFIES FOR RECORD PURPOSES THE
C       DATA INPUT IN THE MAIN ROUTINE AND THE TEMPERATURE DISTRIBUTION
C
        COMMON EX,R,EM,RHOE,PE,UE,HE,REXIT,XEXIT,XT,HO,
      1        DXDX,DRDX,DEMDX,DRHODX,DPEDX,DUEDX,DHEDX,
```

```
      2           CF,COEFF,DELSTR,DELTA,DHIDX,DH1,DH2,DRWDX,
      3           DSVDEL,DSVTH,DSWDX,DTHDX,EMUE,GAS,HAD,HFI,
      4           HI,HJ,HK,HW,IP,IP1,LAWCF,LM,M,N,PAGE,PR,Q,
      5           RE,RECVRY,RETH,REYANL,RHOW,ROE,RW,ST,SUM1,
      6           SUM2,TE,THETA,THVDEL,TW,TX(8),XEND,XPUNCH,
      7           XTRA1,XTRA2,XTRA3,ZE
      DATA AIR/6HAIR    /
C
C
C
      IF (GAS.EQ.AIR) GO TO 30
   10 WRITE ( 6,20) NN,THETA,REXIT,XPUNCH,X0,R0,OMEGA0,HI,LM,IP,J,TX
      WRITE (16,20) NN,THETA,REXIT,XPUNCH,X0,R0,OMEGA0,HI,LM,IP,J,TX
   20 FORMAT (1H0/41H0NITROGEN TURBULENT BOUNDARY LAYER NUMBER I5//
     * 8H0THETA = 1PE14.7,8X,7HREXIT = 1PE14.7,9X,9HXPUNCH = 1PE14.7/
     * 8H0   X0 = 1PE14.7,10X,6HR0   = 1PE14.7,9X,9HOMEGA0 = 1PE14.7/
     * 8H0   HI = 1PE14.7,11X,4HLM = I2,11X,4HIP = I2,10X,3HJ = I2//
     * 25H0TEMPERATURE DISTRIBUTION /7X,2HX* 10X,2HT* 10X,2HX1 10X,2HT1
     * 10X,2HX2 10X,2HT2 10X,2HXE 10X,2HTE/ 4(0PF12.6,F12.4) // )
      GO TO 50
   30 WRITE ( 6,40) NN,THETA,REXIT,XPUNCH,X0,R0,OMEGA0,HI,LM,IP,J,TX
      WRITE (16,40) NN,THETA,REXIT,XPUNCH,X0,R0,OMEGA0,HI,LM,IP,J,TX
   40 FORMAT (1H0/36H0AIR TURBULENT BOUNDARY LAYER NUMBER I5//
     * 8H0THETA = 1PE14.7,8X,7HREXIT = 1PE14.7,9X,9HXPUNCH = 1PE14.7/
     * 8H0   X0 = 1PE14.7,10X,6HR0   = 1PE14.7,9X,9HOMEGA0 = 1PE14.7/
     * 8H0   HI = 1PE14.7,11X,4HLM = I2,11X,4HIP = I2,10X,3HJ = I2//
     * 25H0TEMPERATURE DISTRIBUTION /7X,2HX* 10X,2HT* 10X,2HX1 10X,2HT1
     * 10X,2HX2 10X,2HT2 10X,2HXE 10X,2HTE/ 4(0PF12.6,F12.4) // )
C
   50 GO TO (60,80), LAWCF
   60 WRITE ( 6,70)
      WRITE (16,70)
   70 FORMAT (46H0LAWCF = 1     (SPALDING-CHI SKIN FRICTION LAW) )
      GO TO 100
   80 WRITE ( 6,90)
      WRITE (16,90)
   90 FORMAT (80H0LAWCF = 2              (LUDWIEG-TILLMANN SKIN FRICTION LAW
     * WITH REFERENCE ENTHALPY) )
C
  100 RETURN
      END




      SUBROUTINE LABEL3 (LM)
C
C     REAL GAS TURBULENT BOUNDARY LAYER PROGRAM
C     RGTBLP ------ 1/30/71 ------ W.J.GLOWACKI
C
C
C     THIS SUBROUTINE WRITES A LIST IDENTIFYING THE HEADINGS USED
C     FOR THE TABULATED RESULTS OF THE BOUNDARY LAYER CALCULATION
C
      WRITE (6,10)
   10 FORMAT (1H1////44X,41HIDENTIFICATION OF HEADINGS AND UNITS USED
     * /44X,41H---------------------------------------- ///
     *//38X,55HD--/DX DENOTES THE DERIVATIVE OF -- WITH RESPECT TO X   //
     *//38X,57HCDLSTR    AXISYMMETRIC B.L.MASS CONSERVATION THICKNESS(FT)
     *//38X,57HCF        SKIN FRICTION COEFFICIENT
     *//38X,57HCUTOFF    OPTIMUM CUTOFF POINT OCCURS WHEN CUTOFF = 0
     *//38X,57HD--/DX    DERIVATIVE OF -- WITH RESPECT TO X
     *//38X,57HDELSTR    2-D BOUNDARY LAYER DISPLACEMENT THICKNESS   (FT)
     *//38X,57HDELTA     BOUNDARY LAYER THICKNESS   (FT)
     *//38X,57HDLINCH    BOUNDARY LAYER THICKNESS   (INCH)
     *//38X,57HDLSTRR    AXISYMMETRIC BOUNDARY LAYER THICKNESS   (FT)
     *//38X,57HDSVDEL    DELSTR / DELTA
     *//38X,57HDSVTH     DELSTR / THETA
```

```
      *//38X,57HEM          MACH NUMBER AT EDGE OF BOUNDARY LAYER
      *//38X,56HEMUE        VISCOSITY AT EDGE OF B.L.  (LBF SEC/FT2)            )
      WRITE (6,20)
   20 FORMAT (
      * /38X,57HERROR(1) TRUNCATION ERROR IN INTEGRATION OF DTHETA/DX
      *//38X,57HERROR(2) TRUNCATION ERROR IN INTEGRATION OF DHI/DX
      *//38X,57HHAD          ADIABATIC WALL ENTHALPY  (BTU/LBM)
      *//38X,57HHE           ENTHALPY AT EDGE OF BOUNDARY LAYER  (BTU/LBM)
      *//38X,57HHFI          SHAPE PARAMETER IN TRANSFORMED PLANE FOR DP/DX=0
      *//38X,57HHI           SHAPE PARAMETER IN TRANSFORMED PLANE
      *//38X,57HHW           WALL ENTHALPY  (BTU/LBM)
      *//38X,57HPE           PRESSURE AT EDGE OF BOUNDARY LAYER  (LBF/FT2)
      *//38X,57HQ            HEAT TRANSFER RATE AT NOZZLE WALL (BTU/FT2*SEC)
      */1H1///
      *//38X,57HR            RADIAL DISTANCE FROM AXIS TO EDGE OF B.L.  (FT)
      *//38X,57HRE           REYNOLDS NUMBER PER FOOT AT EDGE OF B.L.
      *//38X,56HRETH         REYNOLDS NUMBER BASED ON THETA                      )
      WRITE (6,30)
   30 FORMAT (
      * /38X,57HRHOE         DENSITY AT EDGE OF BOUNDARY LAYER  (SLUG/FT3)
      *//38X,57HRINCH        RADIAL DISTANCE FROM AXIS TO EDGE OF B.L. (INCH)
      *//38X,57HROE          APPROXIMATE DENSITY AT EDGE OF B.L.  (SLUG/FT3)
      *//38X,57HRW           RADIAL DISTANCE FROM AXIS TO NOZZLE WALL   (FT)
      *//38X,57HRWINCH       RADIAL DISTANCE FROM AXIS TO NOZZLE WALL   (INCH)
      *//38X,57HST           STANTON NUMBER CALCULATED USING REYNOLDS ANALOGY
      *//38X,57HSW           DISTANCE ALONG NOZZLE WALL CONTOUR  (FT)
      *//38X,57HTE           APPROXIMATE TEMPERATURE AT EDGE OF B.L. (DEG K)
      *//38X,57HTHETA        2-D BOUNDARY LAYER MOMENTUM THICKNESS  (FT)
      *//38X,57HTHETAR       AXISYMMETRIC B.L. MOMENTUM THICKNESS  (FT)
      *//38X,57HTW           WALL TEMPERATURE  (DEG K)
      *//38X,57HUE           VELOCITY AT EDGE OF BOUNDARY LAYER  (FT/SEC)
      *//38X,57HX            AXIAL DISTANCE FROM NOZZLE THROAT  (FT)
      *//38X,57HXINCH        AXIAL DISTANCE FROM NOZZLE THROAT  (INCH)
      *//38X,57HZE           APPROXIMATE COMPRESSIBILITY AT EDGE OF B.L.
      *////38X,53HD--/DX DENOTES THE DERIVATIVE OF -- WITH RESPECT TO X )
C
      IF (LM.EQ.0) GO TO 40
      WRITE (16,10)
      WRITE (16,20)
      WRITE (16,30)
C
   40 RETURN
      END




      SUBROUTINE OUT (X,Z,D,ERROR,K,L,H)
C
C     REAL GAS TURBULENT BOUNDARY LAYER PROGRAM
C     RGTBLP ------ 1/30/71 ------ W.J.GLOWACKI
C
C     THIS SUBROUTINE WRITES THE OUTPUT OF THE BOUNDARY
C     LAYER CALCULATION IN THE NOZZLE ON THE SYSTEM TAPE
C     AND, IF LM IS GREATER THAN ZERO, ON TAPE 16 ALSO.
C
      COMMON EX,R,EM,RHOE,PE,UE,HE,REXIT,XEXIT,XT,HO,
     1       DXDX,DRDX,DEMDX,DRHODX,DPEDX,DUEDX,DHEDX,
     2       CF,COEFF,DELSTR,DELTA,DHIDX,DH1,DH2,DRWDX,
     3       DSVDEL,DSVTH,DSWDX,DTHDX,EMUE,GAS,HAD,HFI,
     4       HI,HJ,HK,HW,IP,IP1,LAWCF,LM,M,N,PAGE,PR,Q,
     5       RE,RECVRY,RETH,REYANL,RHOW,ROE,RW,ST,SUM1,
     6       SUM2,TE,THETA,THVDEL,TW,TX(8),XEND,XPUNCH,
     7       XTRA1,XTRA2,XTRA3,ZE
     8       ,CDLSTR,DLSTRR,THETAR,DTHRDX
      DIMENSION Z(5),D(5),ERROR(30)
```

```
      DATA XPREV/-100./
C
      IF (X.EQ.XPREV) GO TO 70
      XPREV=X
      IP1=IP1+IP
      IF (IP1.EQ.1) I=0
      IF (I.GT.0) GO TO 30
C
      I=7
      PAGE=PAGE+1.
      WRITE (6,10) PAGE
   10 FORMAT (1H1 111X,4HPAGE F4.0//)
      WRITE (6,20)
   20 FORMAT (120H0        X                RW            UE           R              HE             E
     *M            RHOE             PE                     DR/DX                      DEM/DX
     */120H       DSW/DX        DRW/DX                        DR/DX                      DEM/DX
     *    DRHOE/DX         DPE/DX          DUE/DX          DHE/DX
     */120H         TW              HW            HAD                       TE
     *        ZE             ROE         ERROR(1)        ERROR(2)
     */120H       CUTOFF          DSVDEL          DSVTH                    XINCH
     *    RWINCH         RINCH         DLSTRR          CDLSTR
     */120H        RE             RETH             ST                      EMUE
     *      DHI/DX        DTHETAR/DX        DELSTR          DELTA
     */120H        POINT            CF              Q                      HFI
     *       HI            THETAR         THETA          DLINCH           )
      IF (LM.EQ.0) GO TO 30
      WRITE (16,10) PAGE
      WRITE (16,20)
C
   30 I=I-1
      CUTOFF=12.*(RW-DELTA-REXIT*(X-XT)/(XEXIT-XT))
      XINCH=12.*X
      RWINCH=12.*RW
      RINCH=12.*R
      DSINCH=12.*DELSTR
      DLINCH=12.*DELTA
      WRITE (6,40) X,RW,R,EM,RHOE,PE,UE,HE,DSWDX,DRWDX,DRDX,DEMDX,
     1 DRHODX,DPEDX,DUEDX,DHEDX,TW,HW,HAD,TE,ZE,ROE,ERROR(1),
     2 ERROR(2),CUTOFF,DSVDEL,DSVTH,XINCH,RWINCH,RINCH,DLSTRR,CDLSTR,RE,
     3 RETH,ST,EMUE,DHIDX,DTHRDX,DELSTR,DELTA,IP1,CF,Q,HFI,HI,THETAR,
     4 THETA,DLINCH
   40 FORMAT (1H /5(1P8E15.6/) I10,5X,1P7E15.6)
      IF (LM.EQ.0) GO TO 50
      WRITE (16,40)X,RW,R,EM,RHOE,PE,UE,HE,DSWDX,DRWDX,DRDX,DEMDX,
     1 DRHODX,DPEDX,DUEDX,DHEDX,TW,HW,HAD,TE,ZE,ROE,ERROR(1),
     2 ERROR(2),CUTOFF,DSVDEL,DSVTH,XINCH,RWINCH,RINCH,DLSTRR,CDLSTR,RE,
     3 RETH,ST,EMUE,DHIDX,DTHRDX,DELSTR,DELTA,IP1,CF,Q,HFI,HI,THETAR,
     4 THETA,DLINCH
   50 IF (X.LT.XPUNCH) GO TO 70
      PUNCH 60,X,RW,R,XINCH,RWINCH
   60 FORMAT (0PF10.5,1P4E15.7)
   70 RETURN
      END




      SUBROUTINE RHOTZ (GAS,P,H,RHO,T,Z)
C
C     REAL GAS TURBULENT BOUNDARY LAYER PROGRAM
C     RGTBLP ------ 1/30/71 ------ W.J.GLOWACKI
C
C     THIS SUBROUTINE COMPUTES RHO, T, AND Z FOR A GIVEN P AND H.
C     FOR NITROGEN, THE CURVE-FITS OF HARRIS ARE USED, WHILE
C     FOR AIR, THE CURVE-FITS OF GRABAU ARE USED.
C
```

```
      DATA C/2.3025851/, RHO0/2.423516E-03/, AIR/6HAIR    /
C
C
      IF (GAS.EQ.AIR) GO TO 60
C
C     NITROGEN CALCULATION
      PATM=P/2116.
      HOVR=H/.127716
      ROAMAG=RHO/RHO0
      DO 30 I=1,50
      X=ALOG10(ROAMAG)
      IF (X.GT.0.) GO TO 10
      Y=0.
      Z=1.
      T=HOVR/3.5
      IF (T.GT.500.) GO TO 20
      ROAMAG=273.16*PATM/T
      GO TO 50
   10 Y=.00482*X*EXP(X)
      Z=1.+Y*X
   20 T=273.16*PATM/(Z*ROAMAG)
      E0=3390./T
      E1=0.
      IF (T.GT.500.) E1=EXP(-3390./T)
      IF (E0.LE..01) E2=T/(1.-E0*(.5-E0/6.))
      IF (E0.GT..01) E2=3390./(1.-E1)
      F=HOVR-(Z+2.5)*T-E1*E2
      F1=T*(Z+(2.5+E1*(E2/T)**2)*(1.+Y*(X+2.)/Z/C))/ROAMAG
      ROAMAG=ROAMAG-F/F1
      Q=ABS(-F/F1/ROAMAG)
      IF (Q.LE..000001) GO TO 50
   30 CONTINUE
      WRITE (6,40) Q
   40 FORMAT (28H0   NO CONVERGENCE IN RHOTZ,    3HQ =F9.7)
   50 RHO=ROAMAG*RHO0
      GO TO 130
C
C     AIR CALCULATION
   60 X4=ALOG10(RHO/0.0025089296)
      X=ALOG10(P/2116.0)
      Y4=H-ENTHLP(X4,X)
      X2=X4
      Y2=Y4
      X4=0.95*X4
      X3=X4
      Y4=H-ENTHLP(X4,X)
      Y3=Y4
      DX=X3-X2
      DY=Y3-Y2
      X4=X3-Y3*DX/DY
      Y4=H-ENTHLP(X4,X)
      DO 100 I=1,20
      X1=X2
      Y1=Y2
      X2=X3
      Y2=Y3
      X3=X4
      Y3=Y4
      DXP=DX
      DYP=DY
      DX=X3-X2
      DY=Y3-Y2
      DIV=DXP*DY-DX*DYP
      IF(DIV.EQ.0.) GO TO 70
      DELINV=(DX+DXP)*DXP/DIV
      RADIC=(DX+DY*DELINV)**2-4.*Y3*DX*DELINV
```

```
      IF(RADIC.LT.0.) GO TO 80
      XX=SQRT (RADIC)
      XL=X3+X2-DY*DELINV
      X4=.5*(XL+XX)
      XL=.5*(XL-XX)
      XBAR=X3-Y3*DX/DY
      DXR=ABS (X4-XBAR)
      DXL=ABS (XL-XBAR)
      IF(DXR.LE.DXL) GO TO 90
      X4=XL
      GO TO 90
   70 X4=X3-Y3*DX/DY
      GO TO 90
   80 X4=Y3-.25*(DX+DY*DELINV)**2/(DELINV*DX)
   90 Y4=H-ENTHLP(X4,X)
      TEST=ABS ((X4-X3)/X4)
      IF (TEST.GT..0001) GO TO 100
      IF (Y4.GE.-.001.AND.Y4.LE..001) GO TO 120
  100 CONTINUE
      WRITE(6,110)
  110 FORMAT (28H0  NO CONVERGENCE IN RHOTZ,   6HTEST = F7.5)
  120 R=0.0025089296*EXP (X4/0.43429448)
      RHO=R
      Z=COMP(X4,X)
      T=3.2373132E-04*P/Z/RHO
C
  130 RETURN
      END




      SUBROUTINE RHOTZE
C
C     REAL GAS TURBULENT BOUNDARY LAYER PROGRAM
C     RGTBLP ------ 1/30/71 ------ W.J.GLOWACKI
C
C
C     THIS SUBROUTINE EVALUATES THE DENSITY, TEMPERATURE, AND
C     COMPRESSIBILITY (ROE,TE,ZE) AT THE EDGE OF THE BOUNDARY
C     LAYER.  FOR NITROGEN, THE VALUES ARE ONLY APPROXIMATE IF THE
C     ISENTROPIC EXPANSION DATA USED IN DETERMINING THE INVISCID
C     CORE WAS OBTAINED FROM WOOLLEYS PROGRAM.  IF THE DATA WAS
C     OBTAINED FROM THE EXPANSION PROGRAMS LABELED AIETP OR NIETP,
C     THEN THE VALUES ARE EXACT AS THE SAME EQUATIONS ARE USED.
C
      COMMON EX,R,EM,RHOE,PE,UE,HE,REXIT,XEXIT,XT,HO,
     1       DXDX,DRDX,DEMDX,DRHODX,DPEDX,DUEDX,DHEDX,
     2       CF,COEFF,DELSTR,DELTA,DHIDX,DH1,DH2,DRWDX,
     3       DSVDEL,DSVTH,DSWDX,DTHDX,EMUE,GAS,HAD,HFI,
     4       HI,HJ,HK,HW,IP,IP1,LAWCF,LM,M,N,PAGE,PR,Q,
     5       RE,RECVRY,RETH,REYANL,RHOW,ROE,RW,ST,SUM1,
     6       SUM2,TE,THETA,THVDEL,TW,TX(8),XEND,XPUNCH,
     7       XTRA1,XTRA2,XTRA3,ZE
      DATA AIR/6HAIR   /,RHOO,PO/.0025089296,2116./
C
C
      ROE=RHOE
      IF (GAS.EC.AIR) GO TO 10
C
C     NITROGEN CALCULATION
      CALL RHOTZ (GAS,PE,HE,ROE,TE,ZE)
      GO TO 20
C
C     AIR CALCULATION
```

```
   10 U=ALOG10(RHOE/RHO0)
      X=ALOG10(PE/P0)
      ZE=COMP(U,X)
      TE=3.2373132E-04*PE/ZE/RHOE
C
   20 RETURN
      END




      SUBROUTINE SHAPE (X0,Y0,DYDX0,X,Y,JMAX,K0,I)
C
C     REAL GAS TURBULENT BOUNDARY LAYER PROGRAM
C     RGTBLP ------ 1/30/71 ------ W.J.GLOWACKI
C
C
C
C     THIS SUBROUTINE DETERMINES THE SHAPE OF THE SUBSONIC
C     INLET DEFINED BY QUARTIC   Y=(((A*X+B)*X+C)*X+D)*X+E
C     USING R, DR/DX SPECIFIED AT BEGINNING OF INLET (X=X0),
C     AND USING R, DR/DX (=0), D2R/DX2 AT NOZZLE THROAT (X=0)
C     WITH D2R/DX2 DETERMINED BY FITTING A QUADRATIC (WITH ZERO SLOPE
C     AT THROAT) TO THROAT AND FIRST CHARACTERISTIC CORE POINT
C
      DIMENSION X(JMAX),Y(JMAX)
C
      X03=X0**3
      YSTAR=Y(I)
C
C     DETERMINE CONSTANTS FOR QUARTIC INLET GEOMETRY
      E=YSTAR
      D=0.
      C=(Y(I+1)-YSTAR)/X(I+1)**2
      B=(4.*(Y0-YSTAR)-X0*(2.*C*X0+DYDX0))/X03
      A=((C*X0+DYDX0)-3.*(Y0-YSTAR)/X0)/X03
C
C     INITIAL GUESS FOR EX NEAR THROAT FROM TAYLOR SERIES EXPANSION
C     Y-Y* = (X-X*)(DY/DX)* + 0.5(X-X*)**2(D2Y/DX2)* = C(X**2)
      EX=-SQRT((Y(I-1)-YSTAR)/C)
C
C
C     USE NEWTON-RAPHSON METHOD TO INVERT QUARTIC TO OBTAIN X FROM Y
   10 K1=K0+2
      K2=I-1
      DO 50 K=K1,K2
      K3=K1+K2-K
      WY=Y(K3)
      DO 20 L=1,100
      F=((A*EX+B)*EX+C)*EX*EX+E-WY
      F1=((4.*A*EX+3.*B)*EX+2.*C)*EX
      ERROR=-F/F1
      Q=ABS(ERROR)/EX
      EX=EX+ERROR
      IF (Q.LT..000001) GO TO 40
   20 CONTINUE
      WRITE (6,30) WY,EX,ERROR,Q
   30 FORMAT (36H0   INLET ITERATION DID NOT CONVERGE   /1P4E15.7//)
   40 X(K3)=EX
   50 CONTINUE
      X(I)=0.
      RETURN
      END
```

```
      SUBROUTINE SKIN
C
C     REAL GAS TURBULENT BOUNDARY LAYER PROGRAM
C     RGTBLP ------ 1/30/71 ------ W.J.GLOWACKI
C
      COMMON EX,R,EM,RHOE,PE,UE,HE,REXIT,XEXIT,XT,HO,
     1       DXDX,DRDX,DEMDX,DRHODX,DPEDX,DUEDX,DHEDX,
     2       CF,COEFF,DELSTR,DELTA,DHIDX,DH1,DH2,DRWDX,
     3       DSVDEL,DSVTH,DSWDX,DTHDX,EMUE,GAS,HAD,HFI,
     4       HI,HJ,HK,HW,IP,IP1,LAWCF,LM,M,N,PAGE,PR,Q,
     5       RE,RECVRY,RETH,REYANL,RHOW,ROE,RW,ST,SUM1,
     6       SUM2,TE,THETA,THVDEL,TW,TX(8),XEND,XPUNCH,
     7       XTRA1,XTRA2,XTRA3,ZE
      DATA AIR/6HAIR    /
C
C
      GO TO (10,60), LAWCF
C
C
C     SPAULDING - CHI LAW   (REF.   J.FL.MECH.   JAN.64)
   10 GO TO (20,30), N
   20 FTHETA =(HE/HW)**.702*(HAD/HW)**.772
      ASQ=DH2/HW
      IF (ASQ .LT. 0.) ASQ=0.
      B=DH1/HW
      D1=SQRT(4.*ASQ+B**2)
      D2=ARSIN((2.*ASQ-B)/D1)+ARSIN(B/D1)
      FC=DH2/HE/D2**2
      IF (CF.GT.0.) GO TO 30
      FCCF=2./(5.77*ALOG10(FTHETA*RETH)+3.8)**2
      CF=FCCF/FC
   30 UGPLUS=SQRT(2./(FC*CF))
      FTHRTH=FTHETA*RETH
      DO 40 INDEX=1,25
      X=0.4*UGPLUS
      XSQ=X**2
      EXPX=EXP(X)
      FUNC = - FTHRTH + UGPLUS**2/6.+((1.-2./X)*EXPX + 2./X+1. -XSQ*(30.
     1+X*(15.+X*(4.5+X)))/180.)/4.8
      DERIV=UGPLUS/3.+(((XSQ -2.*X+2.)*EXPX - 2.)/XSQ -X*(12.+X*(9.+X*
     1(3.6+X)))/36.)/12.
      ERROR=-FUNC/DERIV
      UGPLUS=UGPLUS+ERROR
      IF (ABS(ERROR)/UGPLUS-.0001) 50,50,40
   40 CONTINUE
   50 FCCF=2./UGPLUS**2
      CF=FCCF/FC
      RETURN
C
C
C     LUDWIEG - TILLMANN LAW WITH REFERENCE ENTHALPY
   60 GO TO (70,90), N
   70 HREF=0.5*(HW+HE)+0.22*(HAD-HE)
      CALL RHOTZ (GAS,PE,HREF,RHOREF,TREF,ZREF)
      IF (RHOREF.LE.0.) RHOREF=3.5*PE/(25030.*HREF)
      IF (GAS.EQ.AIR) CALL EMUAIR (HREF,PE,EMUREF)
      IF (GAS.NE.AIR) CALL EMUN2 (TREF,RHOREF,EMUREF)
   80 REREF=RHOREF*UE/EMUREF
      FACTOR= 0.246*(RHOREF/ROE)**1.268
   90 CF=FACTOR*10.**(-.678*DSVTH)/((REREF*THETA)**0.268)
      RETURN
       END
```

```
      SUBROUTINE SLOPE (X3,DELSTR,DRDX,DRWDX)
C
C     REAL GAS TURBULENT BOUNDARY LAYER PROGRAM
C     RGTBLP ------ 1/30/71 ------ W.J.GLOWACKI
C
C     THIS SUBROUTINE COMPUTES AN APPROXIMATE VALUE OF THE WALL
C     SLOPE (DRW/DX).  THE VALUE OF DRW/DX IS OBTAINED BY ADDING
C     THE CORE SLOPE (DR/DX) TO THE X-DERIVATIVE OF THE DISPLACEMENT
C     THICKNESS (DELSTR).  D(DELSTR)/DX IS OBTAINED BY FITTING A
C     QUADRATIC IN X TO DELSTR AT THREE CONSECUTIVE POINTS.
C
      DATA X2,DX21,DX32/-100.,0.,0./
C
      DRWDX=DRDX
      IF (X3-X2) 10,30,20
   10 X2=-100.
      DX21=0.
      DX32=0.
   20 OKAY=DX21
      DX21=DX32
      DX32=X3-X2
      DR21=DR32
      X2=X3
      R2=R3
      DRDXP=DRDX1
      DRDX1=DRDX
   30 R3=DELSTR
      DR32=R3-R2
      IF (OKAY) 40,50,40
   40 DRWDX2=(DR32*DX21/DX32+DR21*DX32/DX21)/(DX32+DX21)+DRDXP
      DRWDX3=2.*DR32/DX32-(DRWDX2-DRDXP)+DRDX
      DRWDX=DRWDX3
   50 RETURN
      END




      SUBROUTINE TERM(X,Z,D,F)
C
C     REAL GAS TURBULENT BOUNDARY LAYER PROGRAM
C     RGTBLP ------ 1/30/71 ------ W.J.GLOWACKI
C
C     THIS SUBROUTINE PROVIDES THE TERMINATION CONDITION REQUIRED BY
C     FNOL2.  TERMINATION WILL BE AT X = XEND UNLESS XEND EQUALS OR
C     EXCEEDS 999. IN WHICH CASE TERMINATION WILL BE AT NOZZLE EXIT.
C
      COMMON EX,R,EM,RHOE,PE,UE,HE,REXIT,XEXIT,XT,HO,
     1       DXDX,DRDX,DEMDX,DRHODX,DPEDX,DUEDX,DHEDX,
     2       CF,COEFF,DELSTR,DELTA,DHIDX,DH1,DH2,DRWDX,
     3       DSVDEL,DSVTH,DSWDX,DTHDX,EMUE,GAS,HAD,HFI,
     4       HI,HJ,HK,HW,IP,IP1,LAWCF,LM,M,N,PAGE,PR,Q,
     5       RE,RECVRY,RETH,REYANL,RHOW,ROE,RW,ST,SUM1,
     6       SUM2,TE,THETA,THVDEL,TW,TX(8),XEND,XPUNCH,
     7       XTRA1,XTRA2,XTRA3,ZE
      DIMENSION Z(5),D(5)
C
      IF (XEND.CE.999.) GO TO 20
C
C     END AT SPECIFIED LOCATION
   10 F=X-XEND
      GO TO 30
C
C     END AT NOZZLE EXIT
   20 F=X-XEXIT
   30 RETURN
      END
```

```
      SUBROUTINE WALL (X)
C
C     REAL GAS TURBULENT BOUNDARY LAYER PROGRAM
C     RGTBLP ------ 1/30/71 ------ W.J.GLOWACKI
C
C
C
C     THIS SUBROUTINE EVALUATES THE ENTHALPY AND/OR TEMPERATURE
C     AT THE WALL ACCORDING TO THE OPTION SPECIFIED BY M
C
C     IF M=4, READ TEMPERATURE DISTRIBUTION CARD
C     IF M=3, COMPUTE TW FROM ADIABATIC WALL ENTHALPY.  INITIAL
C             GUESS FOR TW AT FIRST POINT MUST BE SUPPLIED.
C     IF M=2, COMPUTE TW AND HW FOR GIVEN TEMPERATURE DISTRIBUTION
C     IF M=1, TW IS CONSTANT ALONG NOZZLE BUT HW VARIES UNLESS Z=1
C
      COMMON EX,R,EM,RHOE,PE,UE,HE,REXIT,XEXIT,XT,HO,
     1       DXDX,DRDX,DEMDX,DRHODX,DPEDX,DUEDX,DHEDX,
     2       CF,COEFF,DELSTR,DELTA,DHIDX,DH1,DH2,DRWDX,
     3       DSVDEL,DSVTH,DSWDX,DTHDX,EMUE,GAS,HAD,HFI,
     4       HI,HJ,HK,HW,IP,IP1,LAWCF,LM,M,N,PAGE,PR,Q,
     5       RE,RECVRY,RETH,REYANL,RHOW,ROE,RW,ST,SUM1,
     6       SUM2,TE,THETA,THVDEL,TW,TX(8),XEND,XPUNCH,
     7       XTRA1,XTRA2,XTRA3,ZE
C
C
      GO TO (60,40,70,10), M
C
C
C     READ M,T*,X1,T1,X2,T2,TEXIT
   10 READ (5,20) M,(TX(I),I=2,6),TX(8)
   20 FORMAT (I5,6F10.5)
      TX(1)=0.
      TX(7)=XEXIT
      TW=TX(2)
C     INITIAL GUESS FOR RHOW
      RHOW=PE/(3196.8*TW)
      GO TO (80,30,80), M
C
C
C     EVALUATE CONSTANTS OF STATEMENT 30 FROM INPUT DATA
   30 DTOE=TX(2)-TX(8)
      F=ALOG(DTOE/(TX(4)-TX(8)))
      E=ALOG(DTOE/(TX(6)-TX(8)))
      D=TX(8)
      C=ALOG10(F/E)/ALOG10(TX(3)/TX(5))
      B=F**(1./C)/TX(3)
      A=DTOE
      GO TO 80
C
C
C     EVALUATE HW FROM TW
   40 IF (X.GE.0.) GO TO 50
      TW=A+D
      GO TO 60
   50 TW=A*EXP(-(B*X)**C)+D
   60 CALL HWALL (GAS,PE,TW,HW,RHOW)
      GO TO 80
C
C
C     EVALUATE TW FROM ADIABATIC HW
   70 HW=HAD
      CALL RHOTZ (GAS,PE,HW,RHOW,TW,ZW)
   80 RHOW=RHOW
      RETURN
      END
```

```
      SUBROUTINE FNOL2(J,N,G,L,M,NE,X,Y,D,DERIV,TERM,OUTPUT)
      DIMENSION Y(50),D(50),YB(30,6),GI2(30),GI3(30),GI4(30),EF(30),
     1EF1(30),EF2(30),EF3(30),Y1(30),ERROR(30),HA(30),YA(50),DA(50),
     2YC(30),YP(30),YD(50)
      DOUBLE PRECISION XD,YD,YA,YC,YP,Y1
      EC=Y(N+3)
   1  H=G
   2  HZ=H
   3  LN=N+MAX0(L,3)
   4  NA=0
   5  NB=1
   6  NF=0
   7  NG=0
   8  F=0.
   9  FA=0.
  10  FB=0.
  11  FC=0.
  12  FD=0.
  13  ENE=NE
      DO 200 I=1,LN
 200  YD(I)=DBLE(Y(I))
      XD=DBLE(X)
  14  IF(J-3)15,21,15
  15  IF(NE)18,16,18
  16  JA=4
  17  GO TO 22
  18  RE1=10.**(-ENE)
  19  RE2=10.**(-ENE-3.0)
  20  REM=10.**(-ENE-1.5)
  21  JA=1
  22  DO 25 I=1,N
  23  DO 24 IC=1,5
  24  YB(I,IC)=0.
  25  ERROR(I)=0.
  26  CALL DERIV(X,Y,D)
      DO 300 I=1,N
      GI2(I)=D(I)
      GI3(I)=D(I)
      GI4(I)=D(I)
 300  EF(I)=D(I)
  27  CALL OUTPUT(X,Y,D,ERROR,N,L,H)
  28  FD=Y(N+1)
  29  IF(J-2) 30,129,30
  30  GO TO(31,37,35,37),JA
  31  DO 33 I=1,LN
  32  YA(I)=YD(I)
  33  DA(I)=D(I)
  34  GO TO 37
  35  HB=H
  36  H=2.*H
  37  HD2 = .5*H
      DO 39 I=1,N
  38  YB(I,NB)=D(I)
      XL = D(I) * HD2
  39  Y(I)=SNGL(YD(I)+XL)
      X=SNGL(XD+HD2)
  40  CALL DERIV (X,Y,GI2)
  41  DO 42 I=1,N
      XL = GI2(I)*HD2
  42  Y(I)=SNGL(YD(I)+XL)
  43  CALL DERIV (X,Y,GI3)
  44  DO 45 I=1,N
      XL=GI3(I)*H
  45  Y(I)=SNGL(YD(I)+XL)
      X=SNGL(XD+H)
  46  CALL DERIV(X,Y,GI4)
```

C-32

```
 47 HD6 =H/6.
    GO TO(48,55,60,66),JA
 48 DO 52 I=1,N
    XL=(D(I) + 2.*(GI2(I) + GI3(I)) +GI4(I))*HD6
 49 YC(I)=YD(I)+XL
 51 YD(I)=YA(I)
 52 ERROR(I)=0.
 53 JA=3
 54 GO TO 35
 55 DO 57 I=1,N
    XL=(D(I) + 2.*(GI2(I) + GI3(I)) +GI4(I))*HD6
 56 YD(I)=YD(I)+XL
 57 ERROR(I)=SNGL(YD(I)-YP(I))/15.
 58 JA=1
 59 GO TO 681
 60 DO 62 I=1,N
 61 YD(I)=YC(I)
    XL=(D(I) + 2.*(GI2(I) + GI3(I)) +GI4(I))*HD6
 62 YP(I)=YA(I)+XL
 63 H=HB
 64 JA=2
 65 GO TO 681
 66 DO 68 I=1,N
    XL=(D(I) + 2.*(GI2(I) + GI3(I)) +GI4(I))*HD6
 67 YD(I)=YD(I)+XL
 68 ERROR(I)=0.
681 DO 69 I=1,N
 69 Y(I)=SNGL(YD(I))
    XD=XD+H
    X=SNGL(XD)
 70 CALL DERIV(X,Y,D)
 71 FC=F
 72 CALL TERM(X,Y,D,F)
 73 IF(ABS(F)-1.0E-5 )731,731,733
731 NF=5
732 GO TO 124
733 IF(F)74,124,76
 74 FA=1.
 75 GO TO 77
 76 FB=1.
 77 IF(FA-FB)83,78,83
 78 NF=NF+1
 79 JA=4
 80 NB=1
 81 H=H*F/(FC-F)
 82 IF(NF-4)37,37,124
 83 IF(NE)84,117,84
 84 IF(JA-1)117,85,117
 85 IF(J-3)86,117,86
 86 DO 95 I=1,N
    IF(Y(I))886,885,886
885 HA(I)=1000.
    GO TO 95
886 IF(EC)880,890,87
 87 IF(ABS(Y(I))-EC) 880,880,890
880 IF(ABS(ERROR(I))-RE2) 882,94,881
881 IF(ABS(ERROR(I))-RE1)94,94,882
882 HA(I)=H*(REM/(ABS(ERROR(I))+.0000000001))**(.2)
883 GO TO 95
890 IF(ABS(ERROR(I)/Y(I))-RE2)892,94,891
891 IF(ABS(ERROR(I)/Y(I))-RE1)94,94,892
892 HA(I)=H*(REM/(ABS(ERROR(I)/Y(I))+.0000000001))**(.2)
893 GO TO 95
 94 HA(I)=H
 95 CONTINUE
 96 HB=HA(N)
```

```
 97 DO 98 I=1,N
 98 HB=AMIN1(HA(I),HB)
 99 IF(H-HB)100,117,101
100 IF(HZ-H)101,101,116
101 DO 103 I=1,LN
102 YD(I)=YA(I)
    Y(I)=SNGL(YD(I))
103 D(I)=DA(I)
104 IF(NB-6)107,105,105
105 XD=XD-H
106 GO TO 109
107 XD=XD-2.*H
108 HZ=H
109 H=HB
    X=SNGL(XD)
    CALL DERIV(X,Y,D)
110 NB=1
111 XABS=ABS(.000001*X)
112 IF(ABS(H)-XABS)113,113,117
113 NG=NG+1
114 H=SIGN(XABS,HB)
115 IF(NG-10)124,126,126
116 HZ=H
117 IF(M)118,118,121
118 IF(ABS(Y(N+1)-FD)-Y(N+2))29,119,119
119 FD=Y(N+1)
120 GO TO 124
121 NA=NA+1
122 IF(M-NA)123,123,29
123 NA=0
124 CALL OUTPUT(X,Y,D,ERROR,N,L,H)
125 IF(NF-4)29,29,126
126 WRITE (6,127)
127 FORMAT(1H0)
128 RETURN
129 NB=NB+1
130 IF(NB-6)30,131,136
131 DO 134 I=1,N
132 EF3(I)=YB(I,3)
133 EF2(I)=YB(I,4)
134 EF1(I)=YB(I,5)
135 GO TO 137
136 NB=10
137 HD24 =H/24.
    DO 138 I=1,N
    XL =(55.*D(I) -59.*EF1(I) +37.*EF2(I) -9.*EF3(I))*HD24
    YP(I)=YD(I)+XL
138 Y(I)=SNGL(YP(I))
    X=SNGL(XD+H)
139 CALL DERIV(X,Y,EF)
140 DO 142 I=1,LN
141 YA(I)=YD(I)
142 DA(I)=D(I)
143 DO 148 I=1,N
    XL = (9.*EF(I) +19.*D(I) -5.*EF1(I) +EF2(I))*HD24
144 YD(I)=YD(I)+XL
145 ERROR(I)=-SNGL(YD(I)-YP(I))/14.
146 EF3(I)=EF2(I)
147 EF2(I)=EF1(I)
148 EF1(I)=D(I)
149 GO TO 681
    END
```

AERODYNAMICS DEPARTMENT
EXTERNAL DISTRIBUTION LIST   (A1)

<div align="right">

No. of Copies
</div>

Commander, Naval Ordnance Systems Command Headquarters
Department of the Navy
Washington, D. C. 20360

Attn: Chief Technical Analyst, ORD 05121	1
Attn: ORD 035	1
Attn: ORD 03A	1
Attn: ORD 9132	2

Commander, Naval Air Systems Command Headquarters
Department of the Navy
Washington, D. C. 20360

Attn: AIR 03B	1
Attn: AIR 03C	1
Attn: AIR 320	1
Attn: AIR 320C	1
Attn: Dr. H. J. Mueller, AIR 310	1
Attn: AIR 604	2

Office of Naval Research
Department of the Navy
Washington, D. C. 20360

Attn: Mr. Morton Cooper, ONR 430B	2

Commanding Officer and Director
Naval Ship Research and Development Center
Washington, D. C. 20007

Attn: Central Library Branch (Code L42, M. H. Brode)	1
Attn: Aerodynamics Laboratory (L46)	1

Commander, Naval Weapons Center
China Lake, California 93555

Attn: Technical Library (Code 753)	1
Attn: Code 406	1
Attn: R. E. Meeker (Code 4063)	1

Director, U. S. Naval Research Laboratory
Washington, D. C. 20390

Attn: Library	1

NASA
Ames Laboratory
Moffett Field, California 94035 1

NASA
Langley Research Center
Langley Station
Hampton, Virginia 23365
  Attn: Library   1
  Attn: Aeronautical and Space Mechanics Division   1
  Attn: Mr. Dennis Brushwell   1
  Attn: Mr. Ivan Beckwith   1

NASA
Lewis Research Center
21000 Brookpark Road
Cleveland, Ohio 44135
  Attn: Library   1
  Attn: Chief, Wind Tunnel and Flight Division   1

NASA
George C. Marshall Space Flight Center
Huntsville, Alabama 35812
  Attn: Mr. T. Reed, R-AERO-AU   1
  Attn: Mr. W. K. Dahm, R-AERO-A   1

NASA
600 Independence Avenue, S. W.
Washington, D. C. 20546
  Attn: Dr. H. H. Kurzweg, Director of Research (Code RR)   1

NASA
P. O. Box 33
College Park, Maryland 20740   1

Technical Library
Director Defense Research and Engineering (DDR+E)
Room 3E-1063, The Pentagon
Washington, D. C. 20301
  Attn: Stop 103   1

Defense Documentation Center
Cameron Station
Alexandria, Virginia 22314   20

Commander (5632.2)
Naval Missile Center
Point Mugu, California 93041
  Attn: Technical Library   1

Commanding Officer
USA Aberdeen Research and Development Center
Aberdeen Proving Ground, Maryland 21005
   Attn: STEAP-TL (Technical Library Div.)   1
   Attn: AMXRD-XSE   1

Commander, U. S. Naval Weapons Laboratory
Dahlgren, Virginia 22448
   Attn: Library   1
   Attn: Mr. Thomas Clare   1
Director, Strategic Systems Project Office
Department of the Navy
Washington, D. C. 20390
   Attn: NSP-2722   2

Director of Intelligence
Headquarters, USAF (AFNINDE)
Washington, D. C. 20330
   Attn: AFOIN-3B   1

Aerospace Research Laboratories
Office of Aerospace Research
Wright-Patterson Air Force Base
Dayton, Ohio 45433
   Attn: Thermo-Mechanics Research Lab. (ARN)   1

Commander
Space and Missile Systems Organization
Air Force Unit Post Office
Los Angeles Air Force Station,
California 90045
   Attn: SMTTM/LT. C. Lee   1

Headquarters, Arnold Engineering Development Center
ARO, Inc.
Arnold Air Force Station, Tennessee 37389
   Attn: Library/Documents - Joe Ashley, Jr.   1
   Attn: Dr. H. K. Doetsch/AELR   1
   Attn: R. W. Henzel, Chief, PWT   1

von Karman Gas Dynamics Facility
ARO, Inc.
Arnold Air Force Station, Tennessee 37388   1
   Attn: Mr. Jack D. Whitfield, Chief

Commanding Officer, Harry Diamond Laboratories
Washington, D. C. 20438
   Attn: Library, Room 211, Bldg. 92   1

Commanding General
U. S. Army Missile Command
Redstone Arsenal, Alabama 35809
   Attn: AMSMI-RR   1
   Attn: Chief, Document Section   1
   Attn: AMSMI-RDK, Mr. R. A. Deep   1

Department of the Army
Office of the Chief of Research and Development
ABMDA, The Pentagon
Washington, D. C. 20350   1

Commanding Officer
Picatinny Arsenal
Dover, New Jersey 07801
   Attn: Mr. A. A. Loeb, SMUPA-VC-3   1

Commander (ADL)
Naval Air Development Center
Johnsville, Warminster,
Pennsylvania 18974   1

Commanding Officer
U. S. Air Force Weapons Laboratory
Kirtland Air Force Base
Albuquerque, New Mexico 87117
   Attn: WLRP   1

U. S. Army Ballistic Missile Defense Agency
1100 Commonwealth Bldg.
1320 Wilson Boulevard
Arlington, Virginia 22209
   Attn: Dr. Sidney Alexander   1

The Johns Hopkins University (C/NOw 7386)
Applied Physics Laboratory
8621 Georgia Avenue
Silver Spring, Maryland 20910
   Attn: Document Library   2
   Attn: Dr. F. Hill   1
   Attn: Dr. L. L. Cronvich   1

Director, Defense Atomic Support Agency
Headquarters DASA
Washington, D. C. 20305
  Attn: STSP (SPAS)   1

Commanding Officer
U. S. Army Mobility Equipment
Research and Development Center
Fort Belvoir, Virginia 22060
  Attn: Technical Documents Center   1

Commander, Naval Intelligence Command   1
Naval Intelligence Command Headquarters
2461 Eisenhower Avenue
Alexandria, Virginia   22314

Commanding Officer   1
Naval Scientific & Technical Intelligence Center
4301 Suitland Road
Washington, D.C.   20390

Department of Aeronautics   1
DFAN
USAF, Academy, Colorado 80840
  Attn: Col. D.H. Daley, Prof. & Head

No. of Copies

Aerospace Engineering Program
University of Alabama
P. O. Box 6307
University of Alabama 35486
   Attn: Prof. W. K. Rey, Chm.   1

AME Department
University of Arizona
Tucson, Arizona 85721
   Attn: Dr. L. B. Scott   1

Polytechnic Institute of Brooklyn
Graduate Center Library
Route 110, Farmingdale,
Long Island, New York 11735
   Attn: Dr. J. Polczynski   1

Polytechnic Institute of Brooklyn
Spicer Library
333 Jay Street
Brooklyn, New York 11201
   Attn: Reference Department   1

Brown University
Division of Engineering
Providence, Rhode Island 02912
   Attn: Dr. M. Sibulkin   1
   Attn: Library   1

California Institute of Technology
Pasadena, California 91109
   Attn: Graduate Aeronautical Laboratories
        Aero. Librarian   1
   Attn: Dr. H. Liepmann, Karman Lab-301   1
   Attn: Prof. L. Lees, Firestone Flight Sciences Lab.   1
   Attn: Dr. D. Coles, 306 Karman Lab.   1
   Attn: Dr. A. Roshko   1

University of California
Berkeley, California 94720
   Attn: Dr. M. Holt, Div. of Aeronautical Sciences   1
   Attn: Research Coordinator, College of Engineering   1

GASDYNAMICS
University of California
Richmond Field Station
1301 South 46th Street
Richmond, California 94804
  Attn: A. K. Oppenheim   1

Department of Aerospace Engineering
University of Southern California
University Park
Los Angeles, California 90007
  Attn: Dr. John Laufer   1

University of California - San Diego
Department of Aerospace and Mechanical
 Engineering Sciences
LaJolla, California 92037
  Attn: Dr. P. A. Libby   1

Case Western Reserve University
3306 Clarendon Road
Cleveland. Ohio 44118   1
   Attn: G. Kuerti
The Catholic University of America
Washington, D. C. 20017
  Attn: Dr. C. C. Chang   1
  Attn: Dr. Paul K. Chang, Mechanical Engr. Dept.   1
  Attn: Dr. M. J. Casarella, Mechanical Engr. Dept.   1

University of Cincinnati
Cincinnati, Ohio 45221
  Attn: Department of Aerospace Engineering   1
  Attn: Dr. Arnold Polak   1

Department of Aerospace Engineering Sciences
University of Colorado
Boulder, Colorado 80302   1

Cornell University
Graduate School of Aero. Engineering
Ithaca, New York 14850
  Attn: Prof. W. R. Sears   1
  Attn: Dr. S. F. Shen   1
  Attn: Prof. F. K. Moore, Head, Thermal Engineering Dept.   1
                           208 Upson Hall

University of Delaware
Mechanical and Aeronautical Engineering Dept.
Newark, Delaware 19711
   Attn: Dr. James E. Danberg   1

Georgia Institute of Technology
225 North Avenue, N. W.
Atlanta, Georgia 30332
   Attn: Dr. Arnold L. Ducoffe, Aerospace Engineering Dept.   1

Technical Reports Collection
Gordon McKay Library
Harvard University
Div. of Eng'g. and Applied Physics
Pierce Hall, Oxford Street
Cambridge, Massachusetts 02138   1

Illinois Institute of Technology
3300 South Federal
Chicago, Illinois 60616
   Attn: Dr. M. V. Morkovin   1
   Attn: Prof. A. A. Fejer, M.A.E. Dept.   1

University of Illinois
101 Transportation Building
Urbana, Illinois 61801
   Attn: Aeronautical and Astronautical Engineering Dept.   1

Iowa State University
Ames, Iowa 50010
   Attn: Aerospace Engineering Dept.   1

The Johns Hopkins University
Baltimore, Maryland 21218
   Attn: Prof. S. Corrsin   1

University of Kentucky
Wenner-Gren Aero. Lab.
Lexington, Kentucky 40506
   Attn: C. F. Knapp   1

Department of Aero. Engineering, ME 106
Louisiana State University
Baton Rouge, Louisiana 70803
   Attn: Dr. P. H. Miller   1

University of Maryland
College Park, Maryland 20740
  Attn: Prof. A. Wiley Sherwood, Department of
           Aerospace Engineering   1
  Attn: Prof. Charles A. Shreeve, Department of
           Mechanical Engineering   1
  Attn: Dr. S. I. Pai, Institute for Fluid
           Dynamics and Applied Mathematics   1
  Attn: Dr. Redfield W. Allen, Department of
           Mechanical Engineering   1
  Attn: Dr. W. L. Melnik, Department of Aerospace Engr.   1

Michigan State University Library
East Lansing, Michigan 48823
  Attn: Documents Department   1

Massachusetts Institute of Technology
Cambridge, Massachusetts 02139
  Attn: Mr. J. R. Martuccelli, Rm 33-211   1
  Attn: Prof. M. Finston   1
  Attn: Prof. J. Baron, Dept. of Aero. and Astro., Rm.37-461 1
  Attn: Prof. A. H. Shapiro, Head, Mech. Engr. Dept.   1
  Attn: Aero. Engineering Library   1
  Attn: Prof. Ronald F. Probestein   1
  Attn: Dr. E. E. Covert, Aerophysics Laboratory   1

University of Michigan
Ann Arbor, Michigan 48104
  Attn: Dr. A. Kuethe, Dept. of Aero. Engineering   1
  Attn: Dr. O. Laporte, Dept. of Physics   1
  Attn: Dr. M. Sichel, Dept. of Aero. Engineering   1
  Attn: Engineering Library   1
  Attn: Aerospace Engineering Library   1

Serials and Documents Section
General Library
University of Michigan
Ann Arbor, Michigan 48104   1

Mississippi State University
Department of Aerophysics and Aerospace Engineering
P. O. Drawer AP
State College, Mississippi 39762
  Attn: Dr. Sean C. Roberts   1

U. S. Naval Academy
Annapolis, Maryland 21402
  Attn: Engineering Department, Aerospace Division   1

Library, Code 2124
U. S. Naval Postgraduate School
Monterey, California 93940
  Attn: Technical Reports Section   1

New York University
University Heights
New York, New York 10453
  Attn: Dr. Antonio Ferri, Director of
        Guggenheim Aerospace Laboratories   1
  Attn: Prof. V. Zakkay   1
  Attn: Engineering and Science Library   1

North Carolina State College
Raleigh, North Carolina 27607
  Attn: Dr. R. W. Truitt, Head, Mech. and Aero. Engineering 1
  Attn: Dr. H. A. Hassan, Dept. of Mech. and Aero. Engr. 1

D. H. Hill Library
North Carolina State University
P. O. Box 5007
Raleigh, North Carolina 27607   1

University of North Carolina
Chapel Hill, North Carolina 27514
  Attn: Department of Aero. Engineering   1
  Attn: Library, Documents Section   1
  Attn: AFROTC Det 590   1

Northwestern University
Technological Institute
Evanston, Illinois 60201
  Attn: Department of Mechanical Engineering   1
  Attn: Library   1

Notre Dame University
South Bend, Indiana 46556
  Attn: Dr. J. D. Nicolaides, Dept. of Aero. Engineering 1

Ohio State University
2036 Neil Avenue
Columbus, Ohio 43210
  Attn: Aero. Civil Library   1
  Attn: Prof. J. D. Lee, Aeronautical Research Lab.   1
  Attn: Prof. G. L. Von Eschen, Dept. of Aero-Astro Engr. 1

Ohio State University Libraries
Documents Division
1858 Neil Avenue
Columbus, Ohio 43210   1

Department of Aerospace Engineering
Room 233 Hammond Building
The Pennsylvania State University
University Park, Pennsylvania 16802   1

Pennsylvania State University Library
Documents Section
University Park, Pennsylvania 16802   1

Engineering Library
700 Engineering Hall
University of Pittsburgh
Pittsburgh, Pennsylvania 15213   1

Princeton University
James Forrestal Research Center
Gas Dynamics Laboratory
Princeton, New Jersey 08540
    Attn: Prof. S. Bogdonoff   1
    Attn: Mr. I. E. Vas   1

Purdue University
School of Aeronautical and Engineering Sciences
Lafayette, Indiana 47907
    Attn: Library   1
    Attn: Dr. P. S. Lykoudis, Dept. of Aero. Engineering   1

Rensselaer Polytechnic Institute
Troy, New York 12181
    Attn: Dept. of Aeronautical Engineering and Astronautics   1

Rutgers – The State University
University Heights Campus
New Brunswick, New Jersey 08903
    Attn: Dr. R. H. Page, Dept. of Mech. and Aero. Engineering   1

Stanford University
Stanford, California 94305
    Attn: Librarian, Dept. of Aeronautics and Astronautics   1

Stevens Institute of Technology
Hoboken, New Jersey 07030
  Attn: Mechanical Engineering Department   1
  Attn: Library   1

The University of Texas at Austin
Applied Research Laboratories
P. O. Box 8029
Austin, Texas 78712
  Attn: Director   1

University of Toledo
Department of Aero. Engineering
Research Foundation
Toledo, Ohio 43606   1

Documents Department
Virginia Polytechnic Institute
Blacksburg, Virginia 24061
  Attn: Carol M. Newman Library   1
  Attn: Dr. M..J. Werle, Eng. Mech. Dept.   1
University of Virginia
Charlottesville, Virginia 22901
  Attn: Alderman Library, Science Reference Division   1
  Attn: Dr. G. Matthews, Dept. of Aerospace Engineering   1

University of Washington
Seattle, Washington 98105
  Attn: Engineering Library   1
  Attn: Dept. of Aeronautics and Astronautics   1
  Attn: Prof. R. E. Street, Dept. of Aero. and Astro.   1
  Attn: Prof. A. Hertzberg, Aero. and Astro. Guggenheim Hall 1

West Virginia University
Morgantown, West Virginia 26506
  Attn: Library   1

Federal Reports Center
University of Wisconsin
Mechanical Engineering Building
Madison, Wisconsin 53706
  Attn: S. Reilly   1

Yale University
400 Temple Street
New Haven, Connecticut 06520
   Attn: Dépt. of Engr. and Applied Sciences,
           Library, Dunham Lab.   1
   Attn: Dr. P. P. Wegener   1
   Attn: Prof A. Robinson, Dept. of Mathematics   1

Los Alamos Scientific Laboratory
P. O. Box 1663
Los Alamos, New Mexico 87544
   Attn: Report Library   1

University of Maryland
Baltimore County (UMBC)
5401 Wilkens Avenue
Baltimore, Maryland 21228
   Attn: Dr. R. C. Roberts, Mathematics Department   1

Riverside Research Institute
632 West 125th Street
New York, New York 10027
   Attn: H. K. Cressman   1

Oklahoma State University
Office of Engineering Research
Stillwater, Oklahoma 74074
   Attn: Dr. V. S. Haneman, Jr.   1

Institute for Defense Analyses
400 Army-Navy Drive
Arlington, Virginia 22202
   Attn: Classified Library   1

Kaman Nuclear
1700 Garden of the Gods Road
Colorado Springs, Colorado 80907   1

Kaman Science Corporation
Avidyne Division
83 Second Avenue
Burlington, Massachusetts 01803
   Attn: Dr. J. R. Ruetenik   1

North American Rockwell Corporation
International Airport
Los Angeles, California 90009
   Attn: LAD Library, Dept. 299   1

North American Rockwell Corporation
Engineering Data Services
4300 E. Fifth Avenue
Columbus, Ohio 43216   1

M. I. T. Lincoln Laboratory
P. O. Box 73
Lexington, Massachusetts 02173
  Attn: Library A-082   1

The RAND Corporation
1700 Main Street
Santa Monica, California 90406
  Attn: Library - D   1

Aerojet-General Corporation
6352 N. Irwindale Avenue
Azusa, California 91702
  Attn: M. T. Grenier, Corporate Librarian   1

The Boeing Company
P. O. Box 3999
Seattle, Washington 98124
  Attn: Aerospace Library 8K-38, J. M. MacDonald   1

United Aircraft Corporation
Research Laboratories
East Hartford, Connecticut 06108
  Attn: Dr. William M. Foley   1

United Aircraft Corporation
400 Main Street
East Hartford, Connecticut 06108
  Attn: Library   1

Hughes Aircraft Company
Centinela and Teale Streets
Culver City, California 90230
  Attn: Co. Tech. Doc. Ctr., MS 6/E110   1

Lockheed Missiles and Space Company
Dept. 55-20, Building 102
1111 Lockheed Way
Sunnyvale, California 94088
  Attn: Maurice Tucker   1

Lockheed Missiles and Space Company
P. O. Box 504
Sunnyvale, California 94086
   Attn: Mr. G. M. Laden, Dept. 81-25, Bldg. 154   1
   Attn: Mr. Murl Culp   1

Lockheed Missiles and Space Company
3251 Hanover Street
Palo Alto, California 94304
   Attn: Technical Information Center   1

Lockheed-California Company
Burbank, California 91503
   Attn: Central Library, Dept. 84-40, Bldg. 170, PLT.B-1   1

Vice President and Chief Scientist
Dept. 01-10
Lockheed Aircraft Corporation
P. O. Box 551
Burbank, California 91503   1

Martin Marietta Corporation
P. O. Box 988
Baltimore, Maryland 21203
   Attn: Science-Technology Library (Mail No. 398)   1

Martin Company
3211 Trade Winds Trail
Orlando, Florida 32805
   Attn: Mr. H. J. Diebolt   1

General Dynamics
P. O. Box 748
Fort Worth, Texas 76101
   Attn: Research Library 2246   1
   Attn: George Kaler, Mail Zone 2880   1

Cornell Aeronautical Laboratory, Inc.
4455 Genesee Street
Buffalo, New York 14221
   Attn: Library   1

Air University Library
(SE) 63-578
Maxwell Air Force Base, Alabama 36112   1

McDonnell Company
P. O. Box 516
St. Louis, Missouri 63166
   Attn: R. D. Detrich, Dept. 218, Bldg. 101M   1

McDonnell-Douglas Aircraft Corporation
Missile and Space Systems Division
3000 Ocean Park Boulevard
Santa Monica, California 90405
   Attn: A2-260 Library   1
   Attn: Dr. J. S. Murphy, A-830   1
   Attn: Mr. W. H. Branch, Director   1

Fairchild Hiller
Republic Aviation Division
Farmingdale, New York 11735
   Attn: Engineering Library   1

General Applied Science Laboratories, Inc.
Merrick and Stewart Avenues
Westbury, Long Island, New York 11590
   Attn: Dr. F. Lane   1

General Electric Company
Research and Development Lab. (Comb. Bldg.)
Schenectady, New York 12301
   Attn: Dr. H. T. Nagamatsu   1

The Whitney Library
General Electric Research and Development Center
The Knolls, K-1
P. O. Box 8
Schenectady, New York 12301
   Attn: M. F. Orr, Manager   1

General Electric Company
Missile and Space Division
P. O. Box 8555
Philadelphia, Pennsylvania 19101
   Attn: MSD Library, Larry Chasen, Mgr.   1
   Attn: Dr. J. D. Stewart, Mgr., Research and Engineering   1

General Electric Company
AEG Technical Information Center, N-32
Cincinnati, Ohio 45215   1

General Electric Company
Missile and Space Division
P. O. Box 8555
Philadelphia, Pennsylvania 19101
   Attn: Dr. S. M. Scala   1
   Attn: Dr. H. Lew   1
   Attn: Mr. J. W. Faust   1
   Attn: Mr. W. Daskin   1
   Attn: S. B. Kottock   1
   Attn: S. Kahn   1
   Attn: J. B. Arnaiz   1
   Attn: L. A. Marshall   1
   Attn: A. Martellucci   1

AVCO-Everett Research Laboratory
2385 Revere Beach Parkway
Everett, Massachusetts 02149
   Attn: Library   1
   Attn: Dr. George Sutton   1

LTV Aerospace Corporation
Vought Aeronautics Division
P. O. Box 5907
Dallas, Texas 75222
   Attn: Unit 2-51131 (Library)   1

LTV Aerospace Corporation
Missiles and Space Division
P. O. Box 6267
Dallas, Texas 75222
   Attn: MSD-T-Library   1

Northrop Norair
3901 West Broadway
Hawthorne, California 90250
   Attn: Tech. Info. 3343-32   1

Gifts and Exchanges
The Foundren Library
Rice Institute
P. O. Box 1892
Houston, Texas 77001   1

Grumman Aircraft Engineering Corporation
Bethpage, Long Island, New York 11714
   Attn: Mr. R. A. Scheuing   1
   Attn: Mr. H. B. Hopkins   1
   Attn: Mr. H. R. Reed
                                     1

Marquardt Aircraft Corporation
16555 Saticoy Street
Van Nuys, California 91409
  Attn: Library   1

ARDE Associates
P. O. Box 286
580 Winters Avenue
Paramus, New Jersey 07652
  Attn: Librarian   1

Vitro Laboratories
200 Pleasant Valley Way
West Orange, New Jersey 07052   1

Aeronautical Research Associates of Princeton
50 Washington Road
Princeton, New Jersey 08540
  Attn: Dr. C. duP. Donaldson   1

General Research Corporation
5383 Hollister Avenue
P. O. Box 3587
Santa Barbara, California 93105
  Attn: Technical Information Office   1

Sandia Corporation
Sandia Base
Albuquerque, New Mexico 87115
  Attn: Mr. K. Goin, Div. 9322   1
  Attn: Mrs. B. R. Allen, Div. 3421   1

HERCULES INCORPORATED
Allegany Ballistics Laboratory
P. O. Box 210
Cumberland, Maryland 21502
  Attn: Library   1

General Electric Company
P. O. Box 2500
Daytona Beach, Florida 32015
  Attn: Dave Hovis, Rm. 4109   1

TRW Systems Group
1 Space Park
Redondo Beach, California 90278
  Attn: Technical Library-Document Acquisitions   1

Stanford Research Institute
333 Ravenswood Avenue
Menlo Park, California 94025
   Attn: Dr. G. Abrahamson   1

Aerospace Corporation
111 Mill Street
San Bernardino, California 92402
  Attn: Library   1
  Attn: Dr. Stephen Lubard   1
  Attn: Mr. Farnando Fernandez   1

Hughes Aircraft Company
P. O. Box 3310
Fullerton, California 92634
   Attn: R. H. Sterling, 600-E201   1

Westinghouse Electric Corporation
Astronuclear Laboratory
P. O. Box 10864
Pittsburgh, Pennsylvania 15236
   Attn: Library   1

General Dynamics Corporation
One Rockefeller Plaza
New York, New York 10020
   Attn: Technical Information Center 1

CONVAIR Division of General Dynamics
Library and Information Services
P. O. Box 12009
San Diego, California 92112   2

CONVAIR Division of General Dynamics
P. O. Box 1128
San Diego, California 92112
   Attn: Dr. Jan Raat, Aeroballistics Dept.
         Mail Zone 583-00   1

AVCO Missiles Systems Division
201 Lowell Street
Wilmington, Massachusetts 01887
   Attn: J. H. Grimes, Jr.   1
   Attn: E. E. H. Schormann   1
   Attn: J. Otis   1

Chrysler Corporation
Space Division
P. O. Box 29200
New Orleans, Louisiana 70129
  Attn: G. T. Boyd, Dept. 2781   1

General Dynamics
Pomona Division
Pomona, California 91766
  Attn: Division Library, Mail Zone 6-20   1

North American Rockwell Corporation
Ocean Systems Operations
350 South Magnolia Avenue
Long Beach, California 90802
  Attn: Dr. E. R. van Driest, JB14   1

Philco-Ford Corporation
Aeroneutronic Division
Newport Beach, California 92660
  Attn: Dr. A. Demetriades   1

Raytheon Company
Missile Systems Division
Hartwell Road
Bedford, Massachusetts 01730
  Attn: D. P. Forsmo   1

TRW Systems Group
Space Park Drive
Houston, Texas 77058
  Attn: M. W. Sweeney, Jr.   1

Marine Bioscience Laboratory
527 Las Alturas Road
Santa Barbara, California 93103
  Attn: Dr. A. C. Charters   1

DOCUMENT CONTROL DATA - R & D

(Security classification of title, body of abstract and indexing annotation must be entered when the overall report is classified)

1. ORIGINATING ACTIVITY *(Corporate author)*	2a. REPORT SECURITY CLASSIFICATION
Naval Ordnance Laboratory Silver Spring, Maryland 20910	Unclassified
	2b. GROUP

3. REPORT TITLE

NOL Hypervelocity Wind Tunnel Report No. 2: Nozzle Design

4. DESCRIPTIVE NOTES *(Type of report and inclusive dates)*

5. AUTHOR(S) *(First name, middle initial, last name)*

Walter J. Glowacki

6. REPORT DATE	7a. TOTAL NO. OF PAGES	7b. NO. OF REFS
30 April 1971	124	27

8a. CONTRACT OR GRANT NO.	9a. ORIGINATOR'S REPORT NUMBER(S)
b. PROJECT NO.	NOLTR 71-6
c.	9b. OTHER REPORT NO(S) *(Any other numbers that may be assigned this report)*
d.	

10. DISTRIBUTION STATEMENT

Approved for public release; Distribution Unlimited

11. SUPPLEMENTARY NOTES	12. SPONSORING MILITARY ACTIVITY

13. ABSTRACT

The NOL Hypervelocity Wind Tunnel will provide a high Reynolds number turbulent flow simulation in the Mach number range 10 to 20. This facility, much needed for large-scale testing of hypersonic vehicles, is under construction and will be operational late in 1972. Supply pressures up to 40,000 psi will be maintained constant for 1 to 4 seconds during which stable, condensation-free flow conditions will prevail. Very high Reynolds numbers, ranging from 6.5×10^6 at Mach number 20 to 46×10^6 at Mach number 10 (based on the nozzle exit diameter), are obtained by operating with nitrogen at temperatures just sufficient to avoid test section condensation. This report presents the detailed procedure used to design three nozzles for this facility. The nozzles are forty feet long with five foot exit diameters and are designed to operate at Mach numbers 10, 15, and 20 with supply pressures of 430, 2365, and 3110 atmospheres, respectively. Pressure and temperature effects on the thermo-dynamic properties of nitrogen are important at these elevated supply conditions and are taken into account in both the inviscid core and the boundary layer calculations. The supersonic portion of the inviscid core is calculated by the method of characteristics and the subsonic portion is approximated as a one-dimensional flow. The boundary layer calculation procedure is based on an integral moment of momentum equation and is valid for thick as well as thin boundary layers. The design conditions and the coordinates of both the nozzle wall and the inviscid core contours are given.

DD FORM 1473 (PAGE 1)
1 NOV 65

14. KEY WORDS	LINK A		LINK B		LINK C	
	ROLE	WT	ROLE	WT	ROLE	WT
Hypervelocity Wind tunnel Aerodynamic design Nozzles Turbulent Boundary Layer						

1. Hypersonic wind tunnels — NOL

2. " " — Design

3. Nozzles —

4. Hypersonic "